

NASA Technical Paper 1551

LOAN COPY:
AFWL TECH
KIRTLAND AFB



Flight Evaluation of Stabilization and Command Augmentation System Concepts and Cockpit Displays During Approach and Landing of a Powered-Lift STOL Aircraft

James A. Franklin, Robert C. Innis,
and Gordon H. Hardy

NOVEMBER 1980

NASA



NASA Technical Paper 1551

Flight Evaluation of Stabilization
and Command Augmentation System
Concepts and Cockpit Displays
During Approach and Landing of
a Powered-Lift STOL Aircraft

James A. Franklin, Robert C. Innis,
and Gordon H. Hardy
*Ames Research Center
Moffett Field, California*

NASA

National Aeronautics
and Space Administration

**Scientific and Technical
Information Branch**

1980

TABLE OF CONTENTS

	Page
SUMMARY	1
INTRODUCTION	1
RESEARCH AIRCRAFT	4
STABILIZATION AND COMMAND AUGMENTATION SYSTEM AND DISPLAY CONCEPTS	15
Attitude Control	18
Flightpath Control	27
Cockpit Displays	38
FLIGHT RESEARCH PROGRAM	41
RESULTS	45
Attitude Control	45
Flightpath Control	49
Cockpit Displays	57
Summary of Control-Display Results	68
CONCLUSIONS	70
APPENDIX A – LONGITUDINAL AND LATERAL-DIRECTIONAL DYNAMICS FOR BASIC AIRCRAFT AND SCAS CONFIGURATIONS	72
APPENDIX B – SUMMARY OF PILOT COMMENTS	76
APPENDIX C – NOTATION	83
REFERENCES	89

**FLIGHT EVALUATION OF STABILIZATION AND COMMAND AUGMENTATION
SYSTEM CONCEPTS AND COCKPIT DISPLAYS DURING APPROACH
AND LANDING OF A POWERED-LIFT STOL AIRCRAFT**

James A. Franklin, Robert C. Innis, and Gordon H. Hardy

Ames Research Center

SUMMARY

A flight research program was conducted to assess the effectiveness of manual control concepts and various cockpit displays in improving attitude (pitch, roll, and yaw) and longitudinal path control during STOL approaches and landings. The NASA-Ames Powered-Lift Augmentor Wing Jet STOL Research Aircraft was used in the research program. Satisfactory flying qualities were demonstrated to minimum-decision heights of 30 m (100 ft) for selected stabilization and command augmentation systems and flight director combinations. Precise landings at low touchdown sink rates were achieved with a gentle flare maneuver.

INTRODUCTION

The flight experiments discussed in this report were conducted to determine the influence on flying qualities of stabilization and command augmentation systems (SCAS) and cockpit displays during the approach and landing of a powered-lift STOL transport aircraft. Considerable experience obtained during flight tests of experimental STOL aircraft and during ground-based simulation of a variety of such configurations (refs. 1-13) has exposed deficiencies in flying qualities for either VFR or IFR operations. The deficiencies are associated with performing a precision approach to a landing on a short field with acceptable touchdown sink rates. In general, these deficiencies can be attributed to the sluggish and highly coupled response characteristics of these aircraft; these characteristics are associated with low-speed operation, high wing-loading, and substantial thrust turning representative of such designs.

When longitudinal control is considered, it is noted that precision of pitch attitude control is compromised by poor static stability, by substantial trim changes due to thrust and flaps, by turbulence disturbances, and by an easily excited phugoid mode. Left unattended, the phugoid substantially upsets flightpath and airspeed and will either degrade glide-slope tracking or increase pilot workload during the approach. Even if precise attitude control is achieved, the aircraft's response to pitch attitude is adversely influenced by operation at low speed and on the backside of the drag curve (at speeds where induced drag exceeds profile drag). Sluggish initial flightpath response to pitch attitude and the inability to sustain long-term path corrections with a change in attitude make path control with attitude unsuitable. Although thrust is a very powerful path control, coupling of flightpath and airspeed (as a consequence of large effective thrust turning angles) and thrust response lags can make thrust control of flightpath unsatisfactory or even unacceptable.

In the case of lateral-directional control, roll control capability has been compromised by poor lateral control force characteristics, low control power, and roll damping. Low directional stability, low Dutch-roll damping, and large unfavorable yawing moments from lateral controls, tend to combine to degrade heading control.

In the 1960's, flight evaluations were conducted on the Lockheed NC-130B and on the Breguet 941 to determine their characteristics for STOL operations. These tests revealed many deficiencies in flying qualities which in turn made it difficult to perform a precision IFR approach. The NC-130B (ref. 1) had particularly objectional lateral-directional flying qualities due to poor lateral control force characteristics, low directional stability and damping, and adverse aileron yaw. Longitudinal flying qualities were somewhat better although still unsatisfactory because of low pitch-control power and an easily excited phugoid mode. Attempts to improve the directional control characteristics with a stability augmentation system were successful (ref. 2) and satisfactory turn coordination and directional damping were achieved. The poor lateral control characteristics were not improved, however, and the overall flying qualities for an IFR approach were considered only marginally acceptable.

The Breguet 941 flying qualities, though not completely satisfactory, were considerably better than those of the NC-130B. Lateral control force and response characteristics were satisfactory and yawing moments due to lateral control were essentially eliminated with the combination of spoilers and differential propeller pitch. Although directional stability and damping were low, they did not approach unacceptable levels. Longitudinal flying qualities were acceptable though unsatisfactory due to low static stability. Trim changes with variations in power setting were large and objectionable. This objection was overcome by a mechanical interconnect between the throttles and elevator and, as noted in reference 4, use of power for control of the glide slope was considered satisfactory. Overall flying qualities for the IFR approach were considered to be generally satisfactory with the exceptions noted above; approaches to minimum decision heights of 61 m (200 ft) were feasible.

In the early 1970's, attention shifted to jet STOL configurations, and a number of simulation investigations were conducted to improve the flying qualities for the IFR approach of a number of individual STOL transport conceptual designs. A wide variety of SCAS concepts were applied to the longitudinal and lateral-directional control of these aircraft. Pitch and roll attitude control augmentation ranging from simple rate dampers to rate-command-attitude-hold and attitude-command-hold systems were considered in all of these investigations. In some instances, airspeed stabilization functions comparable to those provided by current generation auto-throttle systems were explored (refs. 5-7, 9).

Flightpath command and stabilization as well as independent lift and drag control devices to be used by the pilot for such purposes were evaluated in some cases (refs. 6-9). Flight director displays, which provide commands for the powered-lift control, were incorporated in the experiments of references 5 and 8 to provide command guidance appropriate to the particular control system mechanization. Virtually all of these reports indicate that higher levels of control augmentation, such as speed stabilization or flightpath SCAS, might be required to achieve satisfactory flying qualities for operation to Category II instrument minimums. The addition of pitch, roll, and yaw SCAS alone was sufficient to eliminate attitude control deficiencies, but the flying qualities were still considered unsatisfactory though acceptable. The remaining deficiencies associated with manual control for glide-slope and localizer tracking, speed control, and suppression of wind- and

turbulence-induced disturbances could only be eliminated with the more sophisticated augmentation modes and with an appropriately designed flight director.

Recent flight experience has been obtained with a variety of specific control augmentation systems on one of the Princeton Variable Stability Navions (ref. 11) and on the YC-15 and YC-14 Advanced Medium STOL Transport prototype aircraft (refs. 12, 13). The Princeton flight experience was obtained for control systems ranging from attitude stabilization to a completely decoupled attitude-speed-flightpath SCAS. Pilots considered the configuration with only attitude stabilization to have unsatisfactory, though acceptable, flying qualities for the IFR approach and landing. Complete decoupling of the aircraft responses and desensitizing response to turbulence resulted in pilot ratings that were fully satisfactory.

The YC-14 control configuration includes pitch, roll, and yaw SCAS; it modulates thrust, spoilers, and the upper surface blown flap to augment flightpath and airspeed control. An electronic attitude director indicator (EADI) provides integrated status and flightpath information in a head-down format. The YC-15 control system incorporates pitch, roll, and yaw SCAS and a DLC control on the aircraft's throttles to drive the spoilers to augment flightpath control. A visual approach monitor provides flightpath reference with respect to the intended touchdown point in a head-up format. It is generally considered, from the results of flight test programs reported to date, that fully satisfactory flying qualities have been achieved for both aircraft for visual approaches and landings.

The Ames Research Center's Augmentor Wing Research Aircraft, described in references 14 and 15, is a propulsive-lift jet STOL transport that because of its configuration and operational flight conditions exhibits some of the control characteristics (noted in the foregoing discussion) that are typical of its class. The aircraft was developed to demonstrate the augmented jet flap concept for powered-lift STOL operation and to provide a powered-lift STOL transport aircraft for research into flight dynamics, navigation, guidance and control, and STOL operations. It was initially procured with flying qualities sufficient to permit the exploration of its flight envelope and to demonstrate the performance, stability, and control characteristics associated with the augmented jet flap. Following the proof-of-concept flight tests, a versatile digital avionics system and electronic cockpit displays were installed. The avionics system and cockpit displays were added to extend the aircraft's capability to support the STOL research aircraft program noted above.

It was of particular interest that flight experiments be conducted for a variety of control system concepts on the Augmentor Wing Research Aircraft to determine the improvement in flying qualities that could be achieved; the concepts included pitch, roll, and yaw SCAS, airspeed stabilization, and flightpath command augmentation. In conjunction with the investigation of such control concepts, it was also considered worthwhile to explore various types of information that when displayed to the pilot in status or command format and properly associated with the mode of control being used provide guidance for flying a precision approach down to appropriate instrument minimums.

This report describes the research aircraft, the individual control and display concepts that were evaluated, and the results of the flight experiments. The flight evaluations were conducted for manually flown approaches under simulated instrument flight conditions followed by breakout at specified instrument minimums to a visual landing. Although these control systems and displays

have been demonstrated on a specific powered-lift design, the nature of the path-control improvement is considered applicable to other powered-lift aircraft configurations as well.

RESEARCH AIRCRAFT

Before describing the SCAS and display concepts investigated in this research program, the physical characteristics of the basic Augmentor Wing Research Aircraft will be reviewed briefly and the pertinent control response behavior on which the SCAS development is based will be discussed.

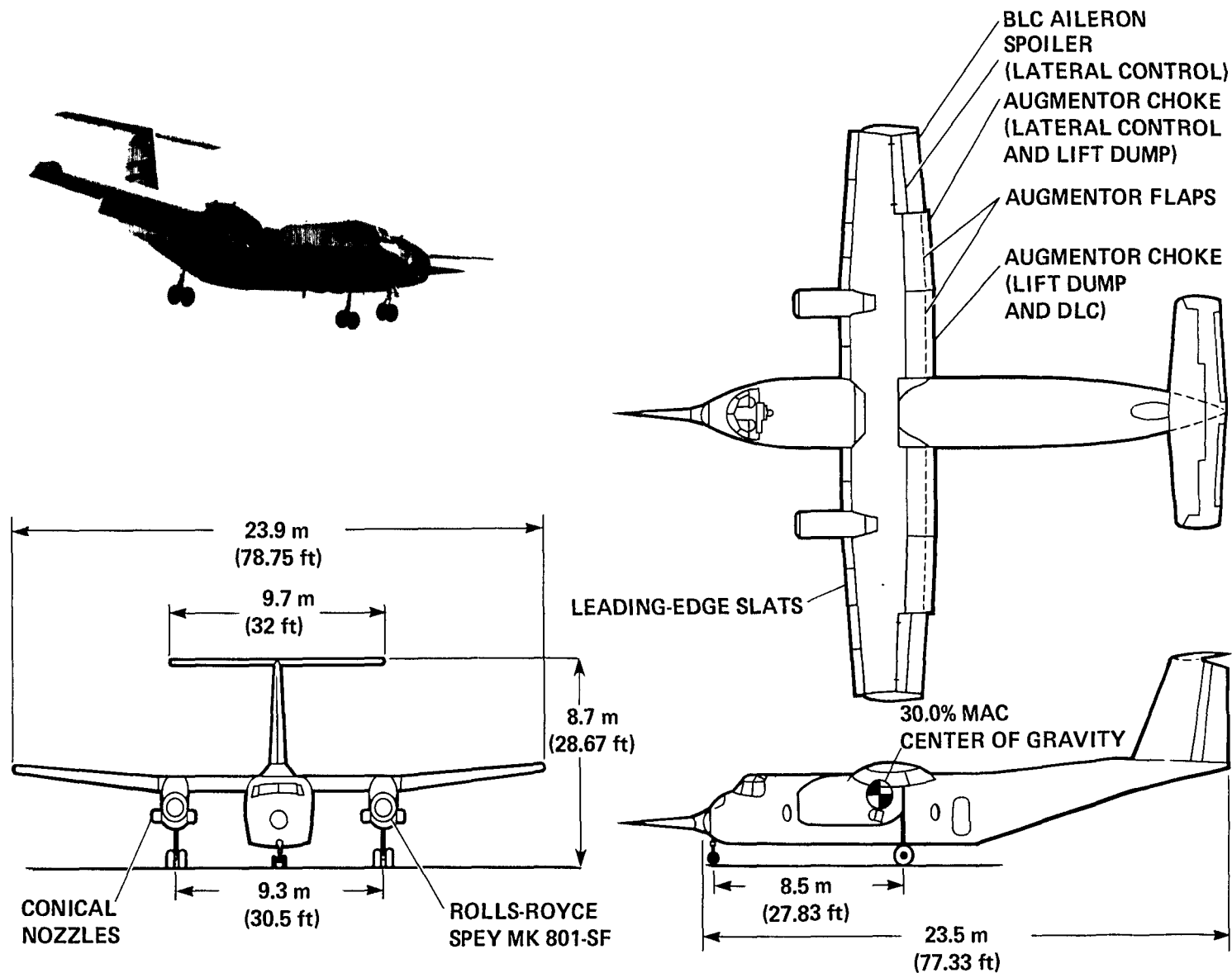
The Augmentor Wing Research Aircraft (fig. 1) is a de Havilland C-8A Buffalo, modified by The Boeing Company, de Havilland of Canada, and Rolls Royce of Canada to incorporate a propulsive-lift system. The aircraft is described in detail in references 14 and 15. It has a maximum gross weight of 21,792 kg (48,000 lb) and a range of operational wing loadings of 215-272 kg/m² (44-55 lb/ft²). The propulsive-lift system utilizes an augmentor jet flap designed for physical flap deflections up to 72°. Two Rolls Royce Spey 801-SF (Split Flow) engines, each providing 46,280 N (10,400 lb) thrust, power the aircraft. Fan air is distributed through bypass ducts to the flaps to augment the basic wing aerodynamics, with the flow from each engine split to supply air through the inner and outer bypass ducts to both right and left flaps to maintain symmetric lift in the event of an engine failure. Hot flow from the engine core passes out of the conical nozzles; the nozzles can be rotated through 98° (6° to 104° relative to the fuselage centerline) to deflect the direct thrust component.

The primary flight controls are fully powered hydraulically. They consist of a single-segment elevator; ailerons, spoilers, and outboard augmentor flap chokes; a two-segment rudder; hot thrust exhaust nozzles; and inboard augmentor flap chokes. The elevator is used for both pitch maneuvering and trim and has a total deflection of -15° to +24° at normal landing approach speeds. Ailerons, spoilers, and outboard augmentor chokes are programmed to deflect together for roll control in response to wheel command inputs. The ailerons have boundary-layer control, and droop as a function of flap position. They can be deflected to ±19° about the nominal droop position for the approach flap angle. The spoilers deflect up to 48° and outboard chokes deflect to close off as much as 55% of the augmentor flap exit area. Full rudder deflection is ±25° for the forward segment, where the aft panel to forward panel gearing ratio is 2:1. The inboard augmentor chokes are controlled symmetrically to modulate lift in flight and to dump lift when on the ground. Their full deflection is 65% closure of the flap exit area for the approach flap configuration.

The pilot's cockpit controls consist of a yoke and wheel, rudder pedals, and overhead throttles and nozzle control levers.

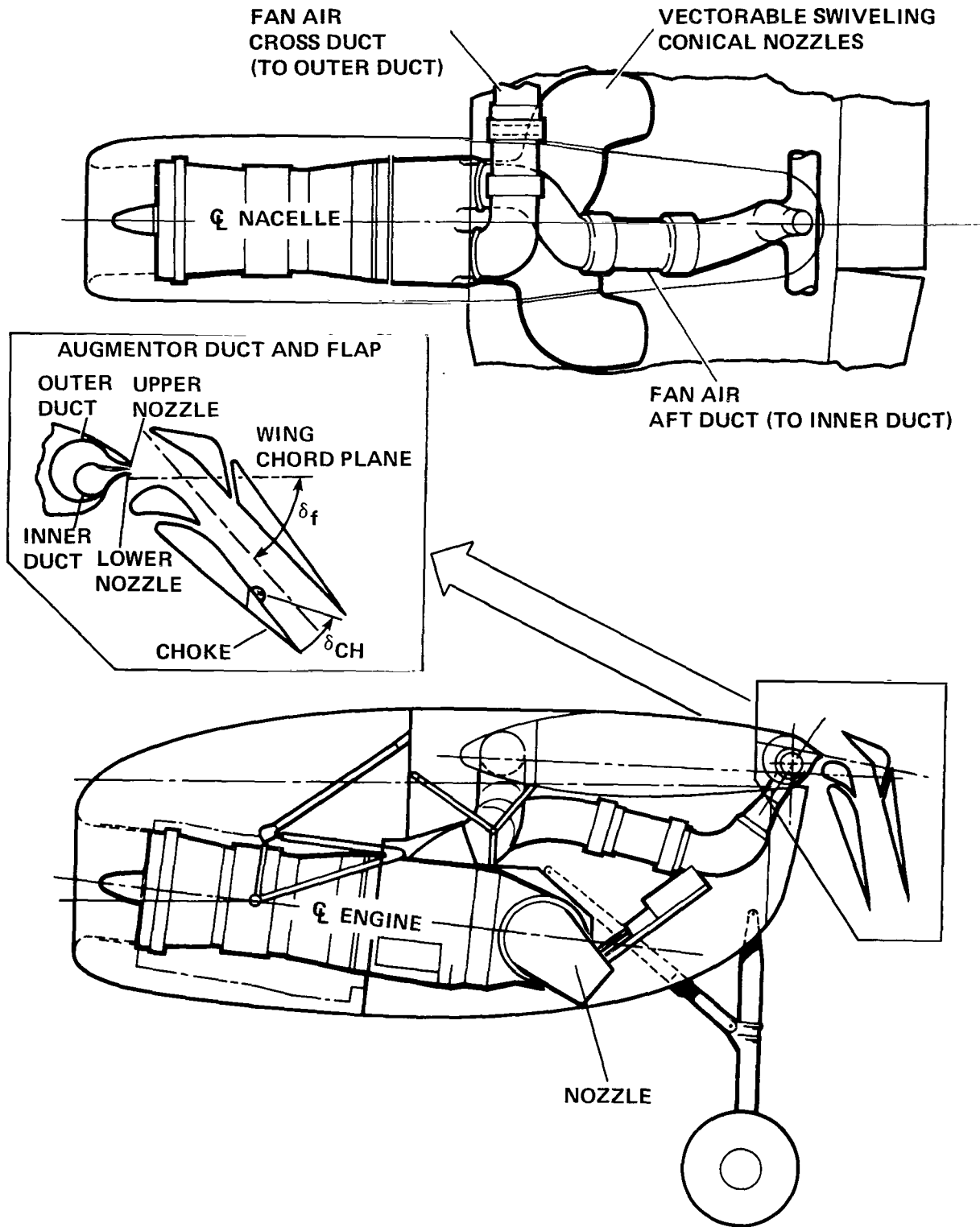
The aircraft's response characteristics for attitude control (pitch, roll, and yaw), longitudinal flightpath control, and airspeed control at the landing approach condition are described in detail in the following discussion.

An indication of the aircraft's longitudinal response is shown in figure 2. The example presented is for a longitudinal control input with the aircraft trimmed for the approach condition. In the short term, the control input commands pitch rate, with a sensitivity of about 0.15°/sec/N



(a) Aircraft three-view.

Figure 1.— Augmentor Wing Research Aircraft.



(b) Augmentor jet flap and propulsion system.

Figure 1.— Concluded.

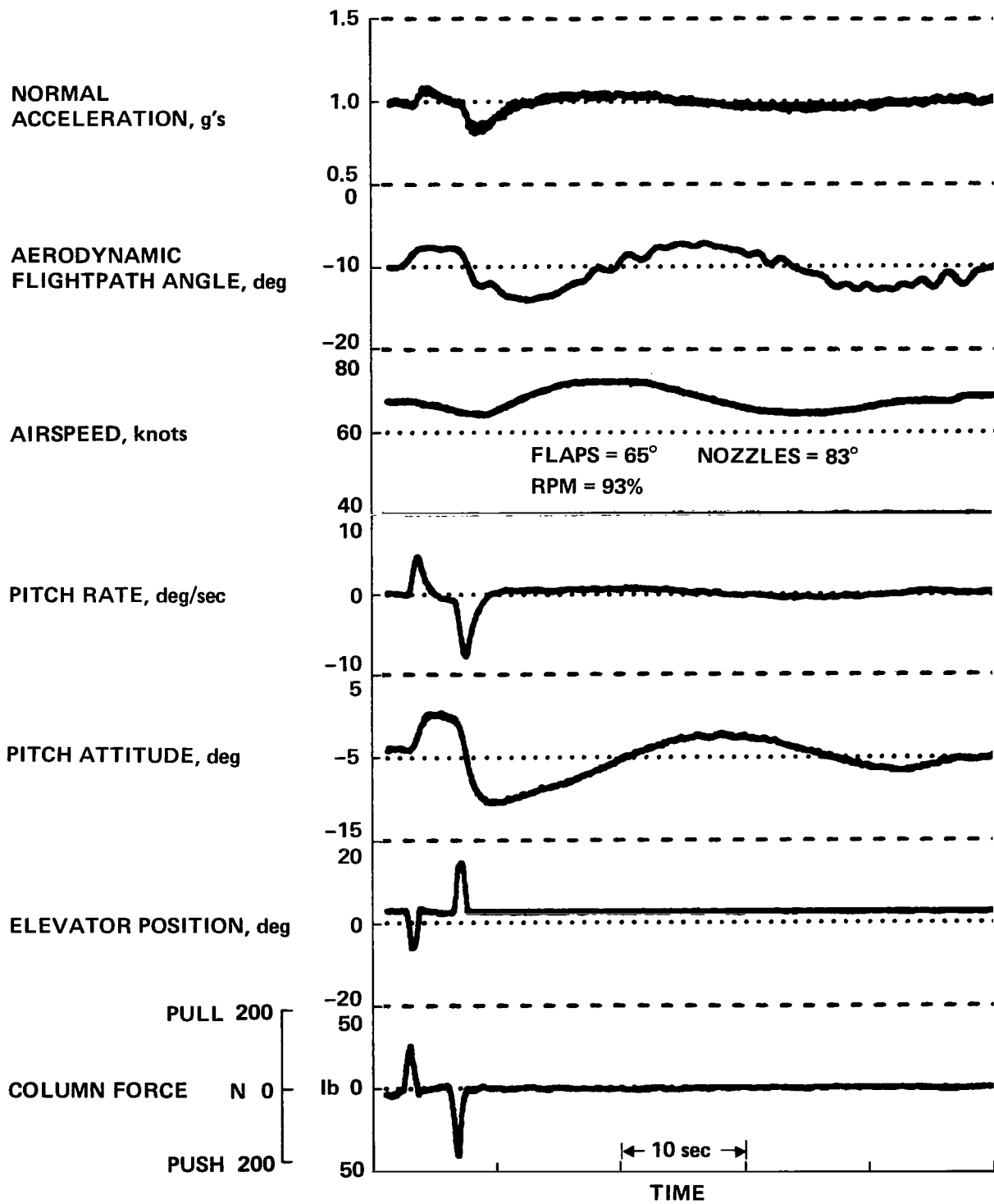
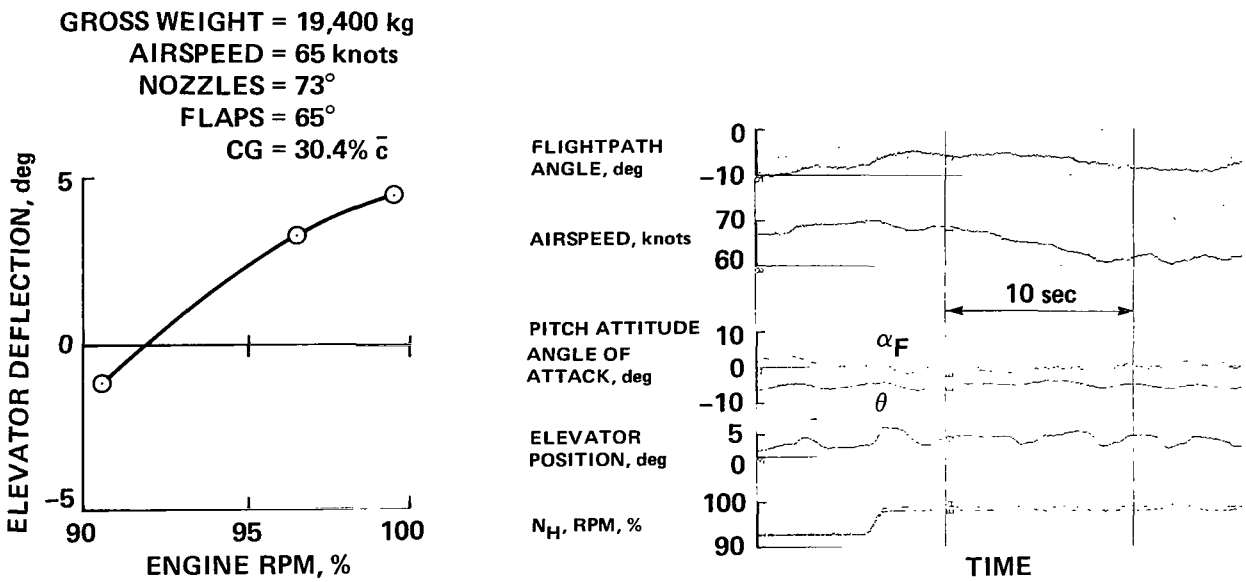


Figure 2.— Longitudinal response to an elevator input.

($0.7^\circ/\text{sec}/\text{lb}$). In the long term, the phugoid is excited to a considerable extent following the change in attitude and, when left unattended, pitch attitude will wander and correspondingly disturb both the flightpath and airspeed.

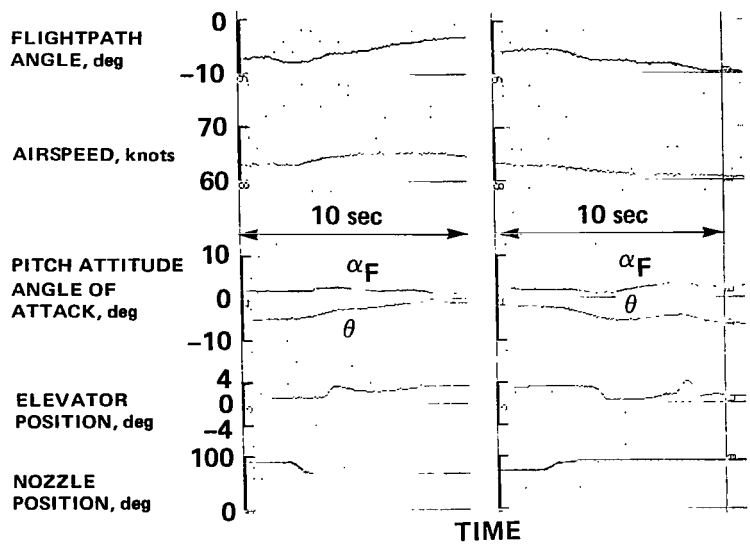
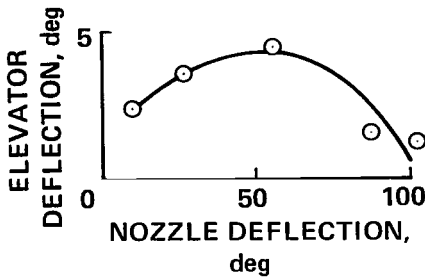
Trim changes and disturbances to flightpath and airspeed that result from variations in thrust or thrust vector angle are shown in figure 3. The variation in elevator deflection required to trim the aircraft for the range of thrust associated with longitudinal path control is not large (fig. 3(a)). As noted in figure 2, however, if pitch attitude is upset, substantial variations in flightpath and airspeed occur that make precision control of longitudinal flightpath difficult. The time history example illustrates the amount of elevator activity required to maintain essentially constant attitude following a step increase in thrust. The amount of deflection needed to trim for a range of nozzle deflection is also not large (fig. 3(b)), but as the time history examples show, the variation in pitch attitude can be significant and can produce correspondingly large variations in flightpath and speed. As a consequence of these characteristics, the pilot must devote considerable attention to attitude control, particularly under IFR conditions, in order to maintain satisfactory glide-slope and speed control.



(a) Trim changes due to thrust.

Figure 3.— Response to thrust and nozzle deflection.

GROSS WEIGHT = 19,400 kg
 AIRSPEED = 65 knots
 RPM = 95%
 FLAPS = 65°
 CG = 30.3% \bar{c}



(b) Trim changes due to nozzles.

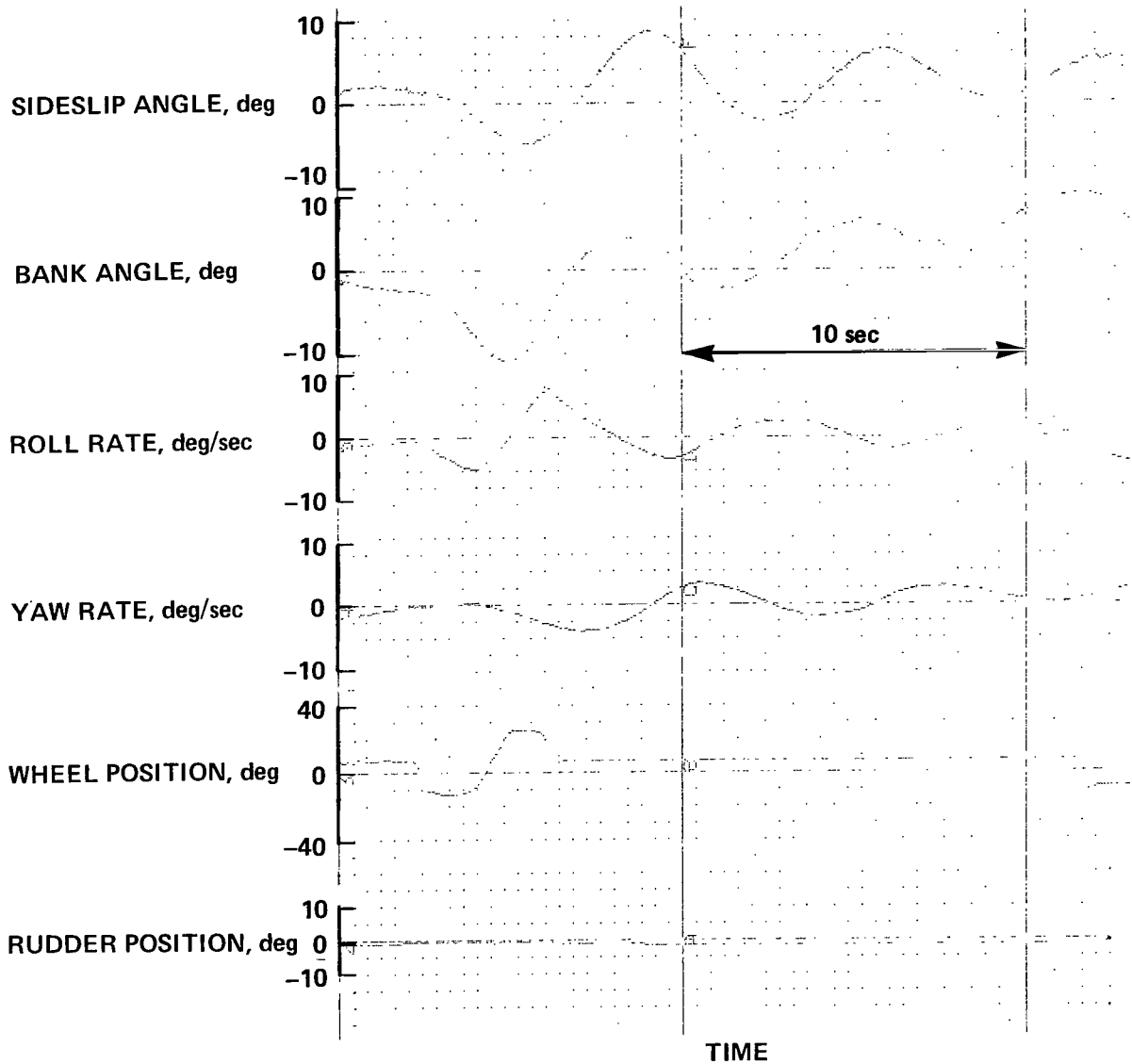
Figure 3.— Concluded.

The basic aircraft's roll and yaw responses to a lateral control input with the aircraft configured for landing approach are shown in figure 4(a). With no inputs from the lateral-directional stability augmentation system, the aircraft exhibits large adverse sideslip, low Dutch-roll damping, low roll damping, and a spiral divergence. These deficiencies combine to make it quite difficult to fly a precision instrument approach and the pilots consider the aircraft to be unacceptable for such operations.

The aircraft was delivered to NASA by Boeing with a lateral-directional stability augmentation system (SAS) that is described in reference 15. The SAS provides spiral-stability augmentation, roll-damping augmentation, lateral-control quickening, turn coordination, and Dutch-roll damping augmentation. With this system engaged, an equivalent of roll-rate command is provided in response to lateral control inputs, and sideslip response is largely suppressed for such maneuvers (fig. 4(b)). When the pilot's lateral control inputs are removed, the aircraft slowly returns to wings-level attitude as a consequence of the augmented spiral stability. Note that for this example the yaw SAS authority was limited to $\pm 5^\circ$ of rudder.

Longitudinal flightpath can be controlled during the approach and landing either by modulating thrust or by deflecting the hot thrust component; however, neither the throttle nor nozzle controls alone are satisfactory for approach or flare control. Since the approach is conducted on the backside of the drag curve, pitch attitude is primarily used for speed control. Sufficient short-term path control in response to attitude exists to provide at least marginally acceptable flare and landing precision. Figure 5 illustrates the aircraft's stabilized path control capability using either throttle or nozzle controls. Throttle control characteristics are shown at the left for the approach flap setting,

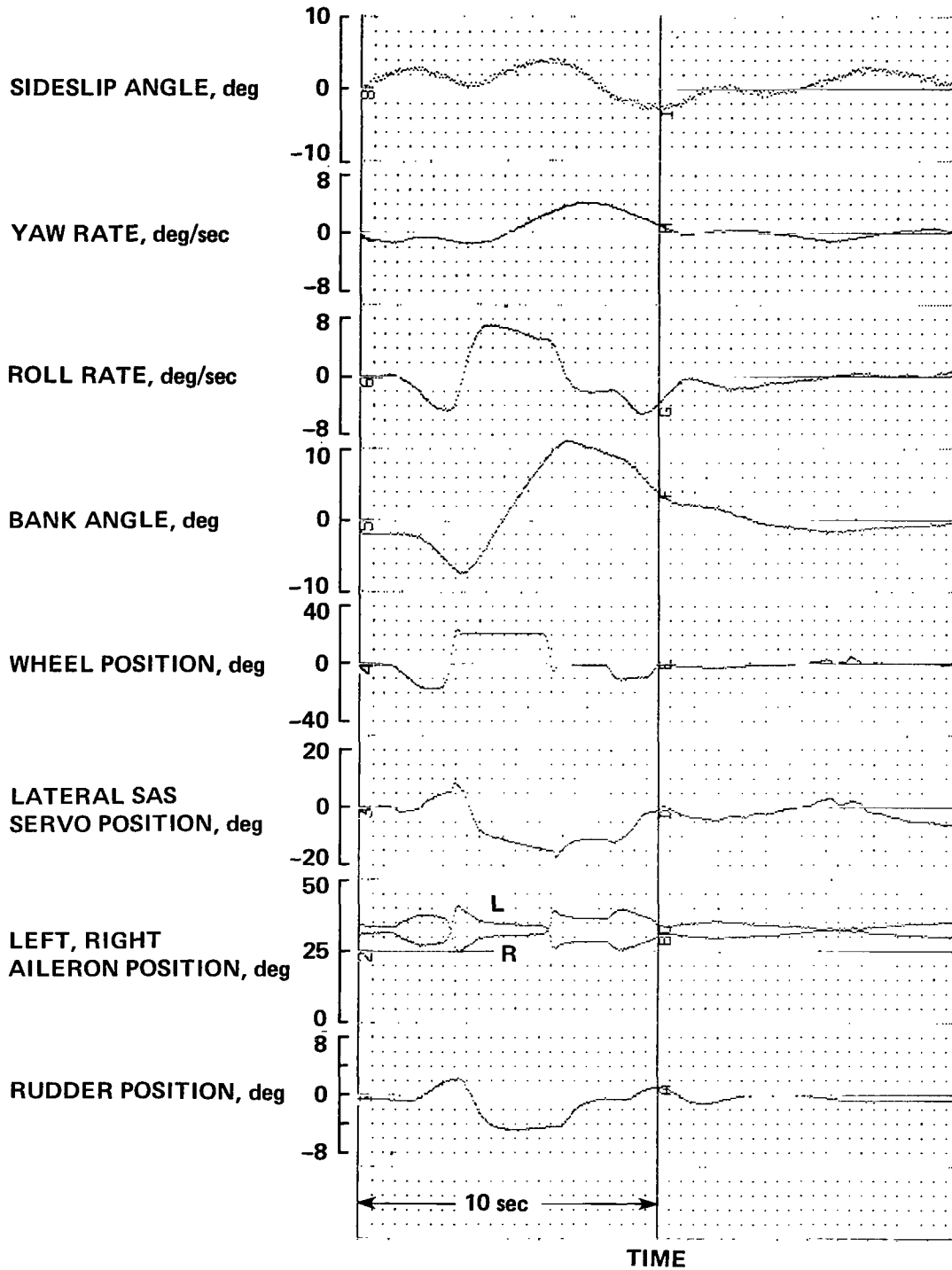
FLAPS = 65° NOZZLES = 87°
AIRSPEED = 61 knots



(a) SAS off.

Figure 4.— Lateral-directional response to a wheel doublet.

FLAPS = 65° NOZZLES = 6°
AIRSPEED = 67 knots



(b) SAS on.

Figure 4.— Concluded.

STANDARD DAY
 ALTITUDE = 300 m (1000 ft)

GROSS WEIGHT = 18,150 kg (40,000 lb)
 FLAPS = 65°

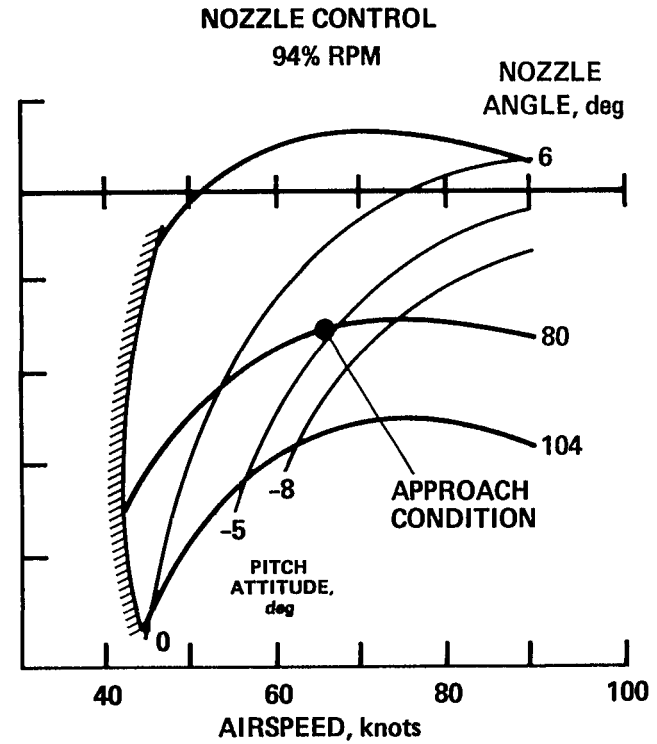
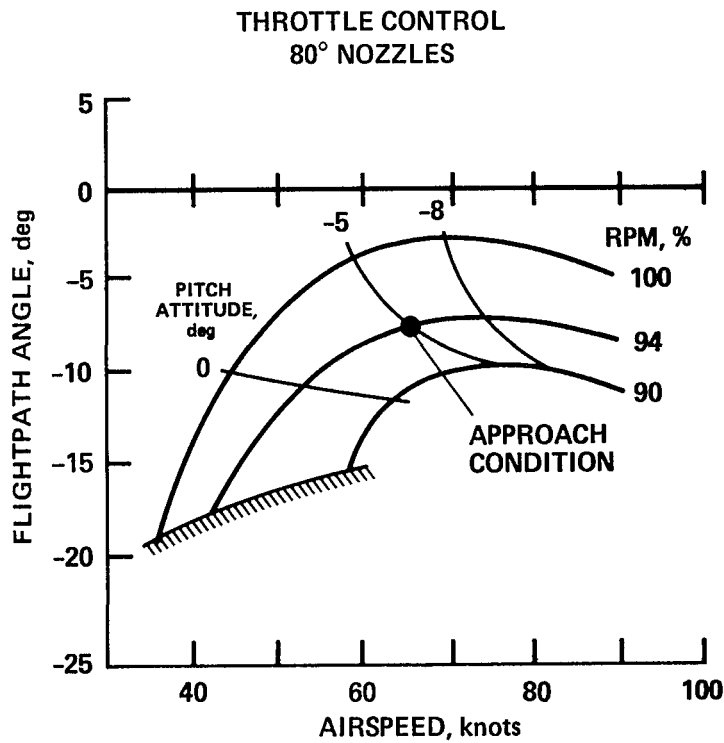


Figure 5.— Performance characteristics for the approach configuration.

a nominal approach thrust vector angle of 80° , and for thrust levels corresponding to engine speeds from 90% rpm to a maximum setting of 100%. A typical approach would be conducted on a 7.5° glide slope at a speed of 65 knots. At the approach speed, the aircraft is capable of achieving flightpath angles from only -4° to -11° for this range of thrust settings. If pitch attitude is kept constant by the pilot or by an attitude stabilization system, this path control capability is reduced to a range from -4.8° to -9.9° as a consequence of coupling between flightpath and airspeed response ($\Delta u_{SS}/\Delta \gamma_{SS} = -2.9$ knot/deg) and of operation on the backside of the drag curve. The steady flightpath-speed relationship at constant thrust for the backside condition is $d\gamma/du = 0.15^\circ/\text{knot}$ and it degrades climb and descent performance when speed is allowed to vary about the approach reference.

Flightpath control capability, which can be achieved by deflecting the nozzles at a nominal approach thrust setting of 94% rpm, is illustrated at the right in figure 5. The flightpath envelope is expanded over that available using thrust control, with the capability of achieving path angles of 2.7° to -13.3° for the maximum range of nozzle angles from 6° to 104° . The relationship of path and speed response to the nozzle control at constant attitude is similar to the response of a conventional aircraft to the throttle control, in that positive path increments are accompanied by increased airspeed, and vice versa. This behavior is expected since the incremental change in force due to nozzle deflection about the nominal nozzle position for the approach condition is nearly aligned with the aircraft's longitudinal axis.

The transient response of flightpath and airspeed to thrust for constant attitude is shown in the time histories of figure 6. Flightpath initially responds quickly to the change in throttle input, and throttle sensitivity is satisfactory ($Z_{\delta_T} = -0.04$ g/cm, or -0.1 g/in.). The equivalent first-order thrust time constant is approximately 0.8 sec; however, the initial path response washes out to a steady-state value that is approximately one-half that observed in the short term ($\Delta \gamma_{max}/\Delta \gamma_{SS} = 2.1$). Airspeed response is decidedly unconventional in that speed decreases following an increase in thrust and is in turn reflected in the constant attitude path-speed coupling noted previously.

Time histories of path and speed response to the nozzle control at constant attitude are also presented in figure 6 for comparison with thrust control characteristics. The initial path response to nozzle deflection is sluggish compared to the response to a thrust increment, and the response may not be sufficient for tight glide-slope tracking in turbulence. If quicker path response is desired, the pilot must initiate the correction with pitch attitude and follow-up with the nozzle control to sustain the long-term correction. Coupling between flightpath and airspeed at constant attitude is conventional, as was previously noted. Consequently, pitch control must be coordinated with the nozzle control if the pilot desires to maintain airspeed.

Flightpath and airspeed responses to a step change in pitch attitude are also shown in figure 6 for constant throttle and nozzle settings. The initial path response follows the change in attitude, although to a significantly lesser degree ($\Delta \gamma_{max}/\Delta \theta_{SS} = 0.55$). The incremental path change eventually reverses direction, however, and establishes a steeper gradient, as indicated by the steady-state performance data of figure 5. Airspeed response is conventional and bears a relationship to pitch attitude similar to that of conventional jet transports ($\Delta u_{SS}/\Delta \theta_{SS} = -2.5$ knots/deg).

STANDARD DAY
ALTITUDE = 300 m (1000 ft)

GROSS WEIGHT = 18,150 kg (40,000 lb)
FLAPS = 65°

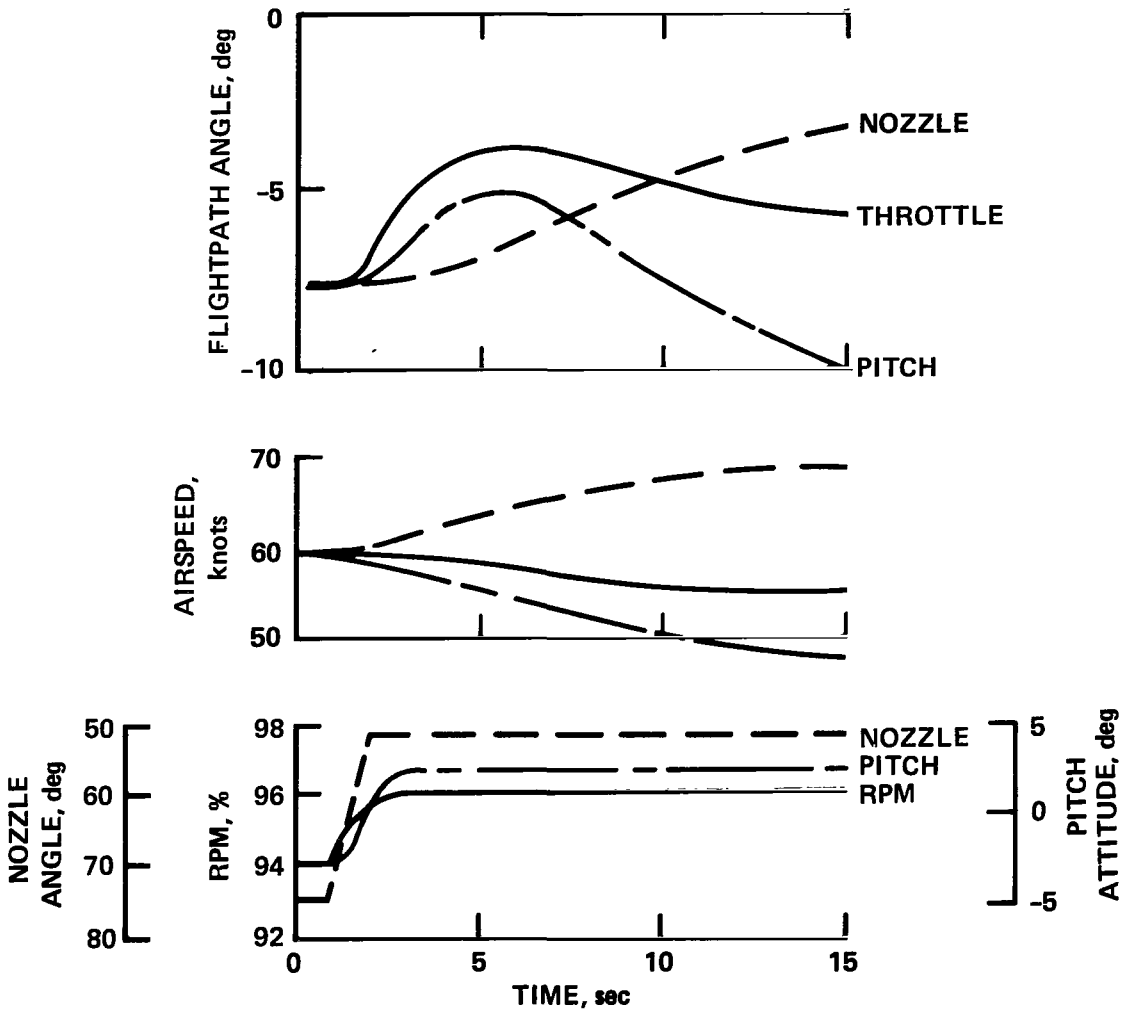


Figure 6.— Longitudinal dynamic response to pitch, throttle, and nozzle controls for the approach configuration.

These response characteristics of flightpath and airspeed to the throttle and nozzle controls dictate that the throttles be used for precise glide-slope tracking and that the nozzles be used to augment thrust control for gross path corrections. Due to the amount of flightpath overshoot and path-speed coupling associated with thrust control, it is difficult for the pilot to anticipate the amount of thrust required to initiate and stabilize a path correction. As a consequence, he must devote considerable attention to path and speed control. Attitude control may be used to reduce path-speed coupling by coordinating attitude changes with the thrust control to minimize the speed excursions. However, this requirement for continuous control in the pitch axis increases the pilot's control workload for glide-slope tracking. Furthermore, the control technique is unfamiliar in that nosedown attitude changes are required to maintain speed while reducing descent rate, and vice versa.

In summary, the coordinated use of three controls is necessary for precise tracking and to establish the proper flare conditions; as a result, pilot workload is unsatisfactorily high. As a consequence, it is desirable to improve approach path control by (1) eliminating the path-speed coupling, (2) reducing the number of controls required for path control, (3) quickening path response for glide-slope tracking and flare, (4) desensitizing response to winds and turbulence, and (5) providing better tracking commands to the pilot.

STABILIZATION AND COMMAND AUGMENTATION SYSTEM AND DISPLAY CONCEPTS

The aircraft's primary flight controls (described previously) can be driven through servos commanded by an experimental digital avionics system (STOLAND) that is installed in the aircraft. This system, developed for Ames Research Center by Sperry Flight Systems, is described in reference 16. A block diagram of the system is presented in figure 7. The major system components are a Sperry 1819A general-purpose digital computer; a data adapter; and the aircraft's sensors, controls, displays, and navigation aids. The controls used for longitudinal path tracking are (1) the elevator for pitch attitude stabilization and control, and (2) the inboard augmentor chokes, throttles, and nozzles for vertical path and airspeed control. The controls used for lateral path tracking and directional control augmentation are the blended lateral controls and the rudder. The pitch stabilization system is driven by an electrohydraulic series servo actuator limited to 40% of the total elevator deflection. The inboard augmentor flap chokes have full mechanical authority (65% closure of the augmentor flap) and are also driven by electrohydraulic servos. In the approach configuration, their authority corresponds to ± 0.12 g. The throttles and nozzle controllers of the Spey engines are driven by electromechanical parallel servos which may be overridden, if desired, by the pilot. Longitudinal acceleration effectiveness of the nozzles in the approach configuration is approximately 0.0037 g/deg for nozzle deflection between 50° and 104° . The roll and yaw stabilization systems are driven by electrohydraulic series servos that have 27% (roll) and 40% (yaw) of full wheel and rudder control authority. Commands to these controls appropriate for the various SCAS modes of interest are generated through suitable combinations of sensor information processed when necessary by complementary filters to retain high-frequency content while removing undesirable sensor noise or atmospheric gust disturbances. The elements of these control commands are shown in figure 8. Control surface and SCAS authorities are noted in table 1. The computer input-output frame time is 50 msec.

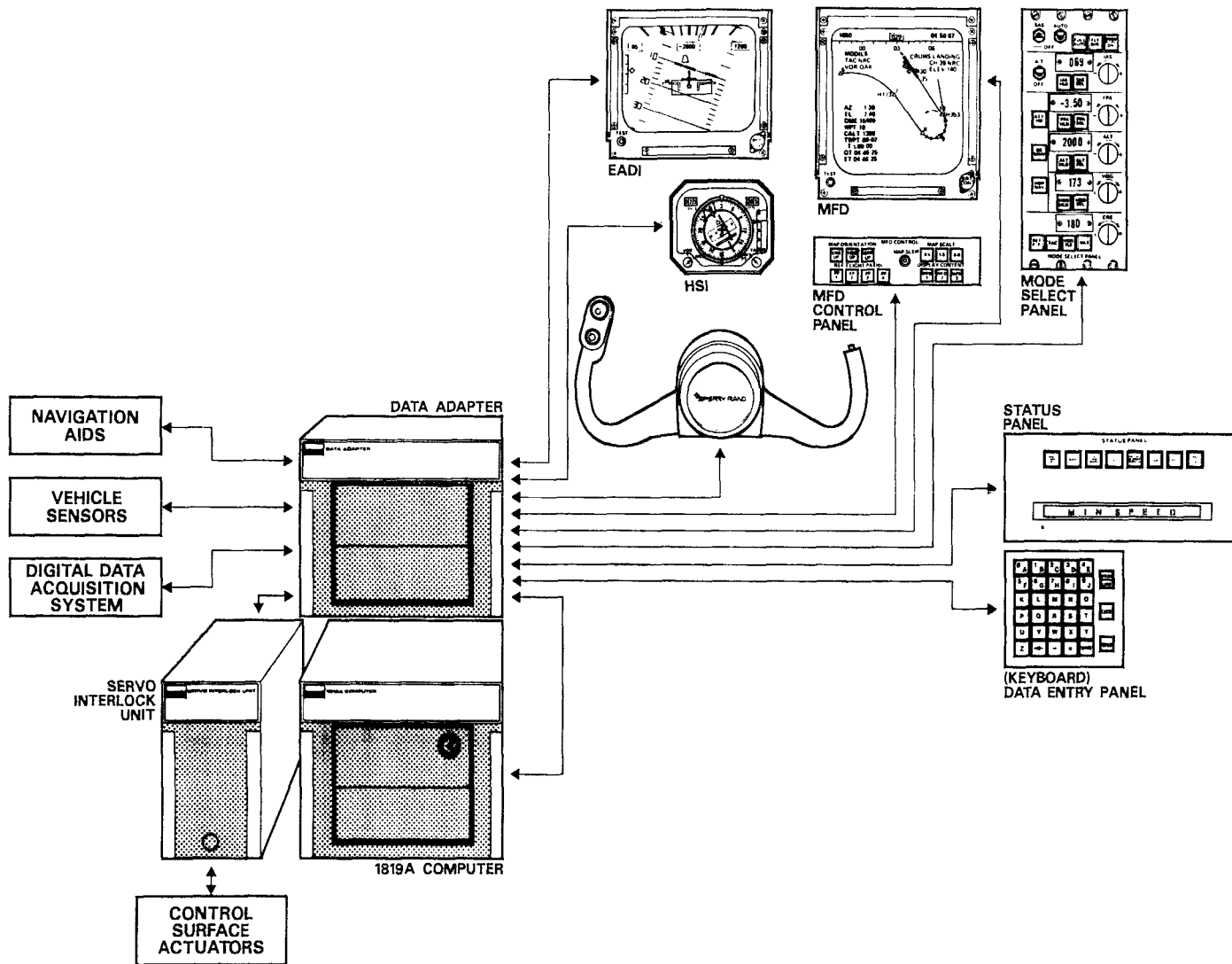


Figure 7.— STOLAND system block diagram.

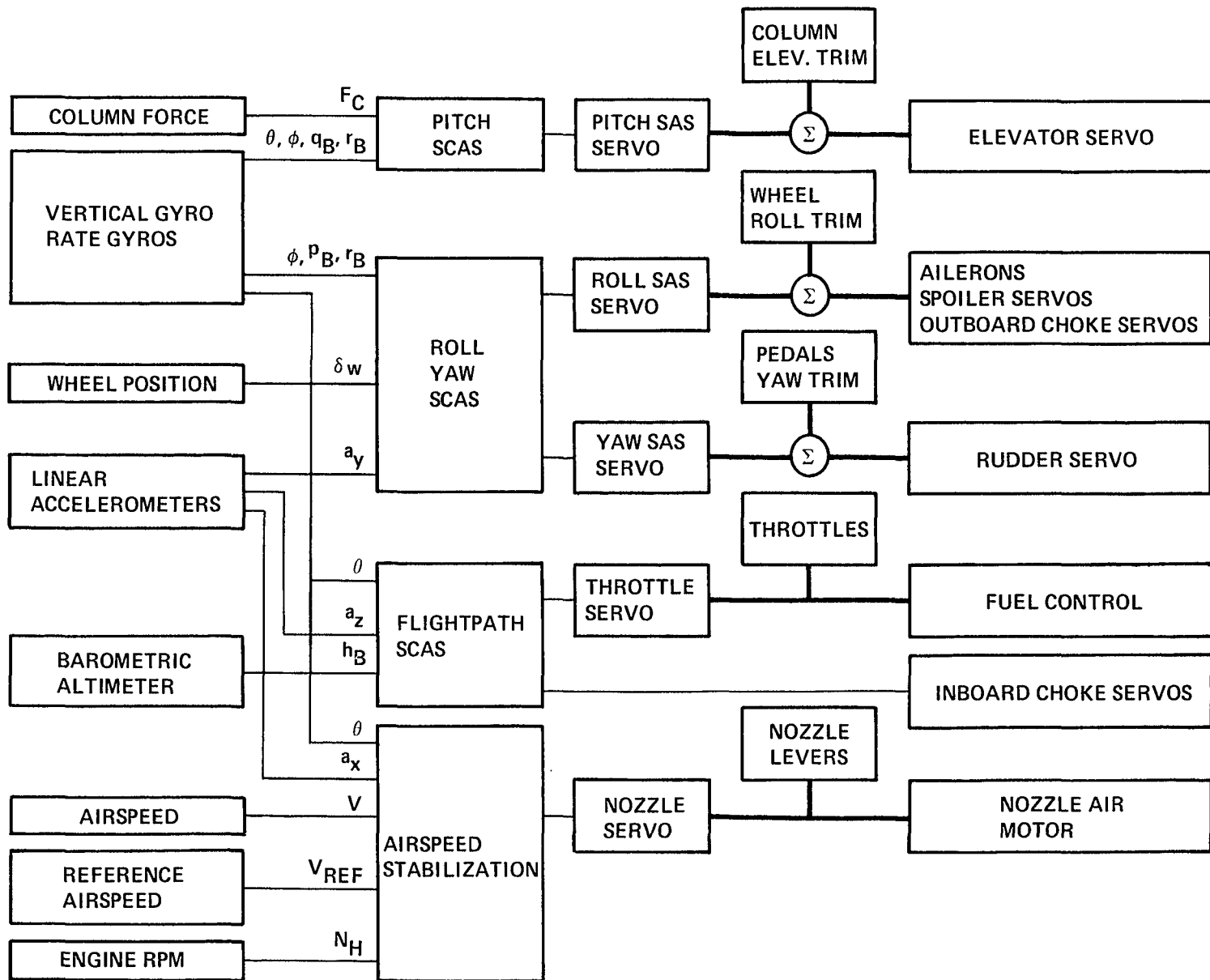


Figure 8.— Control system block diagram.

TABLE 1.— CONTROL DEFLECTION AND ACTUATION RATES

Control	Deflection	Rate Limit
Elevator position servo	+24°, -15° at 65 knots	50°/sec
Pitch SAS servo	+7.9°, -7.5°	33°/sec
Ailerons	±19° at 65° flaps	50°/sec
Spoiler servo	0–48°	120°/sec
Outboard choke servo	0–55% flap exit area closure at 72° flaps	90%/sec
Roll SAS servo	±20° equivalent wheel deflection	50°/sec
Rudder servo	±25°	50°/sec
Yaw SAS servo	±10°	25°/sec
Throttle servo	90–98% rpm	4.2%/sec
Inboard choke servo	0–65% flap exit area closure at 65° flaps	100%/sec
Nozzle air motor	6–104°	90°/sec
Nozzle servo	6–104°	18.4°/sec
Flap actuator	5.6–72°	4°/sec

The primary instrument displays and system mode controls available to the pilot are shown in figure 9. An electronic attitude director indicator (EADI) presents pitch and roll attitude, aerodynamic flightpath, and glide-slope and localizer deviation, as well as digital readouts of calibrated airspeed, vertical speed, and radar altitude. Flight director command bars can be called up on the display when desired. They consist of centrally-located pitch and roll command bars and a throttle command bar positioned on the left wing of the aircraft symbol. An electromechanical horizontal situation indicator (HSI) presents aircraft heading and bearing, related to the navigational aid, and glide-slope and localizer deviation. A mode-select panel provides switches for engaging SCAS modes and the flight director. The keyboard and status display on the center console permits manual entry and readout of instructions to the digital computer.

Attitude Control

Pitch SCAS— To improve pitch attitude control for approach path control and to provide attitude stabilization for unattended operation, pitch-attitude command and stabilization systems were devised for evaluation on the aircraft. The block diagram in figure 10 describes the pitch SCAS concepts. Both pitch-attitude command and pitch rate-command-attitude-hold-systems were evaluated. Attitude stabilization is accomplished through attitude feedback with pitch-rate feedback used to provide suitable closed-loop stability. Attitude- or rate-commands are generated in the feed-forward paths in response to column force, with a pitch trim input provided from the pilot's trim button for the attitude-command system. Gain scheduling, as a function of dynamic pressure, maintains a relatively constant total loop gain over the aircraft's flight envelope; gain scheduling of the column force command, as an inverse function of airspeed, maintains a relatively constant

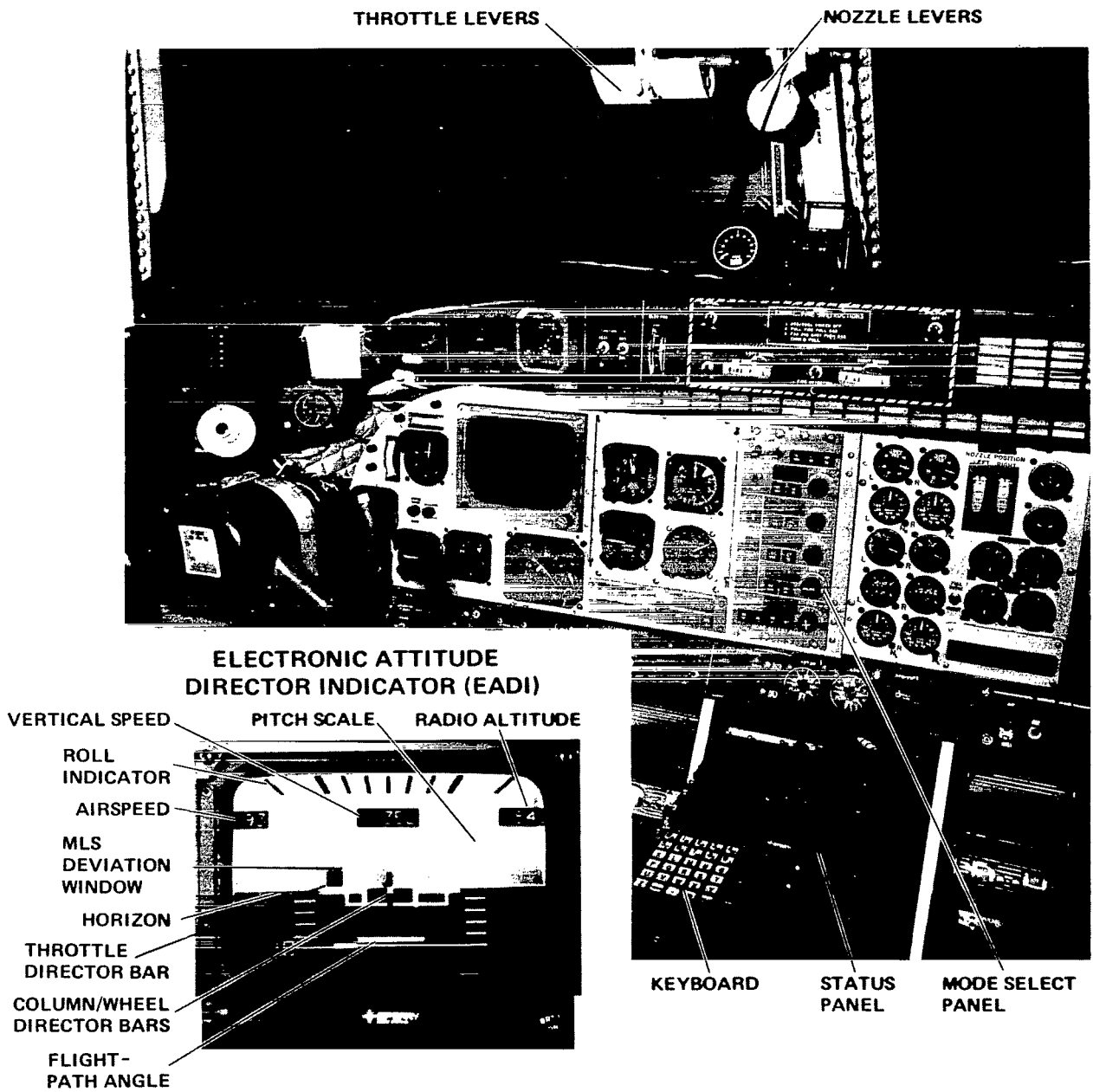
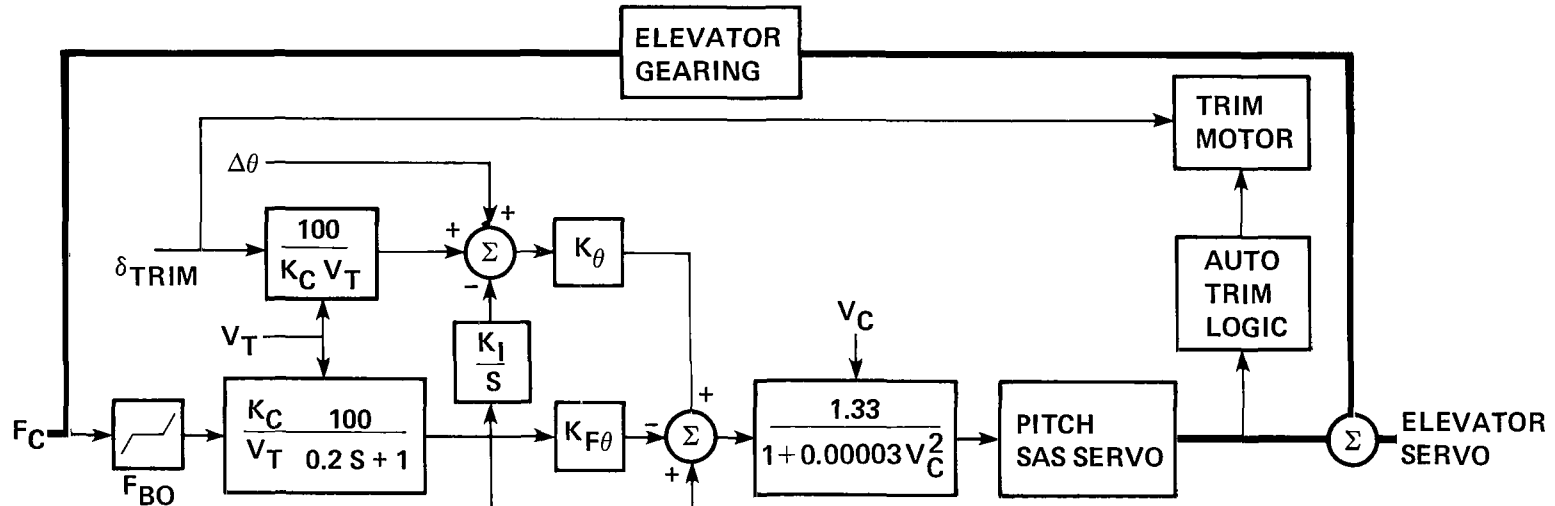


Figure 9.— Flight control and instrument arrangement.



BREAKOUT FORCE

- $F_{BO} = \pm 8.9 \text{ N (2.0 lb)}$

AUTO TRIM

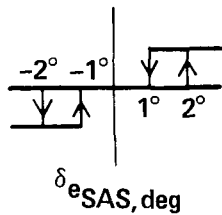
- THRESHOLD (THROUGH 0.5 sec LAG)
- INHIBIT WHEN $F_C > F_{BO}$
- TRIM RATE = $2^\circ/\text{sec}$

MANUAL TRIM

- DISENGAGE WHEN RCAH SCAS ENGAGED

INTEGRATOR GAIN

$$K_I = \begin{cases} 1.0 & \text{RATE COMMAND} \\ 0 & \text{ATTITUDE COMMAND} \end{cases}$$



ELEVATOR GEARING (0 TO 65 knots)

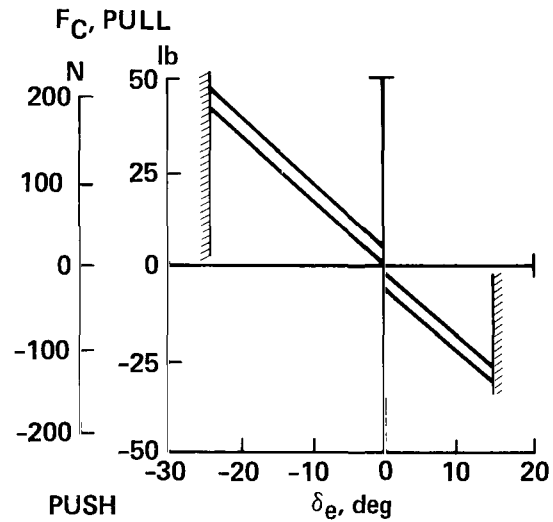


Figure 10.— Pitch SCAS block diagram.

relationship of column force to normal load factor over the envelope. An automatic trim followup on the SCAS actuator acts to reduce long-term trim demands on the SCAS.

The attitude feedback gain K_θ determines how stiff the aircraft is in pitch – in other words, how quickly the aircraft stabilizes following the pilot’s command or a disturbance – and the amount of attitude change associated with pitch disturbances. Pitch-rate feedback is utilized to achieve good closed-loop stability for the degree of attitude stabilization selected. From the viewpoint of the control system designer, the choice of these two feedback gains determines the effective bandwidth of the attitude control and its gain and phase margin. The Bode plot of figure 11 illustrates the pitch-attitude frequency response to the elevator and the contribution of attitude and rate feedback for the approach and cruise flight condition. The proportion of rate to attitude feedback K_q/K_θ , which establishes the break point at $1/T_{L\theta}$, was chosen to achieve essentially rate-command (K/s) characteristics over a broad frequency range for a bandwidth up to 4 to 5 rad/sec at the cruise condition. For the examples shown, a fixed value of $K_q/K_\theta = 0.4$ provides a reasonable approximation of these characteristics over the aircraft’s envelope. Attitude feedback gains from 1 to $4^\circ/\text{deg}$ can then be accommodated to make bandwidth adjustments up to 2 rad/sec at the

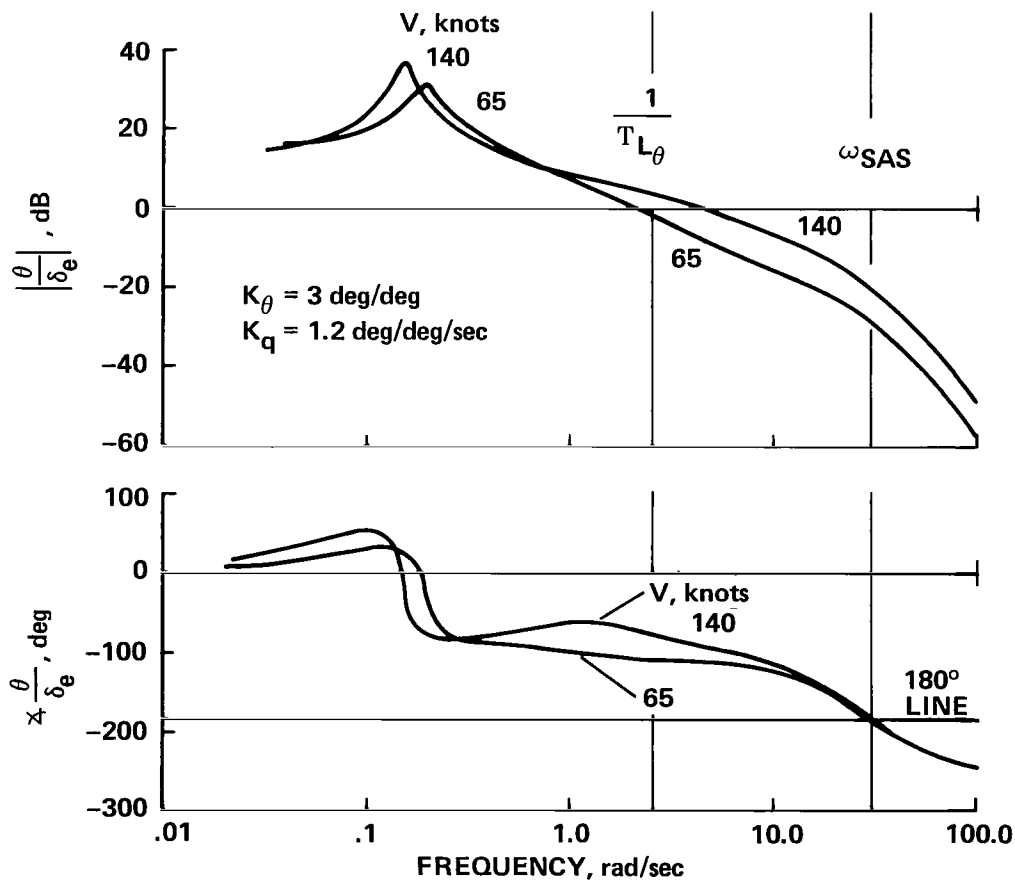


Figure 11.— Pitch attitude control frequency response.



approach condition and up to 5 rad/sec in cruise while maintaining adequate phase margins for closed-loop stability.

For the attitude-command system, the force scaling gain K_c and the feed-forward gain $K_{F\theta}$ can be used to adjust the initial response sensitivity; the ratio of these two gains to the attitude feedback gain will determine the attitude-command sensitivity θ/F_c . The integral feed-forward gain K_I is set to zero for this system. For the rate-command system, the force scaling gain K_c determines the rate-command sensitivity $\dot{\theta}/F_c$. Overshoot in pitch response, when the pilot removes force from the column to stabilize at a new attitude, can be adjusted with the feed-forward gain $K_{F\theta}$.

Configurations for the attitude-command system and for the rate-command-attitude-hold system were established for the initial flight evaluations. Opportunities were allowed to tailor (1) the degree of attitude stiffness with K_θ , (2) the command sensitivities of either system (θ/F_c or $\dot{\theta}/F_c$) using K_c , and (3) the attitude overshoot characteristics for the rate-command system through adjustments of $K_{F\theta}$. Examples of the response of the two systems to the pilot's column force inputs are shown in figures 12 and 13 for the landing approach condition. For the attitude-command system (fig. 12), the respective feedback and feed-forward gains are $K_\theta = 2.0^\circ/\text{deg}$, $K_q/K_\theta = 1.0$, $K_c = 0.17^\circ/\text{N}$ ($0.75^\circ/\text{lb}$) and $K_{F\theta} = 2.0^\circ/\text{deg}$. For the rate-command-attitude-hold system (fig. 13), the corresponding gains are $K_\theta = 3.0^\circ/\text{deg}$, $K_q/K_\theta = 0.4$, $K_c = 0.17^\circ/\text{N}$, and $K_{F\theta} = 1.1^\circ/\text{deg}$.

Roll and yaw SCAS— Lateral-directional stabilization and command augmentation are provided by a SCAS concept that includes roll rate-command-bank-angle hold in the lateral axis in combination with Dutch-roll mode augmentation and sideslip suppression in the yaw axis. Block diagrams of this SCAS concept are shown in figures 14 and 15. For the roll SCAS (fig. 14) bank-angle stabilization is accomplished through the roll-attitude feedback, and roll-rate feedback is used to augment closed-loop stability. Roll-rate command is generated in the integral feed-forward path in response to wheel position. The use of a wheel force command input was rejected since the lateral control feel system force detent was insufficient to isolate the pilot's control wheel from force feedback from the lateral SAS actuator. The yaw SCAS was developed by Sperry as part of the original STOLAND system design; it is shown in figure 15. In this system, lateral acceleration feedback increases the frequency of the Dutch-roll mode and feedback of washed-out yaw rate and bank angle increases the damping ratio of this mode. Turn coordination is provided by bank-angle feedback in the steady state. Yaw SAS authority is $\pm 10^\circ$ of rudder for this system.

Design considerations for the roll SCAS are similar to those for pitch. The attitude feedback gain K_ϕ determines how quickly the aircraft stabilizes in roll and the amount of bank-angle change associated with roll-axis disturbances. Roll-rate feedback is selected in proportion to the amount of roll-attitude feedback to maintain acceptable gain and phase margins for the bandwidth of the roll axis. The Bode plot of figure 16 shows the roll attitude to lateral control transfer function and the contribution of the attitude and rate feedbacks for the landing approach condition. Similar to the pitch-attitude system, the proportion of rate to attitude feedback K_p/K_ϕ was chosen to achieve rate-command characteristics over the frequency range of the pilot's control. For the examples shown, a fixed value of $T_{L\phi} = K_p/K_\phi = 1.2$ produces this relationship over the flight envelope. A roll-attitude feedback gain of the order of $3.3^\circ/\text{deg}$ provides a roll-control bandwidth of about 2.5 rad/sec.

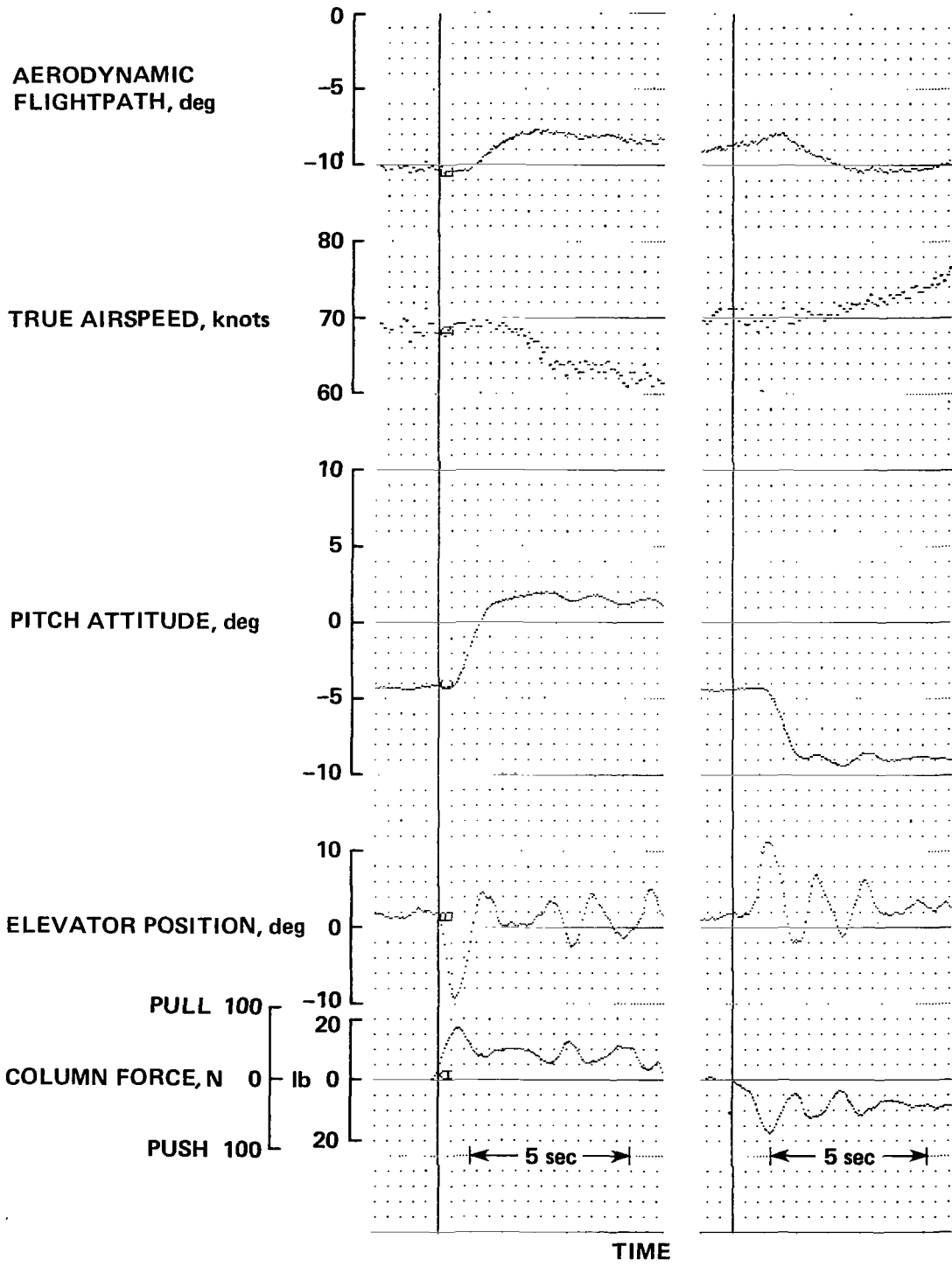


Figure 12.— Longitudinal response to attitude control — attitude-command system on.

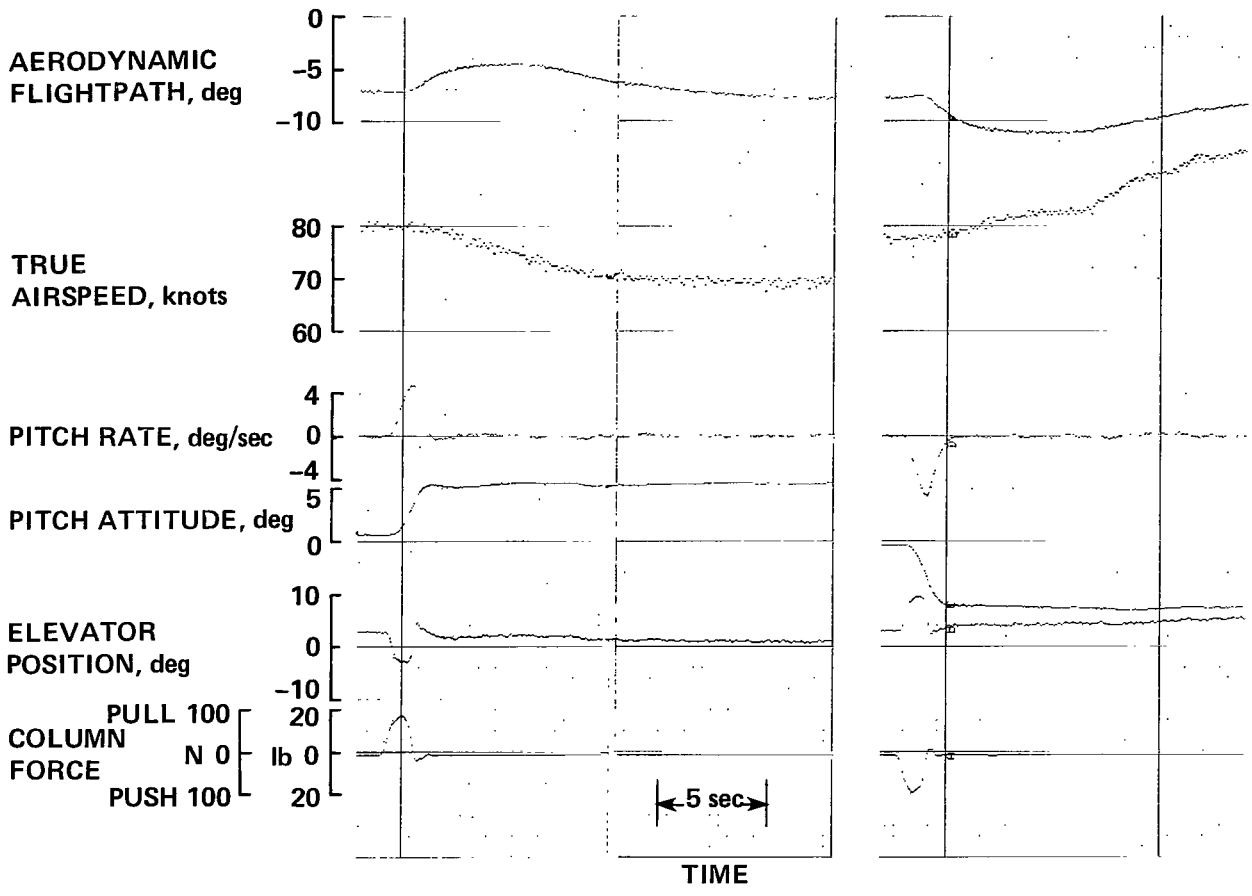


Figure 13.— Longitudinal response to attitude control — rate-command-attitude-hold system on.

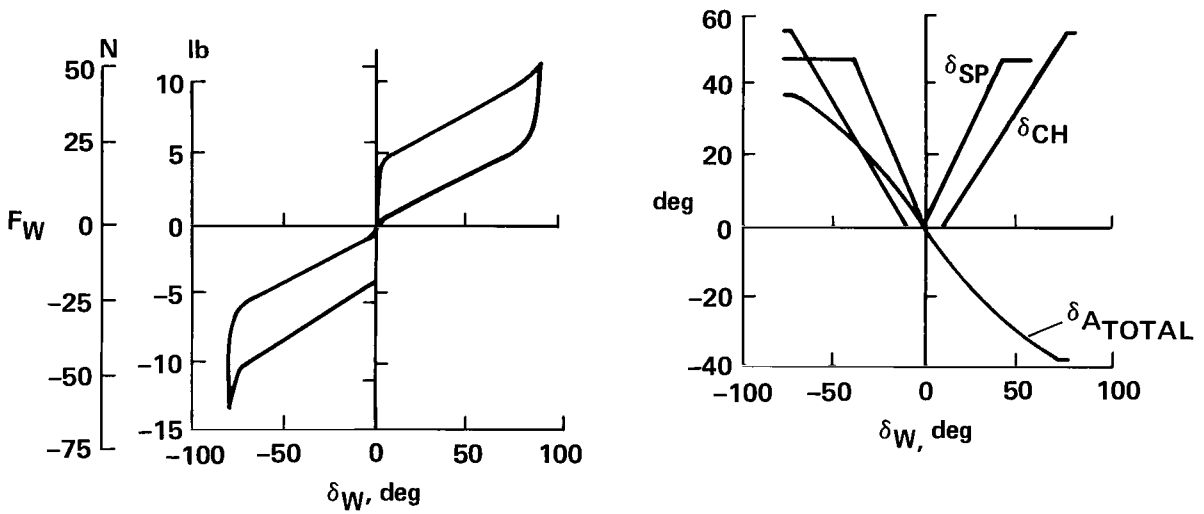
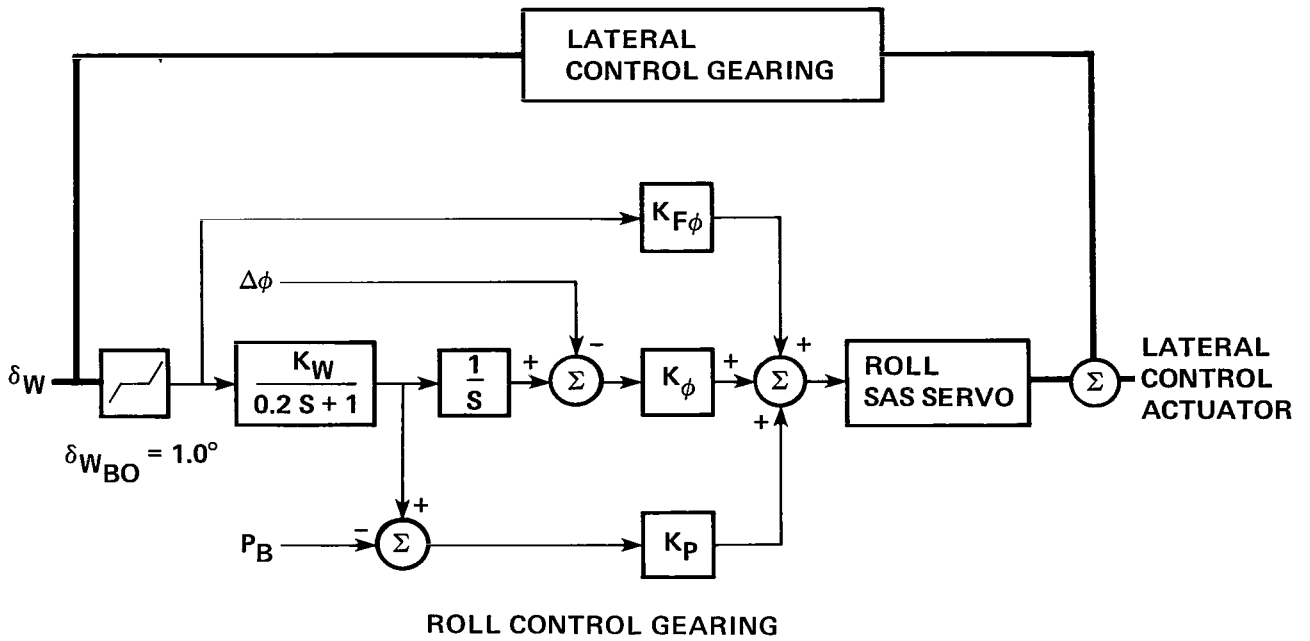
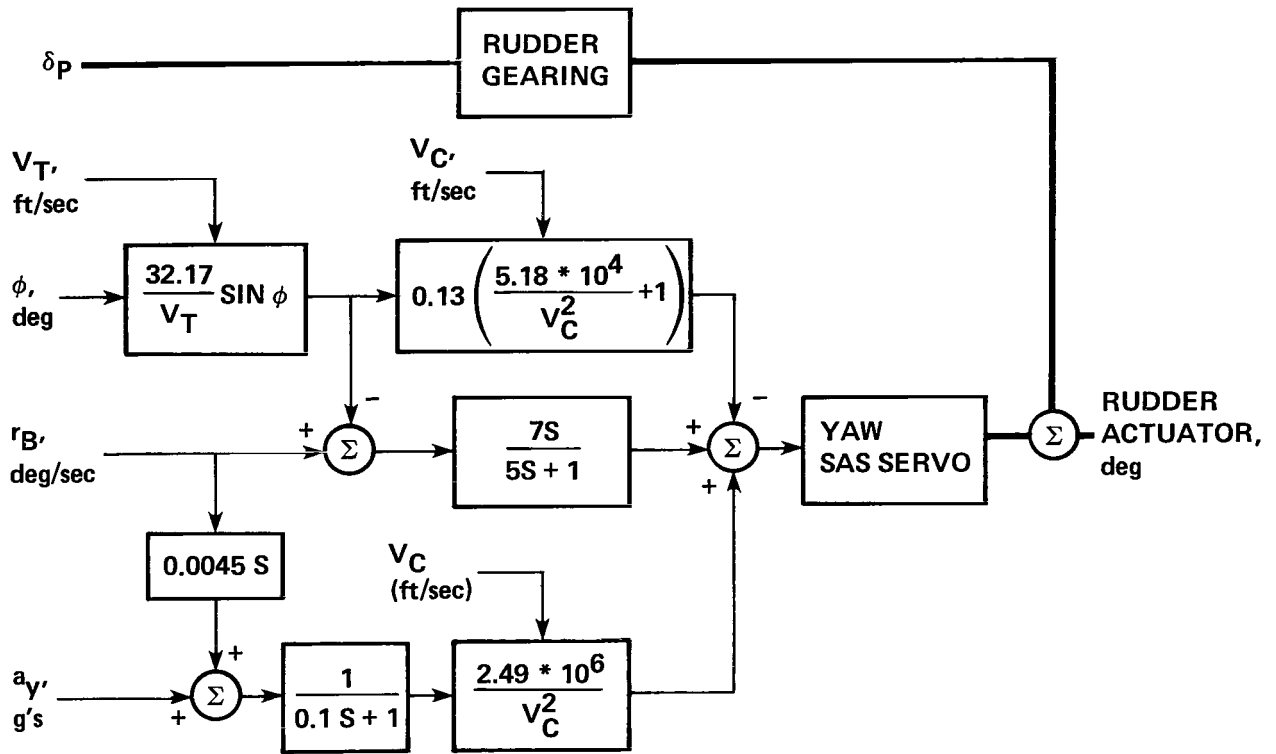


Figure 14.— Roll SCAS block diagram.



RUDDER GEARING

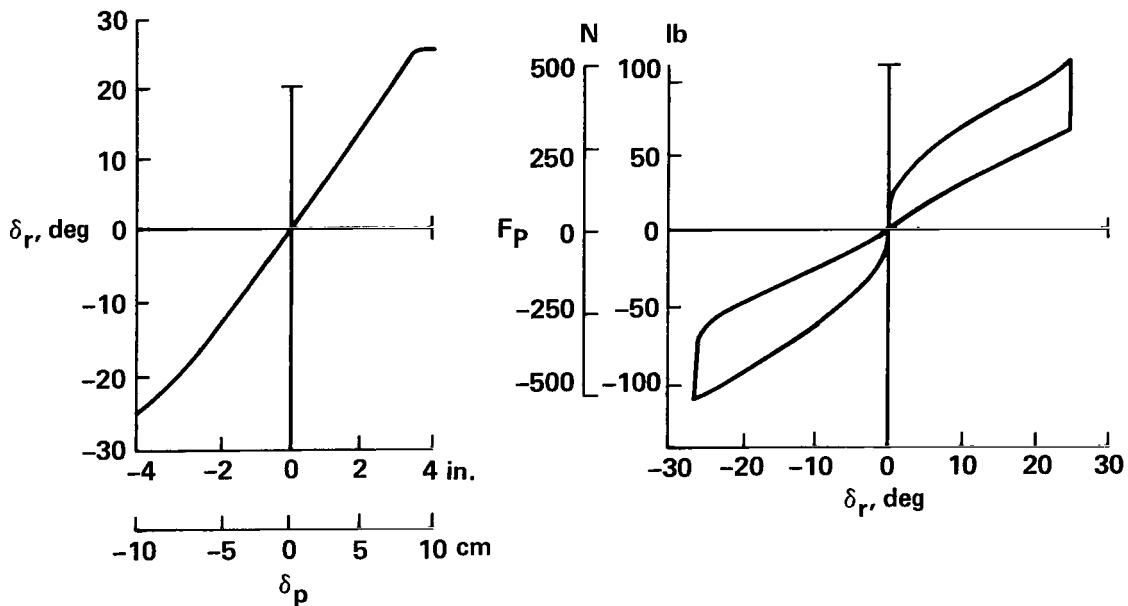


Figure 15.— Yaw SAS block diagram.

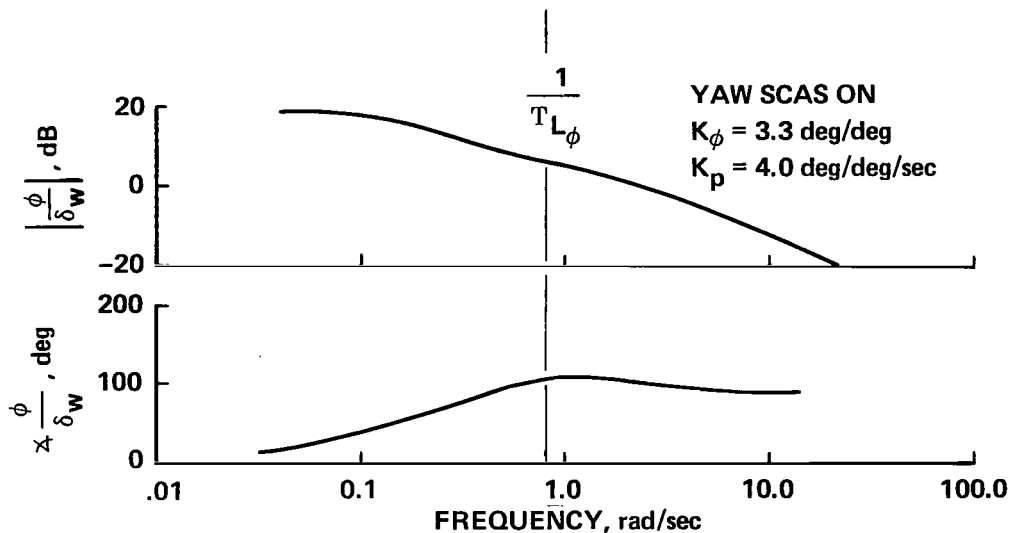


Figure 16.— Roll attitude control frequency response.

The position command gain K_w determines the rate-command sensitivity $\dot{\phi}/\delta_w$. Overshoot in the bank-angle response to a wheel input can be adjusted with the proportional feed-forward gain $K_{F\phi}$.

The configuration for the roll rate-command-bank-angle hold system established for the initial flight evaluations included the feedback and feed-forward gains $K_\phi = 3.3^\circ/\text{deg}$, $K_p/K_\phi = 1.2$, $K_w = 1.5^\circ/\text{deg}$, and $K_{F\phi} = -3.8^\circ/\text{deg}$. Yaw SCAS gains are shown in figure 15. An example of the response of the aircraft to a control wheel input when the roll and yaw SCAS is engaged is shown in figure 17. Roll-rate response follows the pilot's wheel command and bank angle is stabilized without overshoot. Directional oscillations are nonexistent and sideslip disturbances are well suppressed ($\Delta\beta/\Delta\phi \leq 0.1$). Opportunities were provided in the flight program to adjust (1) the attitude stiffness K_ϕ , (2) the command sensitivity ($\dot{\phi}/\delta_w$) using K_w , and (3) bank-angle overshoot through $K_{F\phi}$. Yaw SCAS gains, as established by Sperry, were not altered during the flight evaluations.

Flightpath Control

Throttle-nozzle interconnect— A simple means for reducing the flightpath-airspeed coupling and for improving closed-loop flightpath control for the basic aircraft can be provided by interconnecting the aircraft's throttle and nozzle controls. This interconnect is mechanized by a constant-gain linear command from engine to the nozzles (fig. 8). The sense of this interconnect is to reduce the hot thrust deflection for an increase in thrust and vice versa. An illustration of the influence of this interconnect on the aircraft's performance envelope is presented in figure 18 for a value of the interconnect gain $K_{NT} = -5^\circ/\% \text{ rpm}$; as shown, path-speed coupling is virtually eliminated at constant attitude for the approach condition. The contours on the γ - V diagram are for constant throttle and nozzle angles. In comparison to the performance envelope of the basic aircraft shown previously (fig. 5) this control configuration provides a substantial increase in path control capability. A positive climb angle of 1.7° can now be generated at 100% rpm, and a descent of -14.5° can be obtained at 90% rpm. Improvements in dynamic path response can also be recognized in the

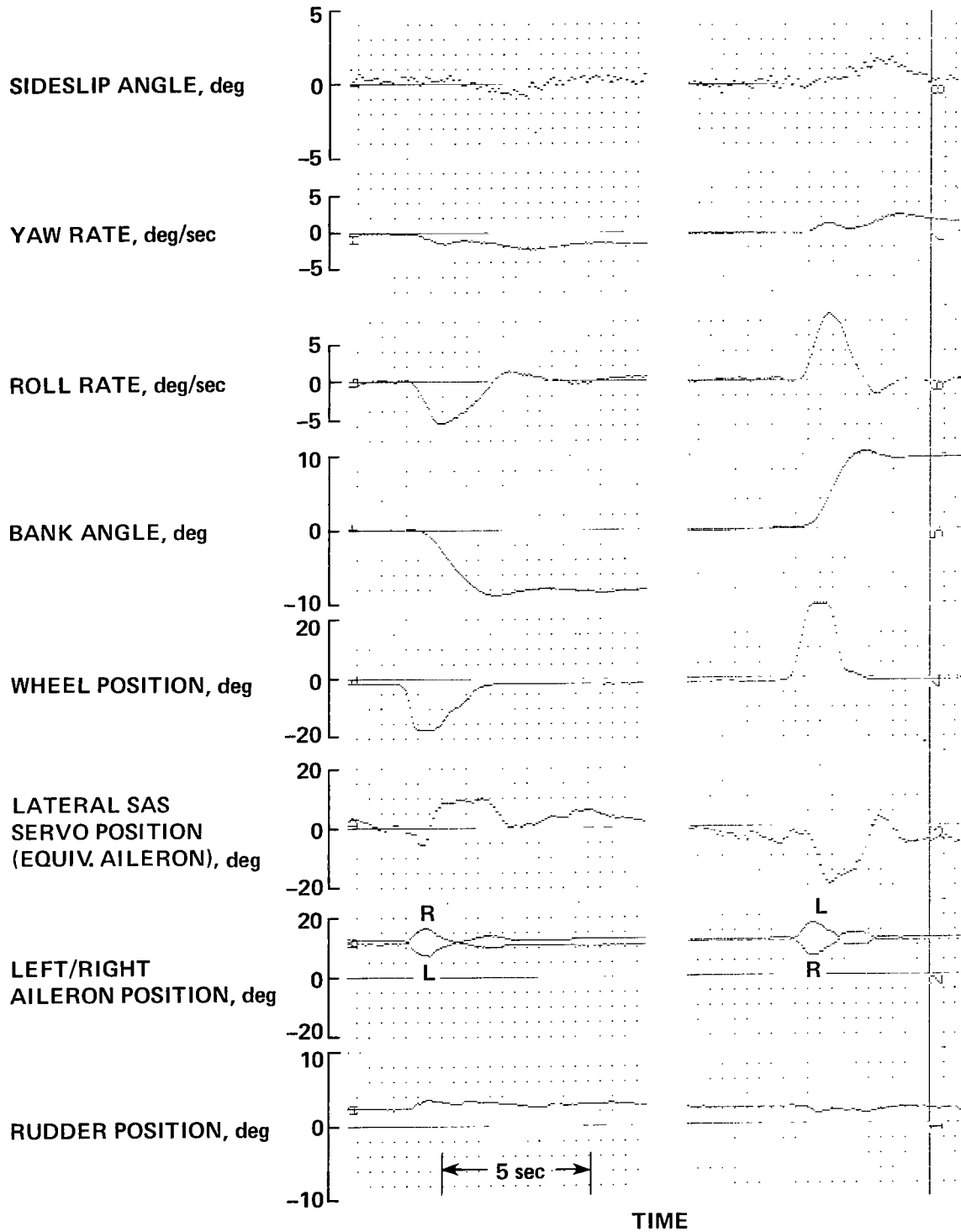


Figure 17.— Lateral-directional response to roll control — roll-yaw SCAS on.

STANDARD DAY
ALTITUDE = 300 m (1000 ft)

GROSS WEIGHT = 18,150 kg (40,000 lb)
FLAPS = 65°

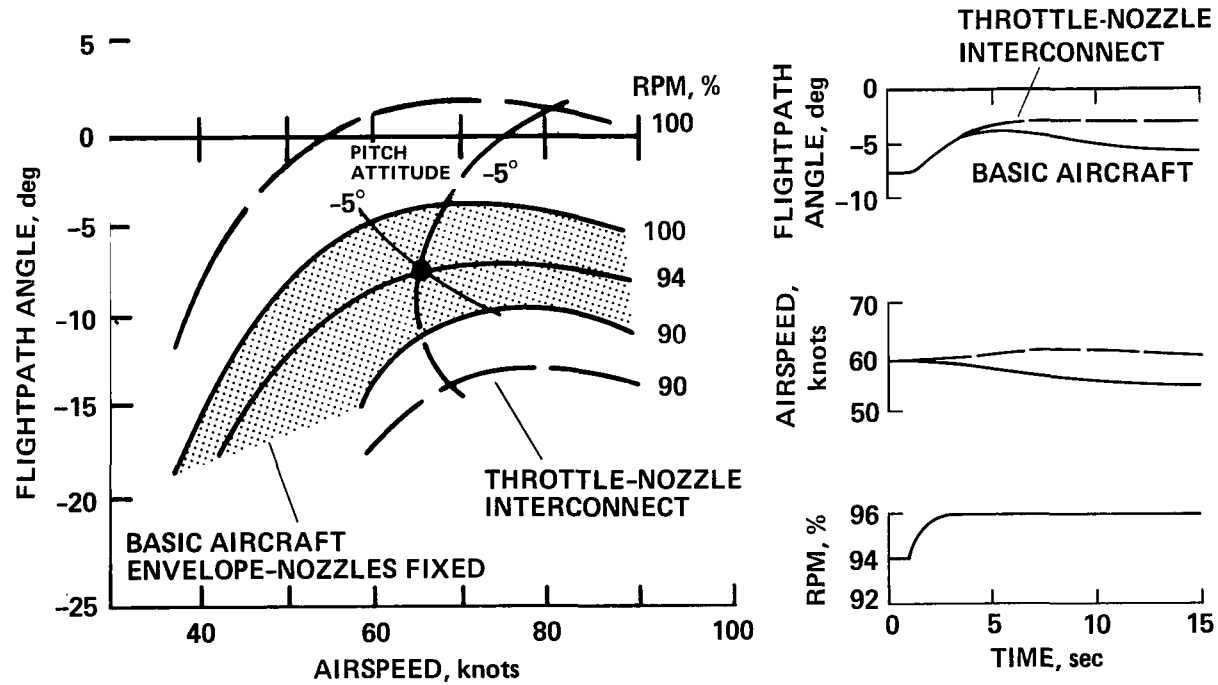


Figure 18.— Performance and dynamic response characteristics for the throttle-nozzle interconnect configuration.

time histories for a step thrust application shown in figure 18. Flightpath responds quickly with no overshoot, and very little change in airspeed is noted. This behavior would permit the pilot to track the glideslope with the throttle alone – no significant pitch control, to improve path response or maintain speed, would be involved.

Airspeed stabilization– Another means of eliminating the flightpath-airspeed coupling induced by thrust control is to stabilize airspeed at the selected approach condition. By prohibiting significant variation in airspeed response to thrust, the dynamics of flightpath response to thrust can be improved to the same extent as that provided by the throttle-nozzle interconnect. Speed stabilization makes it appear to the pilot that the aircraft is flying on the front side of the drag curve; thus, it permits attitude to be used for flightpath control. This system also reduces variations of speed and flightpath in response to longitudinal gust components.

The system operates by driving the nozzles in proportion to speed error, as indicated in figure 19, and is designed for operation with the aircraft configured for the landing approach. In the approach configuration with the nozzles deflected 80° , incremental changes in nozzle deflection provide essentially longitudinal force control and can produce up to ± 0.1 g of longitudinal acceleration within the nozzle control limits of 50° to 104° (the limits used for speed control). With this authority, it is possible to counteract longitudinal force perturbations of a magnitude associated with $\pm 6^\circ$ changes in pitch attitude or for horizontal wind gradients of 1.9 knots/sec.

The speed-error command, which drives the nozzles, is the difference between the reference airspeed selected by the pilot on the cockpit mode-select panel and the actual airspeed, as derived from the airspeed complementary filter. This filter (fig. 19) combines longitudinal acceleration and true airspeed through a second-order filter that removes gust components above about 0.25 rad/sec from the aircraft's pitot static sensors; however, the filter restores the high-frequency component due to aircraft maneuvering by using accelerometer derived inertial data.

Figure 20 illustrates the aircraft's dynamic response to a pitch attitude change at constant thrust with the speed stabilization system operating. It is apparent in the figure that within the authority of the nozzles the aircraft is very markedly operating on the front side of the drag curve. The airspeed feedback gain K_V was chosen to provide good steady-state flightpath control in response to pitch attitude without inducing excessive nozzle control activity. The nominal value selected was $8.4^\circ/\text{knot}$. Substantial changes in flightpath can be obtained with little change in airspeed. The capability exists to achieve level flight with no throttle adjustments, although large attitude changes may be required. The steady-state flightpath-attitude sensitivity ($\Delta\gamma_{SS}/\Delta\theta_{SS}$) is $0.55^\circ/\text{deg}$. The dynamic response of flightpath to change in attitude occurs with no overshoot. Consequently, the pilot may use a control technique for the landing approach that relies primarily on pitch-attitude corrections for glide-slope tracking and requires only infrequent adjustments in thrust for sustaining gross changes in rate of descent. When nozzle limits are reached, the aircraft's response will, of course, revert to the backside characteristics associated with the basic aircraft, and thrust modulation will be required for glide-slope corrections.

The capability of the speed stabilization system to suppress flightpath disturbances due to horizontal wind shear is illustrated by the simulation-generated time histories shown in figure 21. The aircraft's path and speed response to a 15-knot decrease in headwind per each 30-m (100-ft) change in altitude is compared with and without the system operating. Pitch SCAS is engaged to

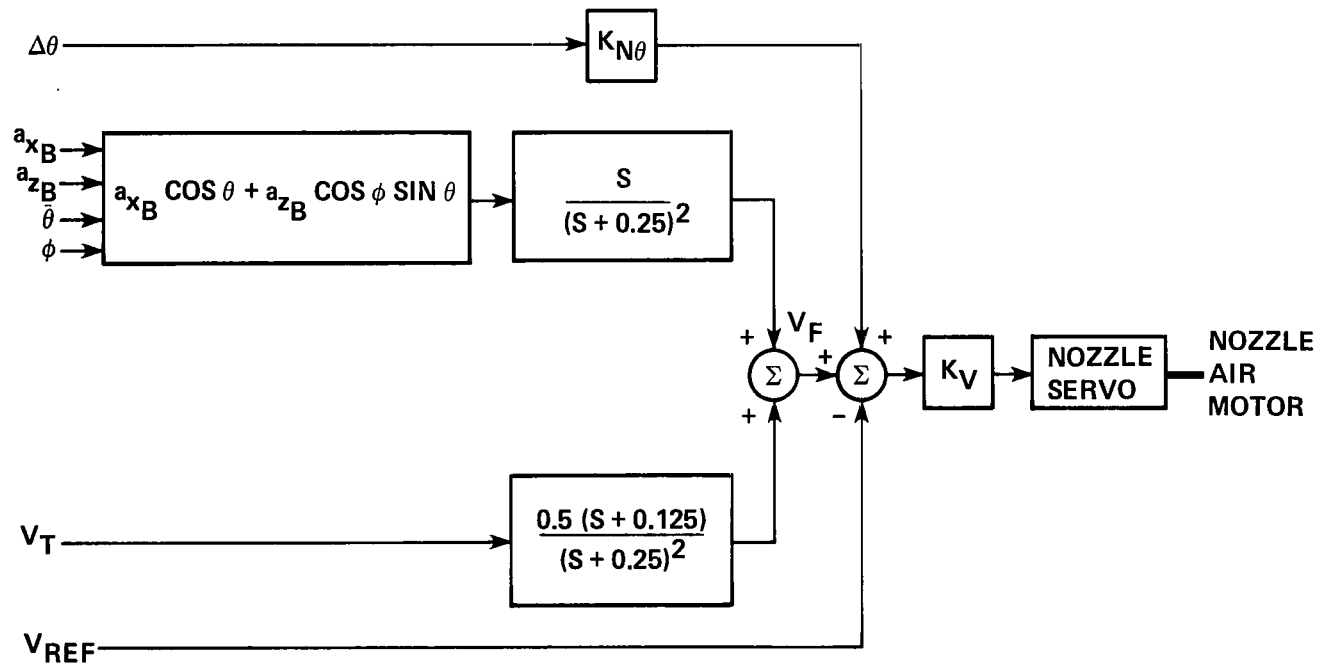


Figure 19.— Speed-stabilization system block diagram.

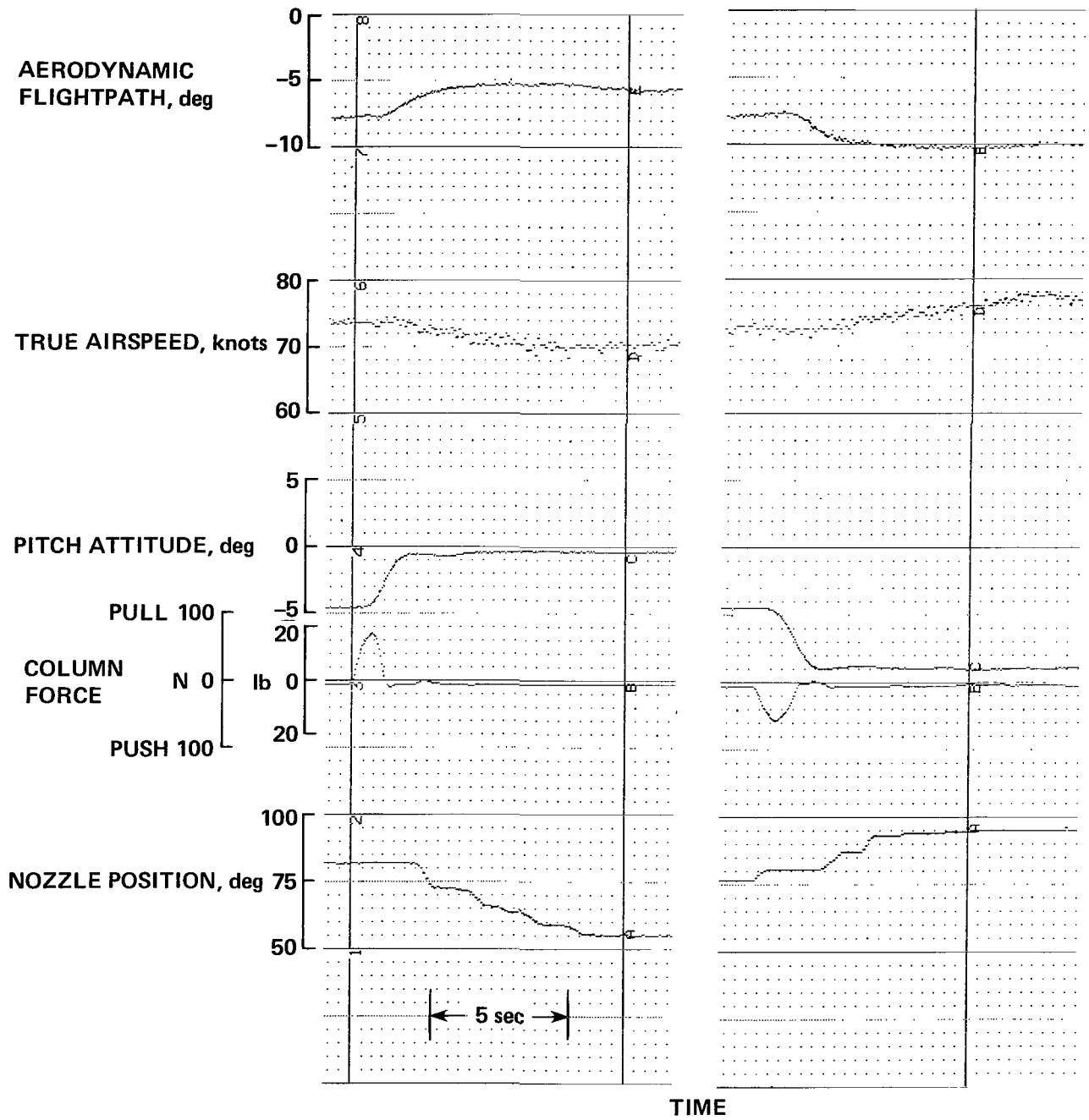


Figure 20.— Longitudinal response to attitude change — airspeed stabilization system on.

SEA LEVEL
GROSS WEIGHT = 18,150 kg
(40,000 lb)

FLAPS = 65°
RPM = 94%
PITCH/ROLL/YAW SCAS ON

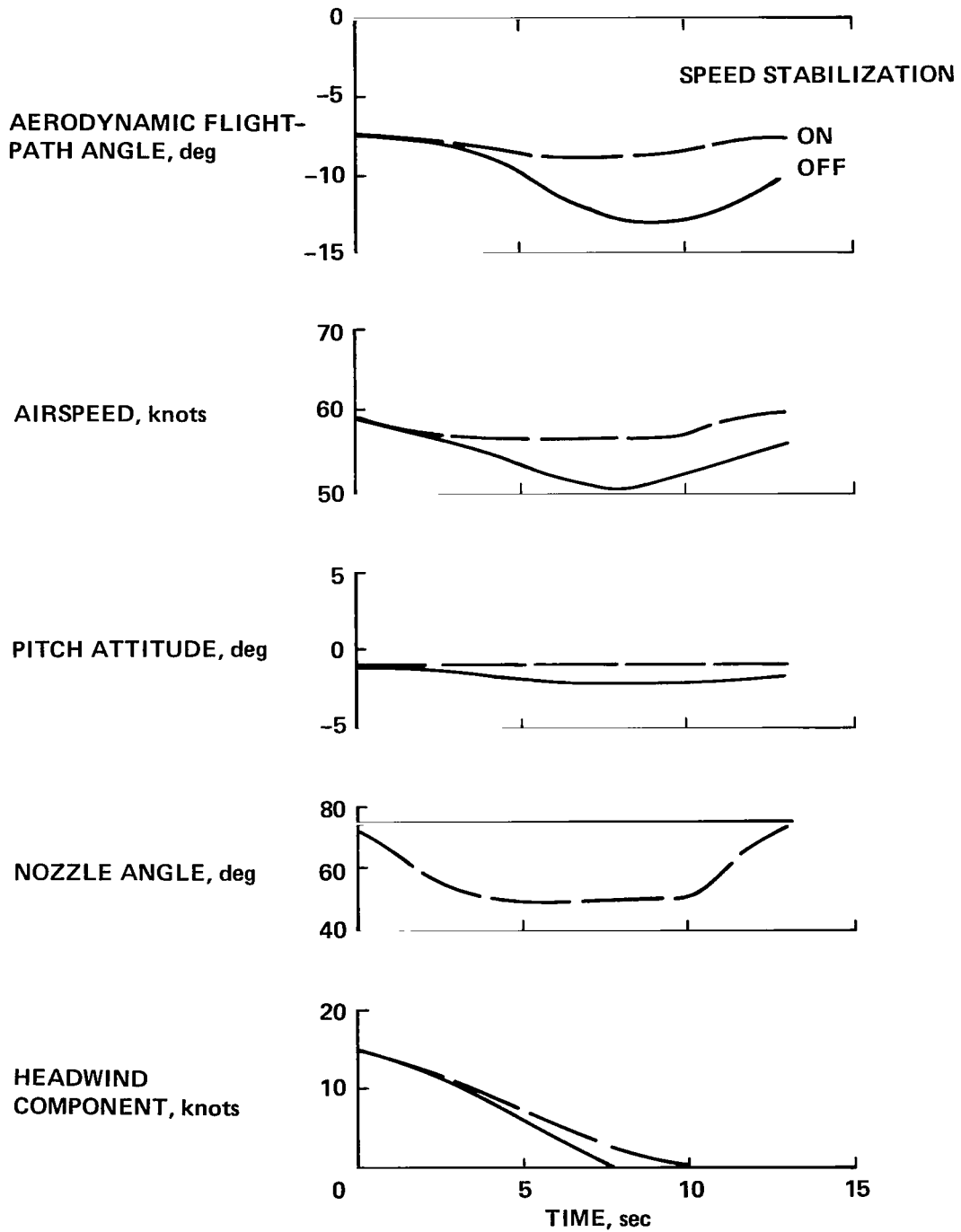


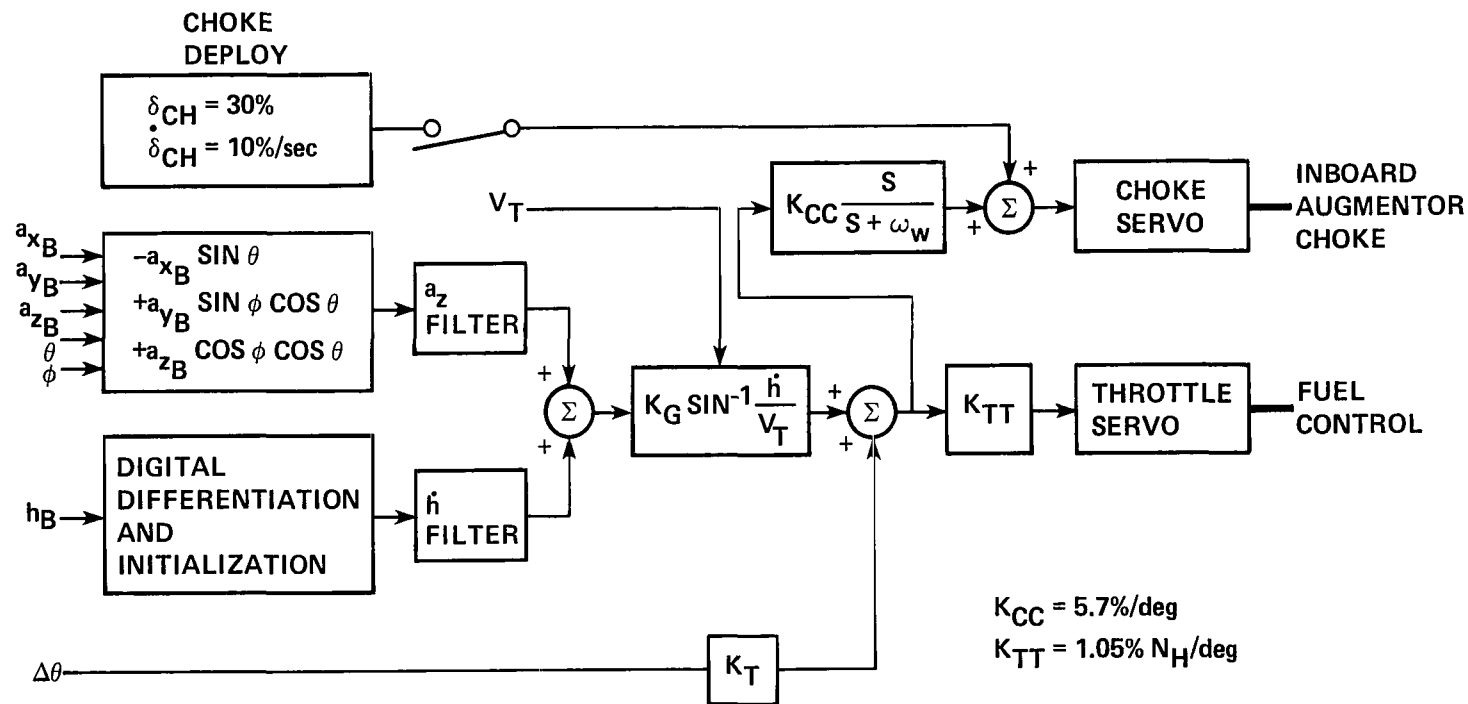
Figure 21.— Response to horizontal wind shear.

hold attitude and no corrective action by the pilot is included. The duration of the wind gradient is 8 to 10 sec, long enough to permit the path and speed perturbations to fully develop when the speed stabilization system is not engaged. When the system is engaged, it drives the nozzles to counteract the deceleration associated with the shear gradient, thereby reducing the magnitude of the change of airspeed, and consequently suppressing the source of the flightpath disturbances. Path excursions are reduced from 6° to 1.8° with the system engaged, with no action by the pilot. As indicated previously, the nozzles have an authority equivalent to 1.9 knot/sec horizontal gradient; for the nominal approach sink rate [4.3 m/sec (14.3 ft/sec) at 65 knots on a 7.5° glide slope] at which this aircraft is operated, this authority corresponds to a spatial gradient of 13.3 knots/30 m (13.3 knots/100 ft). When the nozzles reach an authority limit, the pilot still has substantial capability to counteract subsequent path disturbances with an application of thrust.

In figure 20, some speed variation may be noted in proportion to the magnitude of the change in attitude ($\Delta u_{SS}/\Delta\theta_{SS} = -0.6$ knots/deg); consequently, the system does not provide perfect speed control. An additional command to the nozzles in proportion to the integral of speed error would eliminate the speed variations and would somewhat reduce the attitude required to establish a flightpath correction. It was noted in simulation studies, however, that the integral error command introduced a low-frequency mode in speed and flightpath response that was considered more objectionable than the speed standoff. Hence, the system was mechanized for flight evaluation of the speed control concept using only a speed-error command to the nozzles.

Flightpath command and stabilization—Improvements in flightpath response for glide-slope tracking can be achieved by quickening the initial path response to pitch-attitude control, by providing increased steady-state path-control authority with pitch attitude, and by reducing path disturbances due to winds and turbulence. To obtain these improvements, capability must be incorporated in the flight control system for quickly generating lift increments of the order of ± 0.1 to 0.2 g. As indicated in figure 22, this capability in the Augmentor Wing is provided by the inboard augmentor flap chokes and through control of thrust. This is accomplished in a manner that complements the long-term response to thrust with short-term response to the chokes.

Flightpath stabilization is achieved by driving the throttles and chokes in proportion to an aerodynamic flightpath angle error based on a reference established at the time of system engagement. The system is designed for operation only in the approach configuration. Changes in flightpath can be commanded by the pilot through changes in pitch attitude that also drive the throttles and chokes. Both the flightpath and pitch attitude inputs are sustained in the long term to the throttles and are washed-out to the chokes. The two feedback gains for flightpath and attitude are K_G and K_T , respectively; they are selected to provide the desired transient flightpath response and flightpath authority to pitch attitude. Additional path command quickening could be obtained through a feed-forward of column force; however, simulation studies indicated this additional quickening did not produce significant improvement in path tracking. Note that feedback of equal magnitudes of flightpath and pitch attitude represents feedback of angle of attack, that is, $\alpha = \theta - \gamma$, but without including the contribution of vertical gusts. For transient response considerations, the magnitude of these gains was chosen to increase the aircraft's heave damping to a level corresponding to that of current jet transport aircraft ($Z_w = -0.8 \text{ sec}^{-1}$). Additional attitude feedback is used to increase the steady-state path response to attitude ($\Delta\gamma_{SS}/\Delta\theta_{SS}$). The system gains that were initially selected were $K_G = -0.6$ and $K_T = 1.0$. They were used in conjunction with a choke wash-out time constant of 2 sec.



BARO ALTITUDE	a_z FILTER	\dot{h} FILTER
> 30.5 m (100 ft)	$\frac{1}{S + 0.2}$	$\frac{0.2}{S + 0.2}$
< 30.5 m (100 ft)	$\frac{0.5S(S + 2)}{(S + 1.85)(S^2 + 0.15S + 0.15)}$	$\frac{0.22(S + 0.67)}{(S + 1.85)(S^2 + 0.15S + 0.15)}$

Figure 22.— Flightpath SCAS block diagram.

The speed stabilization system described previously was used in conjunction with the flightpath SCAS to permit a front-side control technique to be adopted for glide-slope tracking. An indication of the quickened response is shown in time histories of figure 23. The incremental changes in path angle in response to a change in attitude are somewhat larger than the attitude increment ($\Delta\gamma_{ss}/\Delta\theta_{ss} = 1.2$). Hence, it is possible to effectively point the flightpath vector in the desired direction with the aircraft's pitch attitude. With this path quickening and path-control authority, glide-slope tracking can be accomplished through attitude control alone, thus considerably simplifying the pilot's longitudinal control workload.

This system also provides a flare capability that permits a less dramatic flare maneuver than that required for the basic aircraft to arrest the sink rate prior to touchdown. Figure 24 provides an illustration of the relative difference in flare performance between the basic aircraft and the aircraft with flightpath SCAS. It can be seen that for a representative flare duration of 7 sec, the flightpath SCAS provides about one-third more sink rate arrestment than the basic aircraft and does

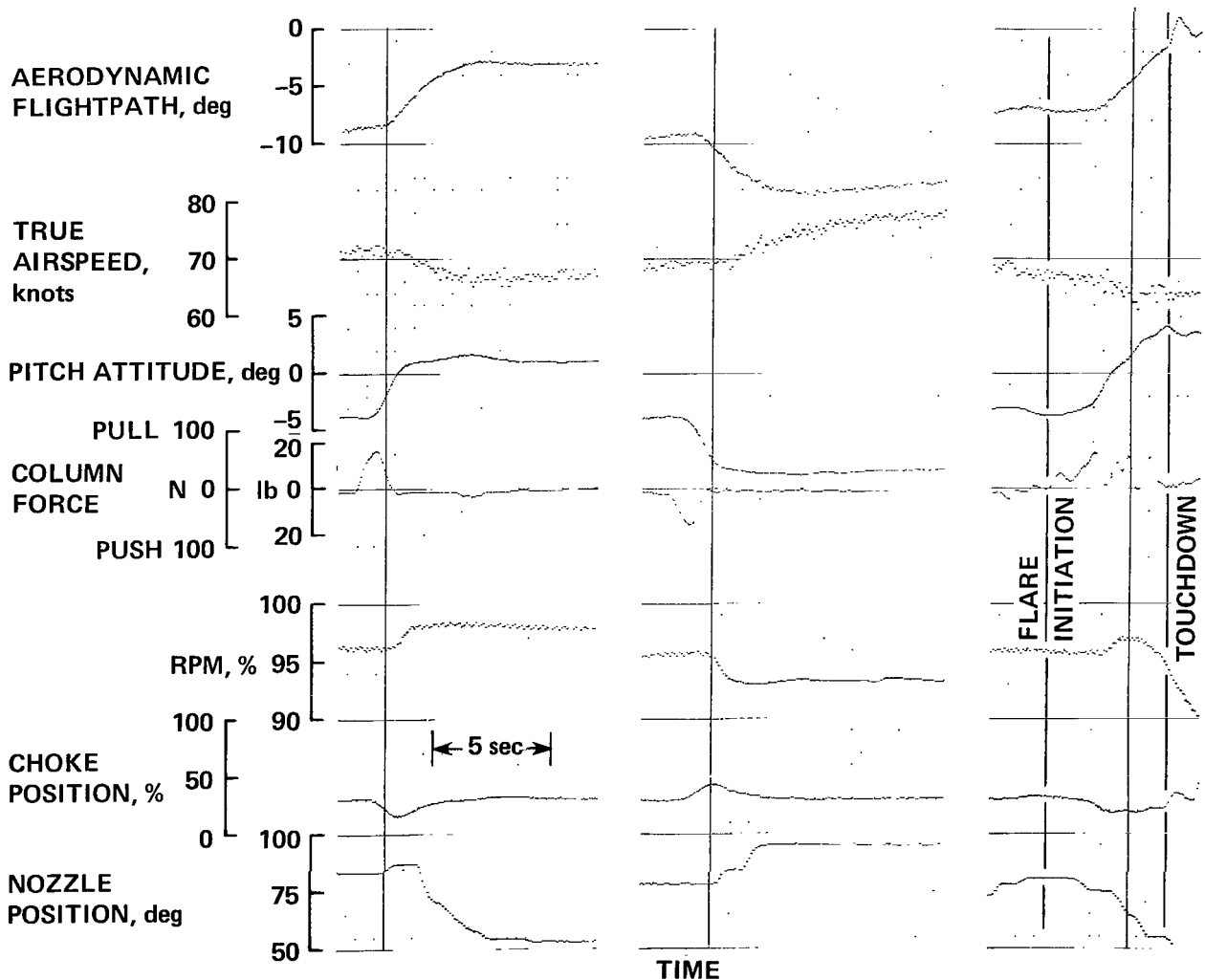


Figure 23.— Longitudinal response to attitude change — flightpath-air speed SCAS on.

STANDARD DAY
SEA LEVEL

GROSS WEIGHT = 18,150 kg (40,000 lb)
FLAPS = 65°

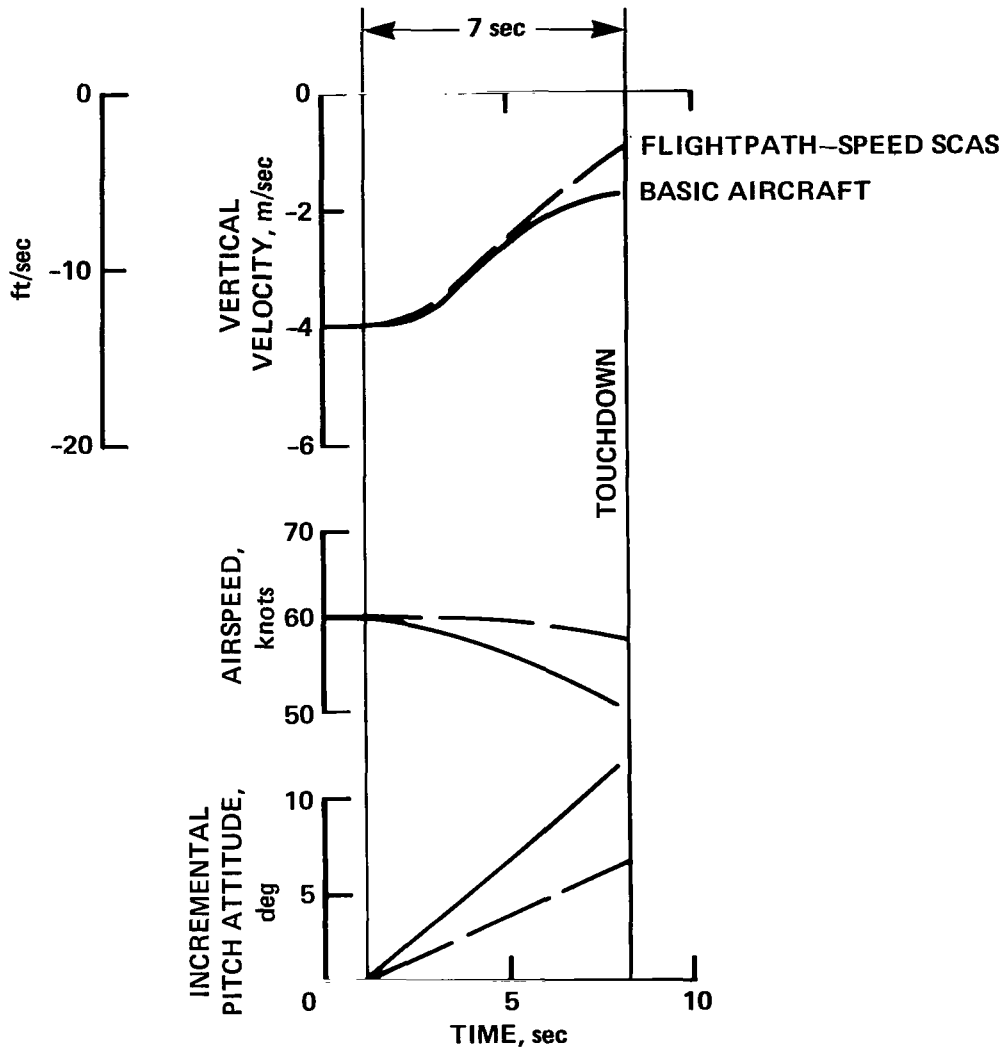


Figure 24.— Flare time history comparison.

so with about one-half the pitch rotation. Although it is possible to achieve comparable sink-rate arrestment with the basic aircraft, it is clear that a much more aggressive flare technique, in terms of rate and magnitude of pitch rotation, would be required.

An alternative concept for flightpath control, which also provides quick path response and path-control authority in response to attitude control, can be mechanized using only a pitch-attitude command to the chokes. In this case, a speed stabilization system is used that includes both airspeed and attitude inputs to the nozzles. The system is engaged to maintain constant airspeed during maneuvers, and a washed-out attitude-error command drives the chokes to quicken

the initial flightpath response. Although this system is conceptually simpler than its counterpart, because there is no derived flightpath information, no suppression of path disturbances in response to short-term gusts is provided. Furthermore, steady-state path-control authority ($\Delta\gamma_{SS}/\Delta\theta_{SS}$) is somewhat less than that for the baseline flightpath SCAS because of the lack of long-term path augmentation with thrust. However, the speed stabilization system does suppress response to wind shears, as noted previously.

An example of the aircraft's response to the pitch control for this alternative system is shown in figure 25. Large flightpath corrections can be sustained in the long term, with essentially no change in airspeed. Initial response is nearly as quick as that observed for the path SCAS shown in figure 23. The speed-to-nozzle gain is the same as for the speed stabilization system ($8.4^\circ/\text{knot}$) and the attitude-to-nozzle gain is $K_{GN} = -6.0$. The attitude-to-choke gain ($K_T = 1.0$) was selected to utilize essentially all of the choke authority for a 5° change in attitude. A choke wash-out time constant of 1 sec was chosen to provide path response with essentially no overshoot or undershoot tendencies.

Cockpit Displays

A variety of displays (fig. 9) useful in providing guidance for following curved-approach profiles and for glide-slope and localizer acquisition and tracking, was available in the aircraft for flight evaluation. These displays ranged from conventional raw glide-slope and localizer data to a sophisticated three-cue STOL flight director. They provided an opportunity to assess the trade-off between control system and display complexity for various degrees of system sophistication and acceptability to the pilot.

The raw data glide-slope and localizer information was provided on the HSI. The sensitivity of the glide-slope needle was changed to account for the steep approach path angle. Sensitivity was set at approximately $1^\circ/\text{dot}$ for both indicators.

A horizontal bar representing aerodynamic flightpath angle in the vertical plane was available on the EADI, superimposed on the pitch-attitude scale. This display was useful in providing lead information for glide-slope acquisition and tracking and for alerting the pilot to incipient glide-slope deviations caused by variations in horizontal and vertical winds and turbulence.

An MLS deviation box, superimposed on the EADI, offered a more integrated display for MLS tracking and a potentially reduced scanning workload for the pilot. Sensitivity of the box was such that a 2.54-cm (1-in.) linear displacement of the center of the box from the reference in either the vertical or lateral axis corresponds to a 30-m (100-ft) displacement from the vertical or lateral flightpath. These display formats were shown previously in figure 9.

The three-cue flight director consisted of commands for the pilot's throttle, column, and wheel controls for vertical and lateral path tracking, and for maintaining the desired airspeed and safe angle of attack margins. This flight director was designed for the Augmentor Wing Aircraft under contract by Systems Technology, Inc.; it is described in detail in reference 17. Figure 26 presents a schematic of the longitudinal flight director, including command generation for the throttle and pitch controls. Complementary filtered vertical velocity, vertical beam deviations, and deviation



Figure 25.— Longitudinal response to attitude change — alternate flightpath-airspeed SCAS.

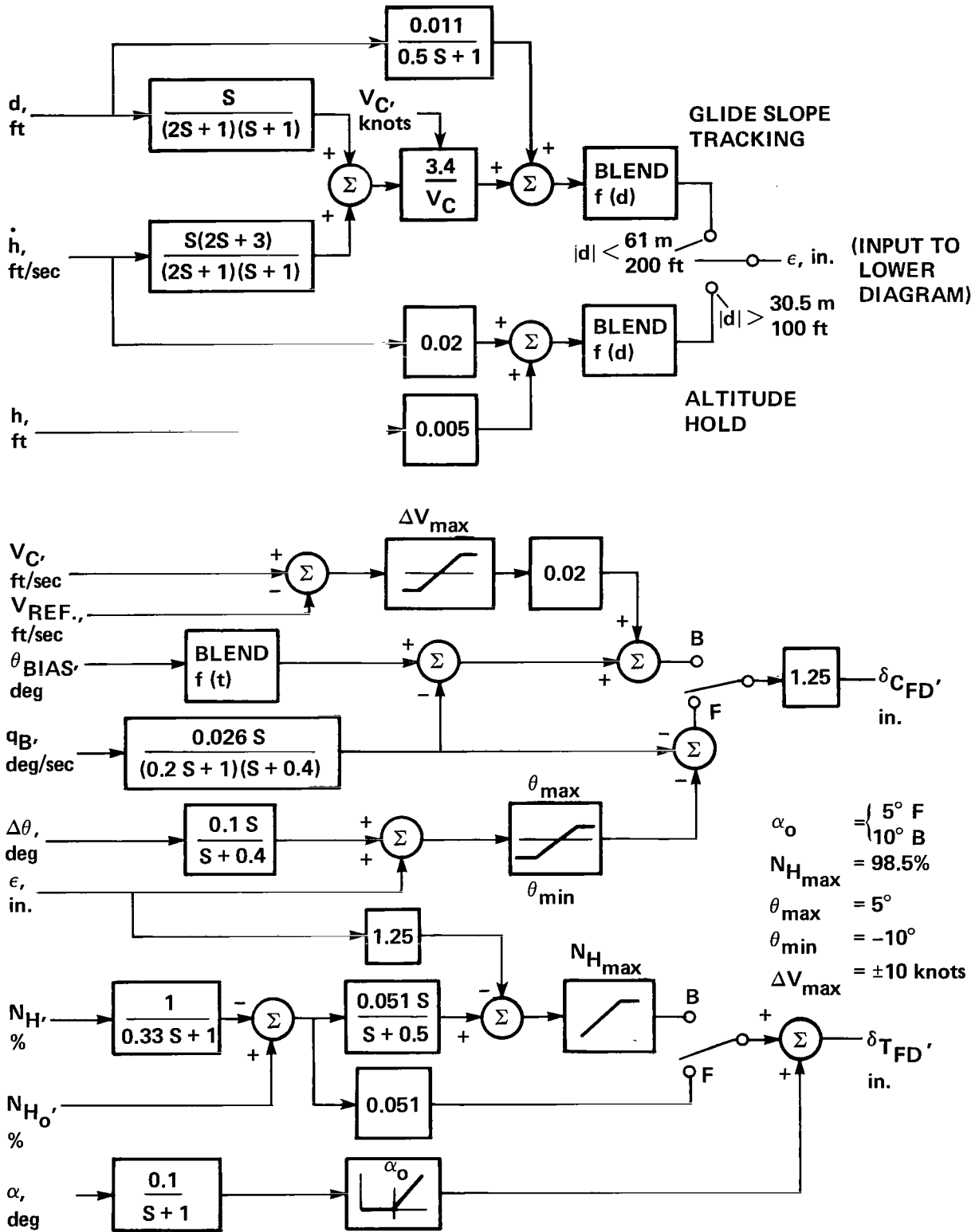


Figure 26.— Longitudinal flight director.

rate are generated for use in holding altitude and in capturing and tracking the glide slope. When in level flight, the inputs to the pitch bar present commands to the pilot to maintain the altitude existing at the time the flight director was engaged. Glide-slope capture is initiated when the aircraft is within 30 m (100 ft) of the glide-slope beam. Subsequent glide-slope tracking may be done either with throttles or pitch control depending on the flight-control system configuration. The tracking mode is selected through the front-side (*F*)/back-side (*B*) switch. Schedule changes in thrust and pitch attitude are commanded as a function of flap angle and initiation of glide-slope capture. Angle-of-attack margins are protected through commands for increased thrust introduced to the throttles when the angle of attack exceeds a specified value that depends on the control configuration. A limit on the thrust command corresponding to maximum authorized thrust ($rpm = 98.5\%$) is included in the throttle logic. Commands to maintain the reference airspeed are introduced to the pitch bar in the event a speed stabilization system is not utilized during the approach, or in the event the system should fail to maintain the selected speed.

Figure 27 presents a block diagram of the lateral flight director. Complementary filtered lateral beam deviation and deviation rate are generated for lateral path capture and tracking. Bank-angle commands can be introduced for executing turns of a prescribed radius associated with a reference flightpath. These commands are introduced 3 sec prior to turn entry and removed 3 sec prior to the turn exit, where the time interval is computed based on distance to the entry and exit waypoints and the current ground speed.

FLIGHT RESEARCH PROGRAM

Combinations of the experimental SCAS and display configurations chosen for evaluation in the flight research program are shown in table 2. Response characteristics of the respective systems and the stability derivatives on which they are based are listed in appendix A. The program proceeded with a buildup in complexity of the attitude control SCAS, starting with pitch, roll, and yaw SCAS, and progressively adding the throttle-nozzle interconnect, speed control, and flightpath SCAS. Selected evaluations of the various displays were obtained for the various SCAS options. Raw data glide-slope and localizer tracking was performed in all cases and the flight director was evaluated for straight-in approaches with the throttle-nozzle interconnect and the flightpath SCAS.

Assessments of glide-slope tracking and flare and landing capability for the configurations described in the foregoing discussion were obtained from landing approaches flown on a 7.5° glide slope at airspeeds from 60 to 65 knots to landings on a 30- by 518-m (100- by 1,700-ft) STOL runway. Landing approach guidance was provided by a prototype microwave landing system (MODILS). Figure 28 shows the runway and approach guidance arrangement at Ames Research Center's experimental flight facility at the Crows Landing Naval Airfield. Straight-in approaches were initiated at about 450 m (1,500 ft).

Research pilots from Ames Research Center, the Canadian Department of Transport, and the Canadian National Aeronautical Establishment conducted the flight evaluations in this program. Both VFR and simulated IFR approaches were flown in calm to light wind conditions. Additional evaluations were obtained when possible with surface conditions that ranged from strong headwinds to light tailwinds and from light to moderate turbulence. Pilot commentary and opinion ratings based on the Cooper-Harper scale of reference 18 were obtained for most configurations. The

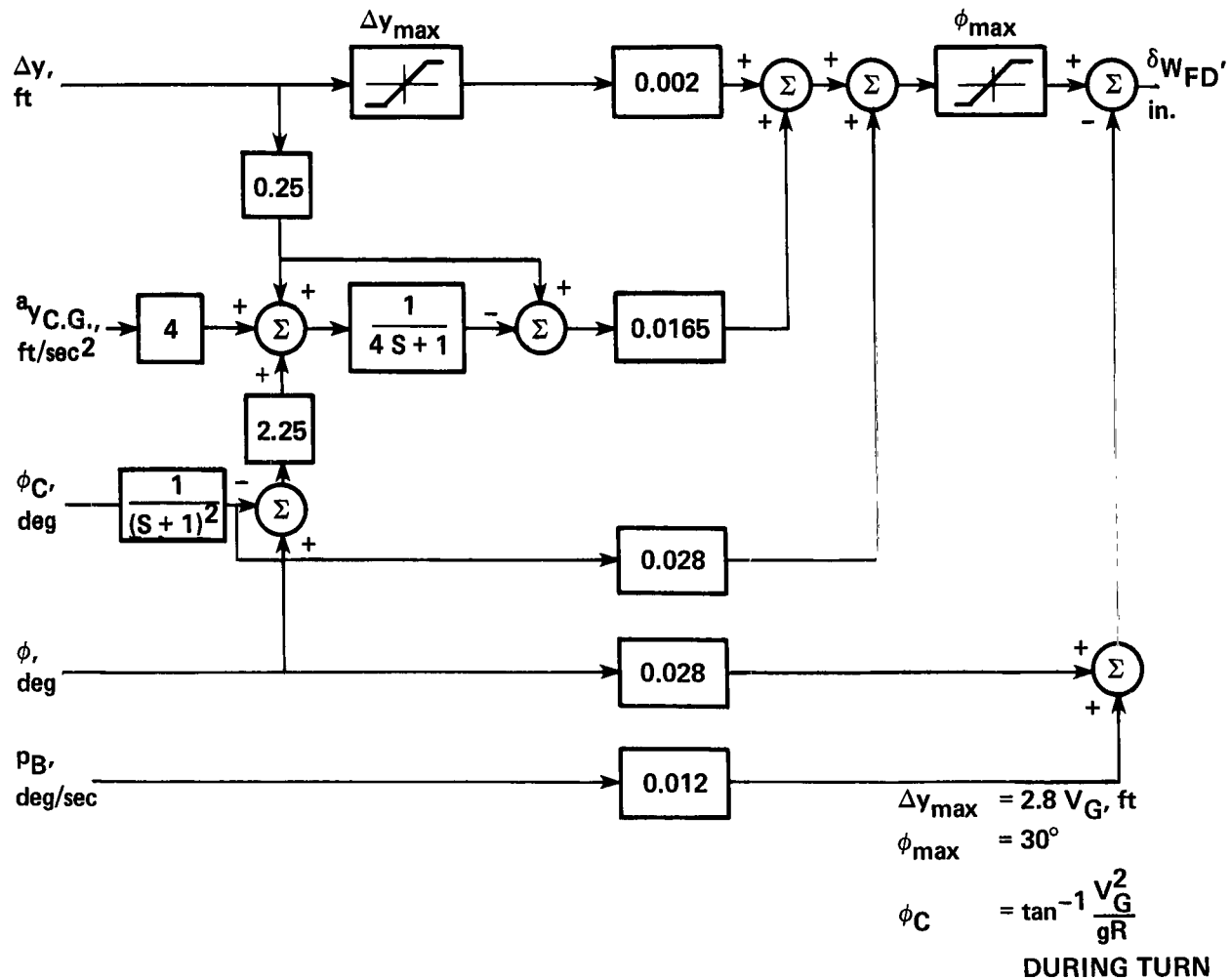


Figure 27.— Lateral flight director.

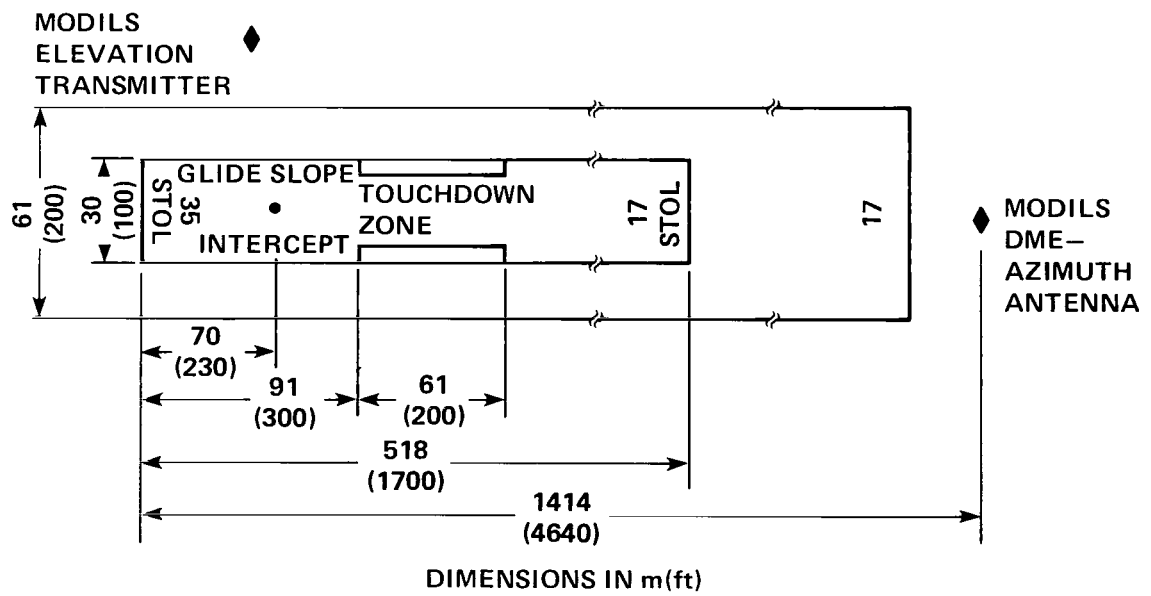
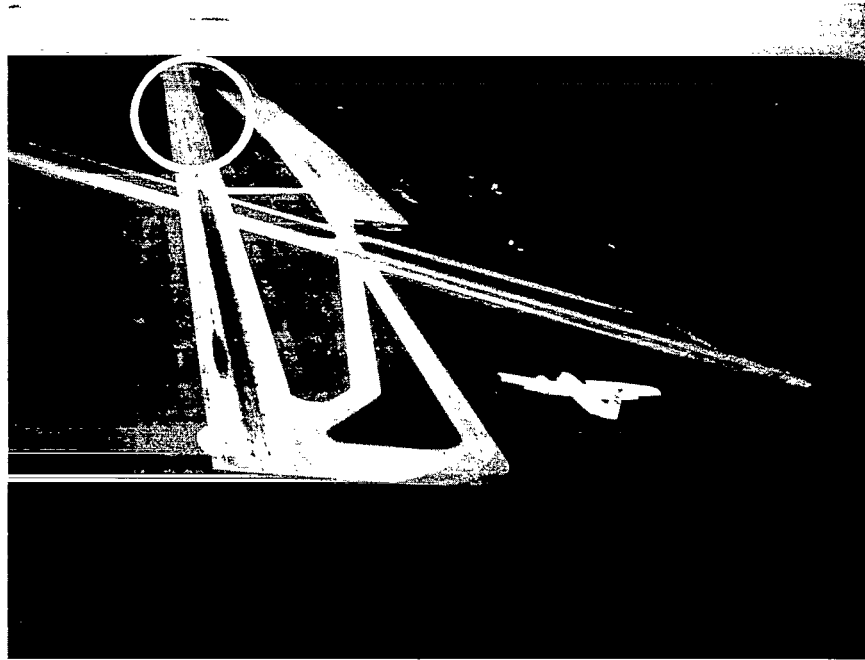


Figure 28.— Crows Landing flight research facility and STOL runway layout.

TABLE 2.— EXPERIMENTAL SCAS AND DISPLAY CONFIGURATIONS

Aircraft and control system configurations			Display configurations	STOL approach control technique
Config.	Attitude control	Flightpath control		
Basic aircraft	Boeing roll-yaw SAS	Basic aircraft	Electronic attitude-director indicator (EADI) Horizontal situation indicator (HSI)	Backside (B) flightpath control with thrust, airspeed control with attitude
Pitch SCAS	Pitch SCAS ● Rate command-attitude hold ● Attitude command Boeing roll-yaw SAS	Basic aircraft	EADI HSI	Backside
Roll-yaw SCAS	Pitch rate-command-attitude hold Roll rate-command-attitude hold Yaw SCAS	Basic aircraft	EADI HSI	Backside
Flightpath-air speed decoupling	Pitch rate command Roll rate command Yaw SCAS	Throttle-nozzle interconnect	EADI ● Flight director HSI	Backside
Air speed stabilization	Pitch rate command Roll rate command Yaw SCAS	Speed control ● Nozzles	EADI HSI	Frontside (F) flightpath control with attitude
Flightpath SCAS	Pitch rate command Roll rate command. Yaw SCAS	Flightpath control ● Throttles/chokes ● Chokes Speed control ● Nozzles	EADI ● Flight director HSI	Frontside

pilot's assessments of the acceptability of the flare and touchdown were based on the consistency of landing performance (touchdown point and sink rate) that could be achieved for a particular configuration. Fully flared landings were performed to reduce the approach sink rate of 4.3 m/sec (14 ft/sec) to levels well below the gear limit of the aircraft – 3.8 m/sec (12.6 ft/sec).

RESULTS

In the material that follows, the pilots' evaluations of the attitude and flightpath control are discussed for the basic aircraft and for the aircraft equipped with the various control and display concepts. In this case, the basic aircraft configuration includes the original Boeing-designed lateral-directional stability augmentation system (described in the "Research Aircraft" section). Attitude and flightpath control SCAS are discussed for the IFR approach in calm air and turbulence. Control of the flare and landing is presented for the final VFR segment under wind conditions similar to those encountered for the approach. Contributions of the flight director and display elements combined with those of the flightpath SCAS are noted where appropriate. A summary of pilot ratings and comments for each of the experimental configurations are provided in appendix B along with selected values of the more significant wind and turbulence conditions experienced throughout the program.

Attitude Control

Basic aircraft— Pitch-attitude control for the basic aircraft was considered unsatisfactory for the approach; it was given pilot ratings from 3 to 5 for calm air operation. Objections concerned the need to continually monitor pitch attitude to stabilize at a desired reference and to suppress disturbances that occurred either when making throttle or nozzle control adjustments or in response to turbulence. It was not possible for the pilot to divert his attention for more than a few seconds without the attitude being upset and consequently the approach path and airspeed being disturbed from a stabilized condition.

Pitch SCAS— Both the attitude-command and rate-command-attitude-hold systems improved pitch-attitude control substantially by suppressing the phugoid mode and minimizing attitude variation during unattended operation. These improvements were particularly appreciated during operation in turbulence. For the attitude-command system, two levels of attitude feedback were tested ($K_\theta = 2.0^\circ/\text{deg}$ and $3.8^\circ/\text{deg}$). The corresponding attitude bandwidth ranged from 1.5 to 3 rad/sec. The lower gain was selected for detailed evaluation. The rate to attitude gain ratio was $K_q \cdot K_\theta = 1.0$ and control sensitivity θ/F_c was $0.13^\circ/\text{N}$ ($0.6^\circ/\text{lb}$). The trim rate was $0.3^\circ/\text{sec}$. Figure 29 presents time histories of the operation of the system during an approach. This attitude-command system was given ratings from 3 to 4 for the VFR approach and ratings as high as 5 for the IFR approach. Although control forces for attitude maneuvering and trim rates were considered satisfactory and attitude stability was good, the necessity to retrim the aircraft during pitch maneuvers on the approach was objectionable to all the evaluation pilots. It is evident in figure 29 that considerable pitch control activity is present during the approach as required for speed control and that it is not appropriate to fly the approach at a fixed attitude. Control forces for the flare maneuver are about 4.5 N (20 lb); pilots objected to sustaining this force level for several seconds.

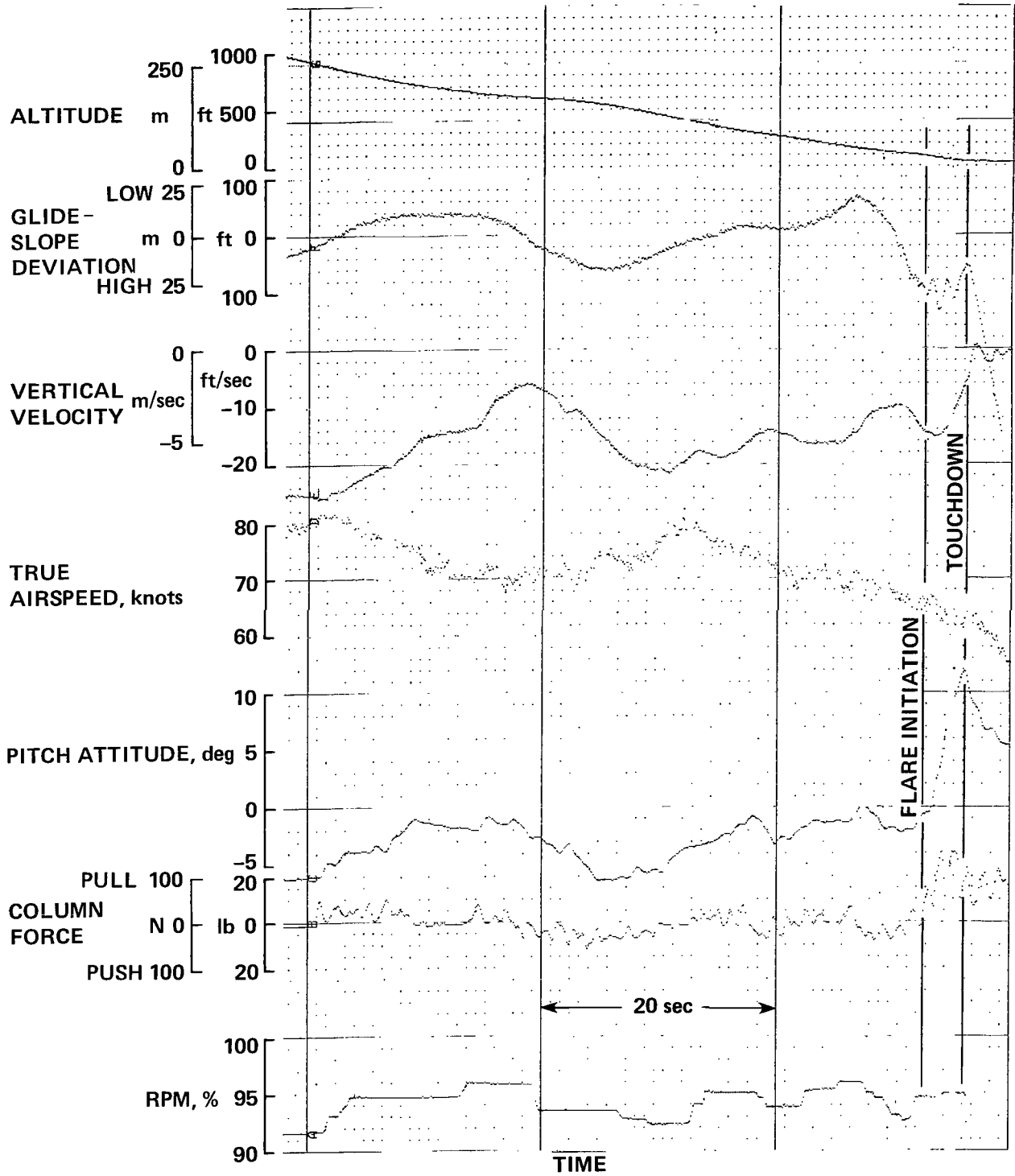


Figure 29.— Landing approach time history — attitude-command system.

For the rate-command-attitude-hold system, variations in the attitude feedback gain ranged from 1.0 to 4.0°/deg, with a rate-to-attitude relationship of $K_q \cdot K_\theta = 0.4$. The corresponding attitude bandwidth varied from 0.7 to 3.0 rad/sec. The configuration selected for detailed evaluation used an attitude gain $K_\theta = 3.0^\circ/\text{deg}$ and a control sensitivity $\dot{\theta}/F_c = 0.09^\circ/\text{sec}/\text{N}$ ($0.4^\circ/\text{sec}/\text{lb}$). Attitude overshoot was adjusted to zero for all configurations. An example of an approach and landing for this configuration is shown in figure 30. This rate-command-attitude-hold system was rated from 2 to 3 for the VFR approach, and up to one rating unit worse for the IFR approach (PR 2 to 4). It was the preference of all the pilots for approach and landing operation of this aircraft. The lack of the requirement to maintain prolonged column forces or to retrim the aircraft while maneuvering in pitch during the approach provided some reduction in pilot workload. As can be seen in figure 30, large and small attitude changes could be made precisely and stabilized easily, and smooth, precise flare rotations could be made for landing. Control forces were satisfactory in both cases. No objections were expressed about the lack of classical speed stability or the use of the rate-command system for the landing flare. Finally, the system performed well in suppressing pitch disturbances for large thrust changes and airspeed variations.

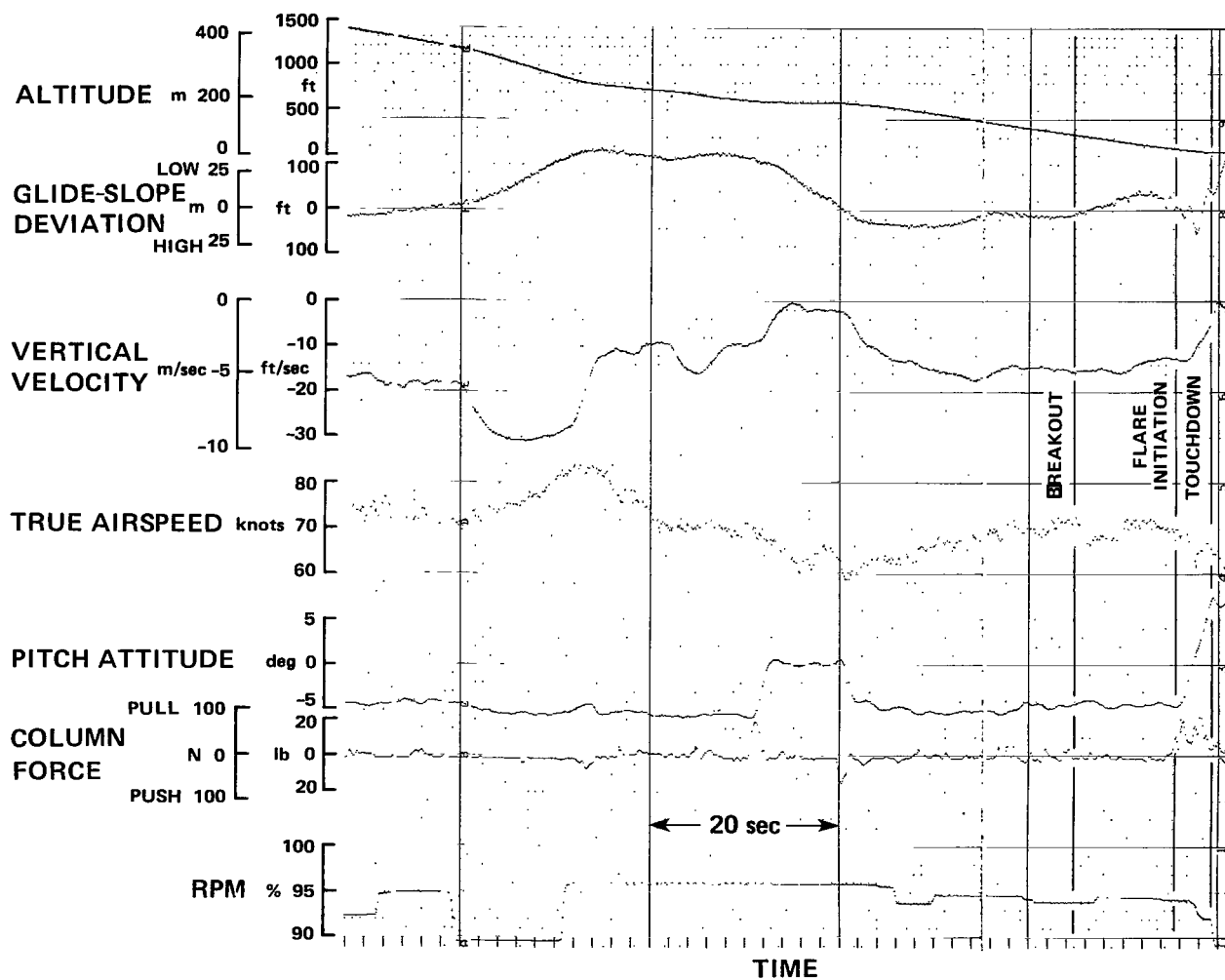


Figure 30.— Landing approach time history — rate-command-attitude-hold SCAS.

The foregoing comments should not be construed to imply that an attitude-command system would be unsatisfactory for STOL operations. For those aircraft that require little or no attitude maneuvering during the approach and flare, such as aircraft with very little speed variation in response to the flightpath controller, an attitude command system may well be preferred to any other concept. When active pitch control is necessary during these flight phases, however, it should be anticipated that the rate-command-attitude-hold system will be preferred over other concepts. For all subsequent SCAS concepts for flightpath and airspeed control, the rate-command-attitude-hold system was used to augment pitch control.

Roll and yaw SCAS— Evaluations of the roll rate-command-bank-angle hold and the directional SCAS were performed for the configuration defined in the section on SCAS and display concepts under the discussion of roll and yaw SCAS. An example of lateral-directional control of the aircraft during the landing approach is shown in figure 31. Roll control sensitivity was $\dot{\phi}/\delta_w = 0.33^\circ/\text{sec}/\text{deg}$, which corresponded to $\dot{\phi}/F_w = 0.94^\circ/\text{sec}/\text{N}$ ($4.2^\circ/\text{sec}/\text{lb}$) based on a lateral control force gradient of 0.35 N/deg (0.078 lb/deg). Precise bank-angle and heading control were achieved and sideslip excursions were nominally within $\pm 2^\circ$, with occasional larger perturbations due to lateral gusts. Pilot ratings of 3 were given for lateral-directional control during the IFR approach. With this SCAS operating, the primary difficulty with localizer control was contributed by the instrument scan workload associated with raw data displays, specifically, the raw localizer and heading scan on the HSI and bank angle on the EADI. This difficulty is evident in the oscillatory localizer tracking performance shown in figure 31.

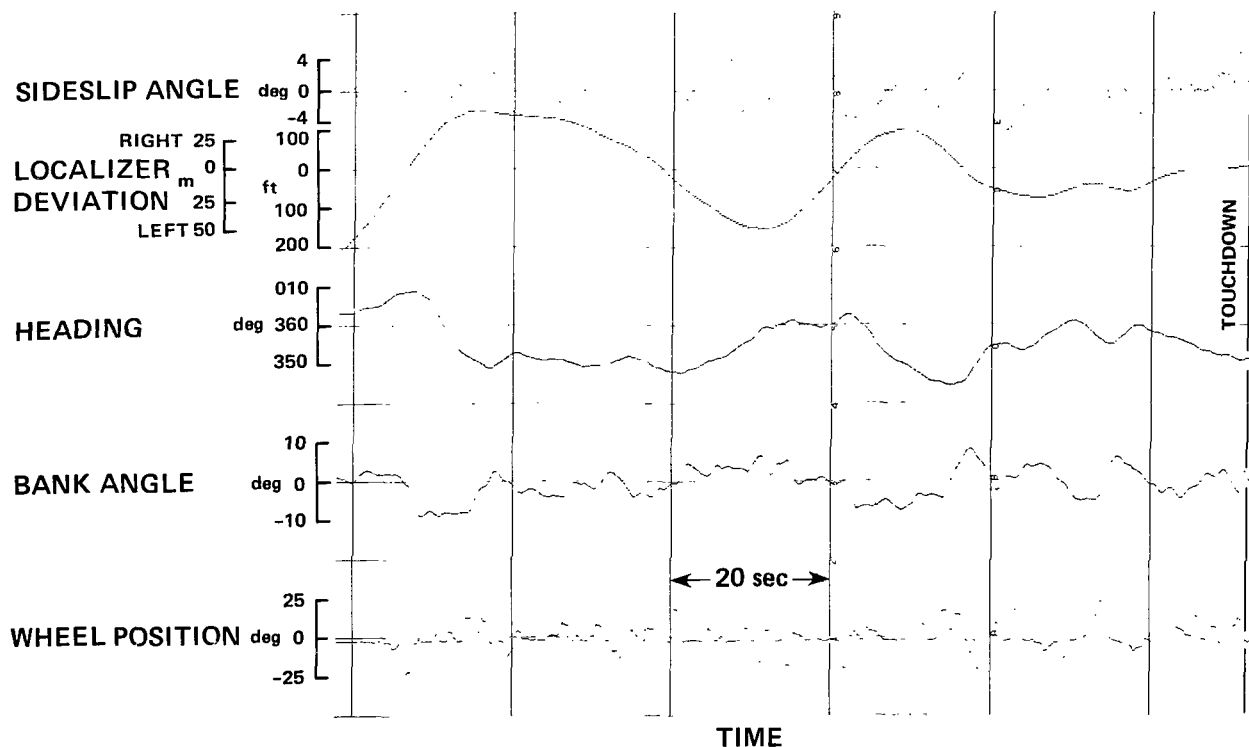


Figure 31.— Landing approach time history – roll-yaw SCAS.

Flightpath Control

Basic aircraft with pitch, roll, yaw SCAS— The pilot's workload for IFR glide-slope tracking down to a decision height of 60 m (200 ft) was considered unsatisfactory when either the throttle or nozzle controls were used alone. The most acceptable technique for tracking the glide slope on an instrument approach utilized the nozzle control for making gross adjustments in rate of descent and the throttles for tight path tracking and setting up the flare.

Glide-slope control with nozzles was considered unsatisfactory due to the sluggish path response to changes in the thrust vector angle or, if attitude is used to quicken the response, due to the coordination required between the attitude and nozzle controls. IFR glide-slope control with the throttles was given a pilot rating of 5 to 6 due to the large path-speed coupling and unpredictable flightpath response. Path control authority with the throttles was also considered insufficient for glide-slope tracking in turbulence. Operation in turbulence up to 4.6 m/sec (15 ft/sec) peak-to-peak vertical gusts and horizontal wind gradients of 1.0 knots/sec sustained up to 10 sec, produced degradations in pilot ratings from one-half to one rating unit worse than the calm air evaluations.

The landing for this aircraft was accomplished with a full flare to low touchdown sink rates. The flare was routinely performed by rotating the aircraft to a touchdown attitude with thrust adjustment as necessary to offset high angles of attack or high sink rates at flare entry or to compensate for any floating tendency. An example of the flare maneuver extracted from flight records is shown in figure 32. Response of the aircraft to the pitch rotation develops adequate normal acceleration to check the sink rate to an acceptable level ($\Delta\gamma_{max}/\Delta\theta_{ss} = 0.55$). However, a pitch rotation of the order of 10° at a rate of $3^\circ/\text{sec}$ to $4^\circ/\text{sec}$ is required to reduce the sink rate to 1 m/sec (3.5 ft/sec); this rate is considered unsatisfactory for passenger comfort in a commercial operation. Flare and landing accomplished primarily using pitch with an assist as required from thrust was given ratings from 3.5 to 5.

Throttle-nozzle interconnect— The improvement in glide-slope control provided by this interconnect is a consequence of eliminating path-speed coupling and increasing the flightpath authority for the thrust control. Pilot ratings from 3.5 to 4 for VFR operation and 4.5 to 5 for raw data IFR operation to a 60-m (200-ft) decision height represented some improvement over the basic aircraft; they were a consequence of the improved path response and reduced workload for speed control. An example of a landing approach for this configuration is shown in figure 33. The requirement to modulate both the nozzle and throttle controls for glide-slope tracking is relieved and the disturbances to speed are reduced substantially so that the approach can be essentially flown with a single control, the throttle. Figure 34 shows an approach in turbulence with peak vertical gusts of ± 5.5 m/sec (18 ft/sec), an average headwind component of 20 knots, and wind shears of 1.4 knots/sec sustained up to 8 sec. Degradations in pilot rating of only one-half to one unit were associated with these wind conditions. Glide-slope tracking performance was good and the throttle control activity was slightly increased over that required for an approach in calm air. Increased path-control authority improves the capability for coping with disturbances due to turbulence and wind shears. The primary deficiency remaining for path tracking that accounts for the unsatisfactory pilot rating is the instrument scan workload associated with the raw data display. No modification of flare control characteristics or technique is associated with this configuration.

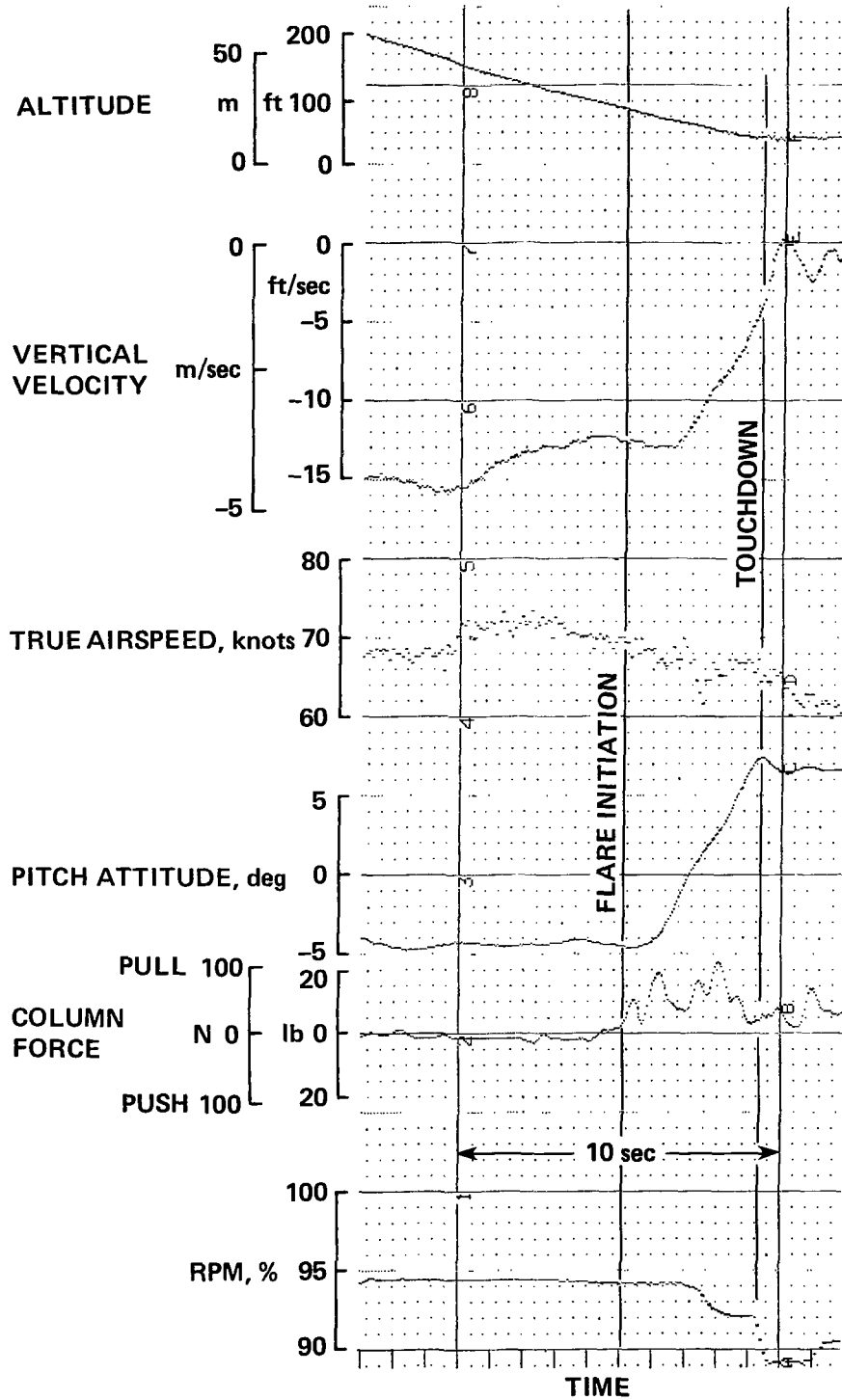


Figure 32.— Flare time history — basic aircraft.

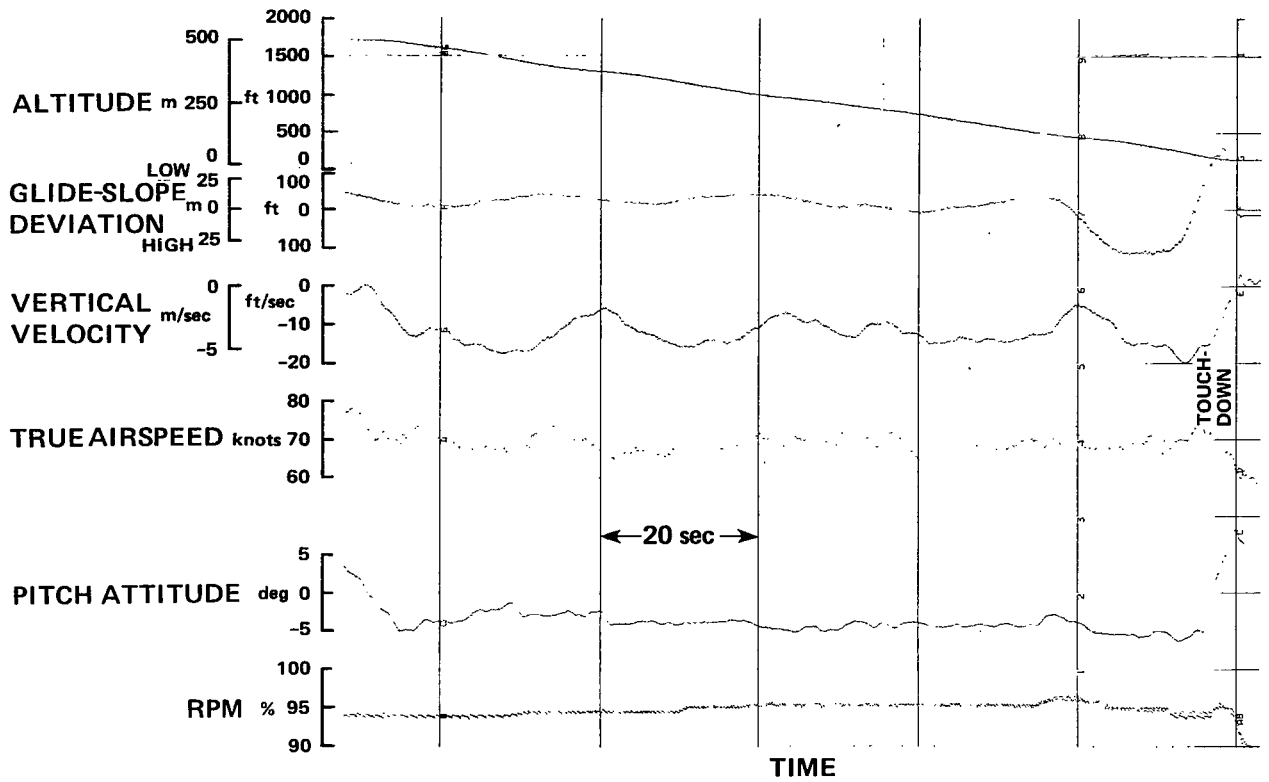


Figure 33.— Landing approach time history — throttle-nozzle interconnect.

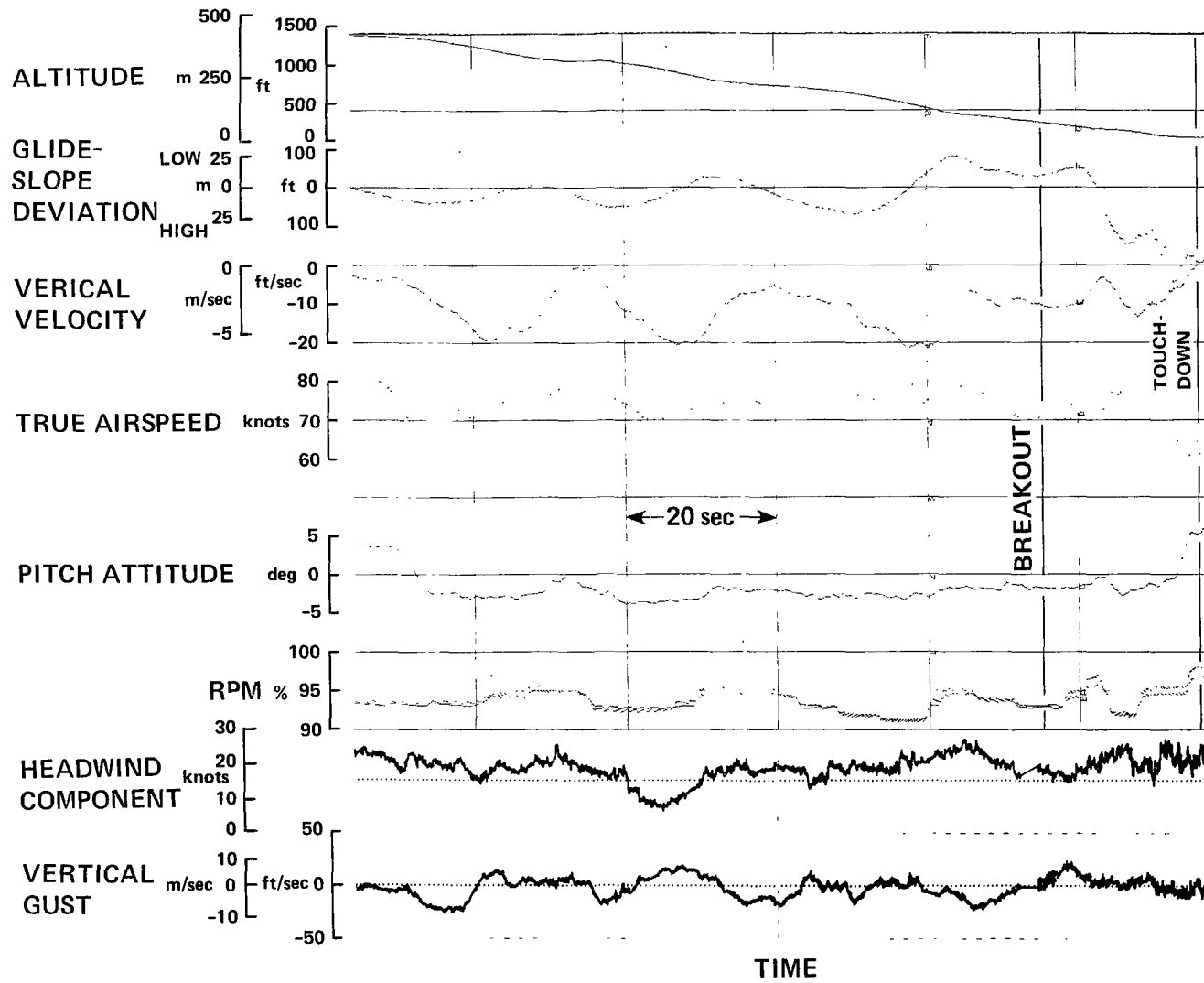


Figure 34.— Landing approach in turbulence — throttle-nozzle interconnect.

Airspeed stabilization— The airspeed stabilization system shown previously in figure 19 used a feedback gain to the nozzles of $K_V = +8.4^\circ/\text{knot}$ and a complementary filter break frequency of 0.25 rad/sec. The resulting flightpath to attitude control sensitivity was $\Delta\gamma_{SS}/\Delta\theta_{SS} = 0.55^\circ/\text{deg}$. This system permitted the pilot to track the glide slope with the pitch control with only occasional adjustments of thrust for large path-angle changes. Figure 35 shows the behavior of the aircraft during an approach. The flare could also be performed with pitch as it could for the basic aircraft, although some thrust reduction was required to inhibit a tendency to float. Some speed bleed-off occurs during the final flare; for this example the bleed-off is approximately 4 knots. These characteristics were the basis for pilot ratings of 3.5 to 4.5 for IFR glide-slope tracking and 3.5 to 5 for flare and landing. The pilots expressed a desire for a more authoritative path control and quicker heave response for flightpath changes on short final and for the flare maneuver. Hence, they were unwilling to give the system clearly satisfactory ratings. Speed excursions during maneuvers and in the presence of turbulence were substantially reduced by the system and hence path disturbances that would ordinarily be induced were largely suppressed. Brief evaluation of the system with a lower speed feedback gain ($K_V = 5.0^\circ/\text{knot}$) yielded more criticism of the magnitude of pitch excursions required for glide-slope corrections. One pilot rated this system one-half rating unit worse than the baseline configuration. A number of approaches were flown with a complementary filter break frequency of 1.0 rad/sec; an example is shown in figure 36. The pilots objected to the amount of nozzle control activity and to the corresponding longitudinal accelerations produced by turbulence in this frequency range. The break frequency of 0.25 rad/sec, which was finally selected, seemed to provide the best compromise for suppressing the aircraft's response to wind gradients while avoiding the disturbing high-frequency control activity associated with horizontal gusts.

It should be reiterated that the mechanization of this speed-control concept, which produced commands to the nozzles as a function of speed error, permitted speed standoff errors to develop during pitch maneuvers for large glide-slope corrections. In part due to these speed variations, steady-state flightpath response to pitch attitude was reduced. If the speed standoff was eliminated during the sustained corrections, for example by introducing a nozzle command in proportion to the integral of speed error, the flightpath response to attitude could be increased to about $\Delta\gamma_{SS}/\Delta\theta_{SS} = 0.9$. As a consequence, the pilot's objections to the performance of this system would be partially alleviated.

Flightpath command and stabilization— The flightpath control configuration described previously in figure 22 consisted of attitude, flightpath, and airspeed feedback gains of $K_T = 1.0^\circ/\text{deg}$, $K_G = -0.6^\circ/\text{deg}$, and $K_V = 8.4^\circ/\text{knot}$, and an airspeed complementary filter break frequency of 0.25 rad/sec. The flightpath control response to attitude was $\Delta\gamma_{SS}/\Delta\theta_{SS} = 1.2^\circ/\text{deg}$ in the steady state. An example of a landing approach in a light tailwind and light turbulence is shown for this configuration in figure 37. Since the approach could be flown using attitude control alone, the pilot was not required to manipulate the throttles, other than to reduce thrust during the latter stages of the flare to counteract any tendency to float. The engine activity indicated in figure 37 is contributed by the flightpath SCAS. Flightpath control authority was satisfactory and response to pitch inputs was crisp and precise. Flightpath authority ranging from level flight down to -13° has been demonstrated for this configuration. As a consequence of the pilot's simplified control procedure and the improved heave response, the workload for glide-slope tracking was reduced and pilot ratings ranging from 2 to 4 were given for IFR operation down to 30-m (100-ft) minimums. These ratings apply for operation in light turbulence, with horizontal shears up to 1.5 knots/sec. The pilot rating of 4 was primarily attributed to the workload associated with the instrument scan for

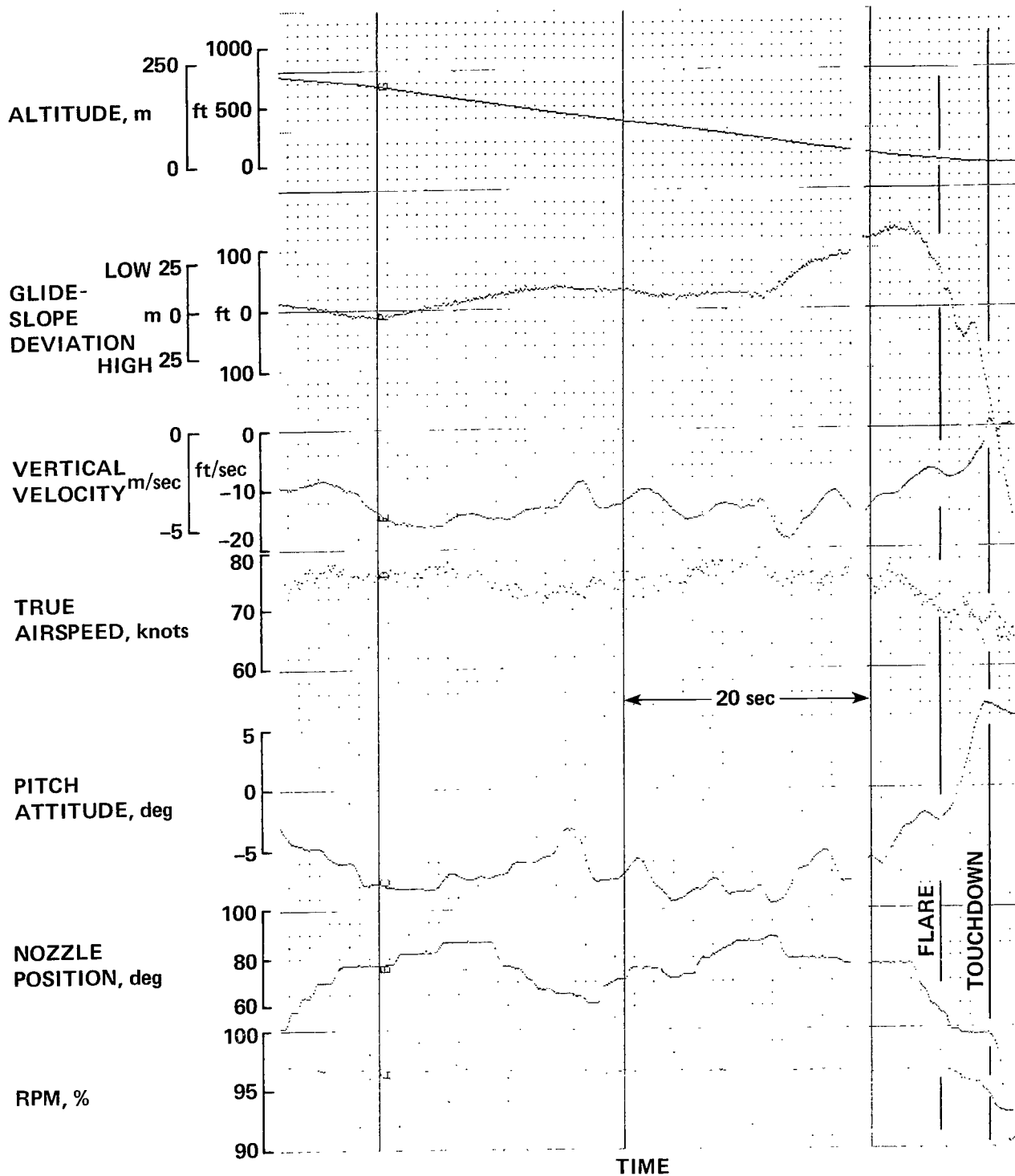


Figure 35.— Landing approach time history — airspeed-stabilization system with 0.25 rad/sec filter.

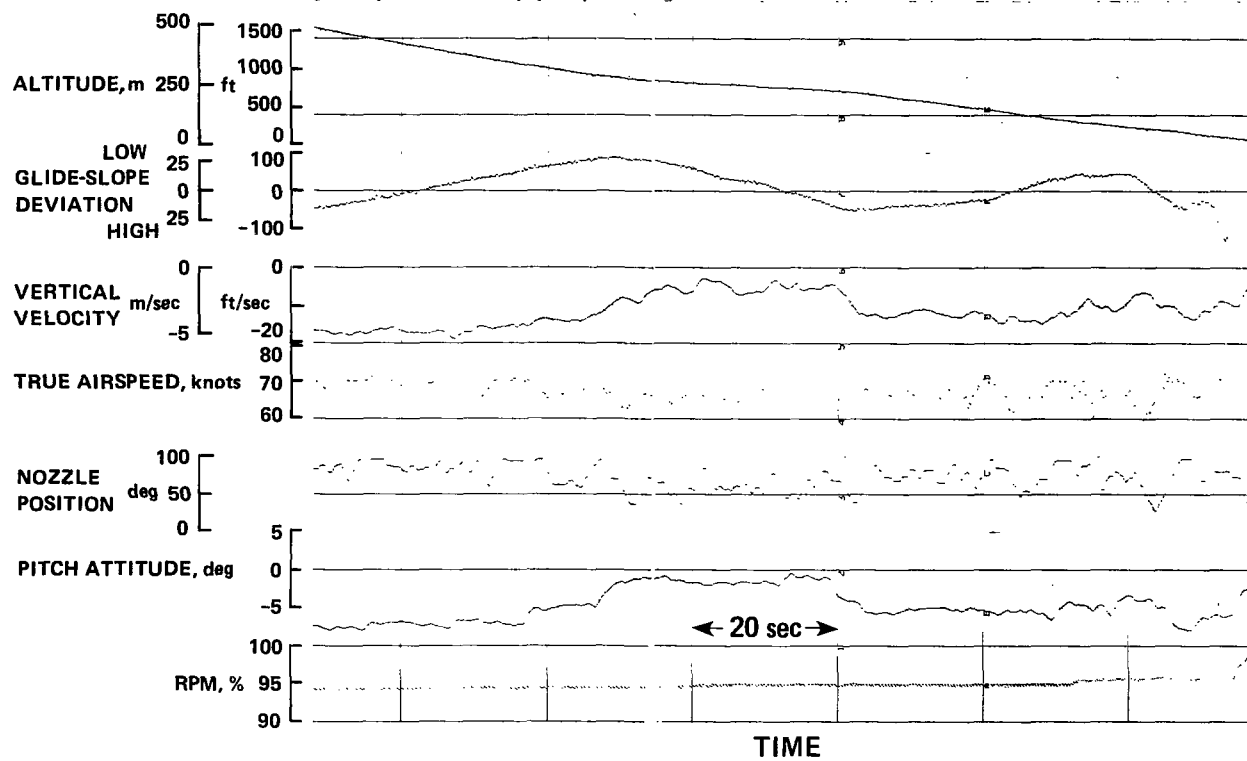


Figure 36.— Landing approach time history — airspeed-stabilization system with 1.0 rad/sec filter.

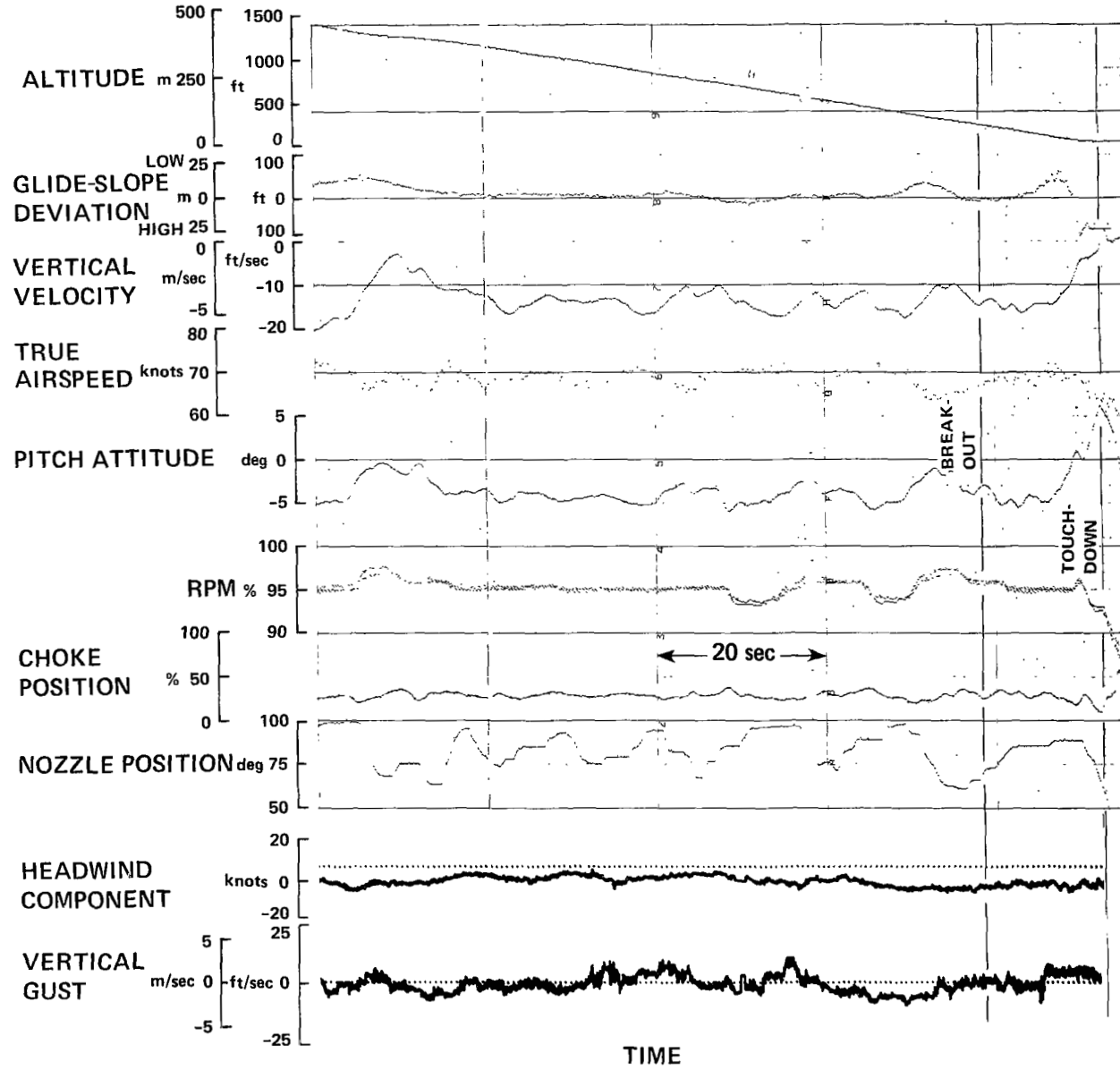


Figure 37.— Landing approach in turbulence – flightpath-airspeed SCAS.

the raw data IFR approach. Improvements in this rating that can be obtained with a flight director will be discussed subsequently.

A brief evaluation was obtained for the system with a somewhat lower attitude feedback gain, $K_T = 0.6^\circ/\text{deg}$, and a flightpath-to-attitude sensitivity of $\Delta\gamma_{SS}/\Delta\theta_{SS} = 0.8^\circ/\text{deg}$. Although the pilots still appreciated the simplified control for this configuration, they objected somewhat to the larger attitude excursions required for glide-slope tracking and to the relatively more sluggish glide-slope corrections. Apparently, $\Delta\gamma_{SS}/\Delta\theta_{SS}$ ratios somewhat exceeding 1:1 are preferred for tracking the 7.5° approach path.

The landing flare for the flightpath SCAS ($K_T = 1.0$), shown in figure 38, proved to be a much more docile maneuver than for the basic aircraft. Based on the improved heave response to pitch and the relatively low workload required to achieve the desired landing precision, pilot ratings of 2.5 to 3 were obtained for the flare. Figure 39 presents a comparison of several of the flare profiles for this configuration and the basic aircraft. The reduction in pitch rotation and the less abrupt maneuver required for the flare are evident. Landing performance, in terms of touchdown dispersions and sink rates, are comparable for both configurations (fig. 40). In either case, the performance falls within acceptable dispersion and landing gear limits. The improvement that the pilots note for the flightpath SCAS over the basic aircraft concern the ease and confidence with which they can obtain the desired level of landing performance.

It should be noted that the aircraft's ground roll could be reduced somewhat by reducing the touchdown velocity. In this regard, it would be advantageous to disable the speed-stabilization control logic by restraining the nozzles at a fixed position that exists at flare entry or at a pre-specified altitude. This would allow more speed to bleed-off during the flare than the 4- to 5-knot reduction that typically occurs with the speed-stabilization system engaged.

The alternative flightpath SCAS configuration, which used washed-out commands to the augmentor chokes while leaving the throttles fixed, also provided quite good glide-slope tracking. This configuration had a flightpath-to-attitude sensitivity of $\Delta\gamma_{SS}/\Delta\theta_{SS} = 0.9^\circ/\text{deg}$; it was not quite as quick in response to commanded flightpath corrections as the system that uses the throttles and chokes in combination. An example of an approach and landing is shown in figure 41. Although the pilots noted the difference in the initial response time, their ratings of the system for glide-slope control were essentially the same as for the baseline flightpath SCAS (PR = 2 to 4). Attitude control activity for glide-slope tracking and flare appear similar in figures 41 and 37. This approach was flown in turbulence with horizontal shears up to 1.0 knot/sec persisting for 7 sec, and with peak vertical gusts of ± 1.8 m/sec (± 6 ft/sec). It can be seen that the system works well to suppress glide-slope disturbances in the presence of the noted wind shear activity.

Cockpit Displays

Raw data information— For the evaluations of the various control configurations discussed previously, objections were registered concerning the instrument scan workload between the EADI and HSI; one pilot could not justify a rating better than 4 for glide-slope tracking with the best flightpath SCAS configuration. Favorable comments were received regarding the use of the flightpath bar as an aid in glide-slope tracking. In some instances, the pilots felt this element provided information to anticipate glide-slope deviations and to lead incremental flightpath corrections.

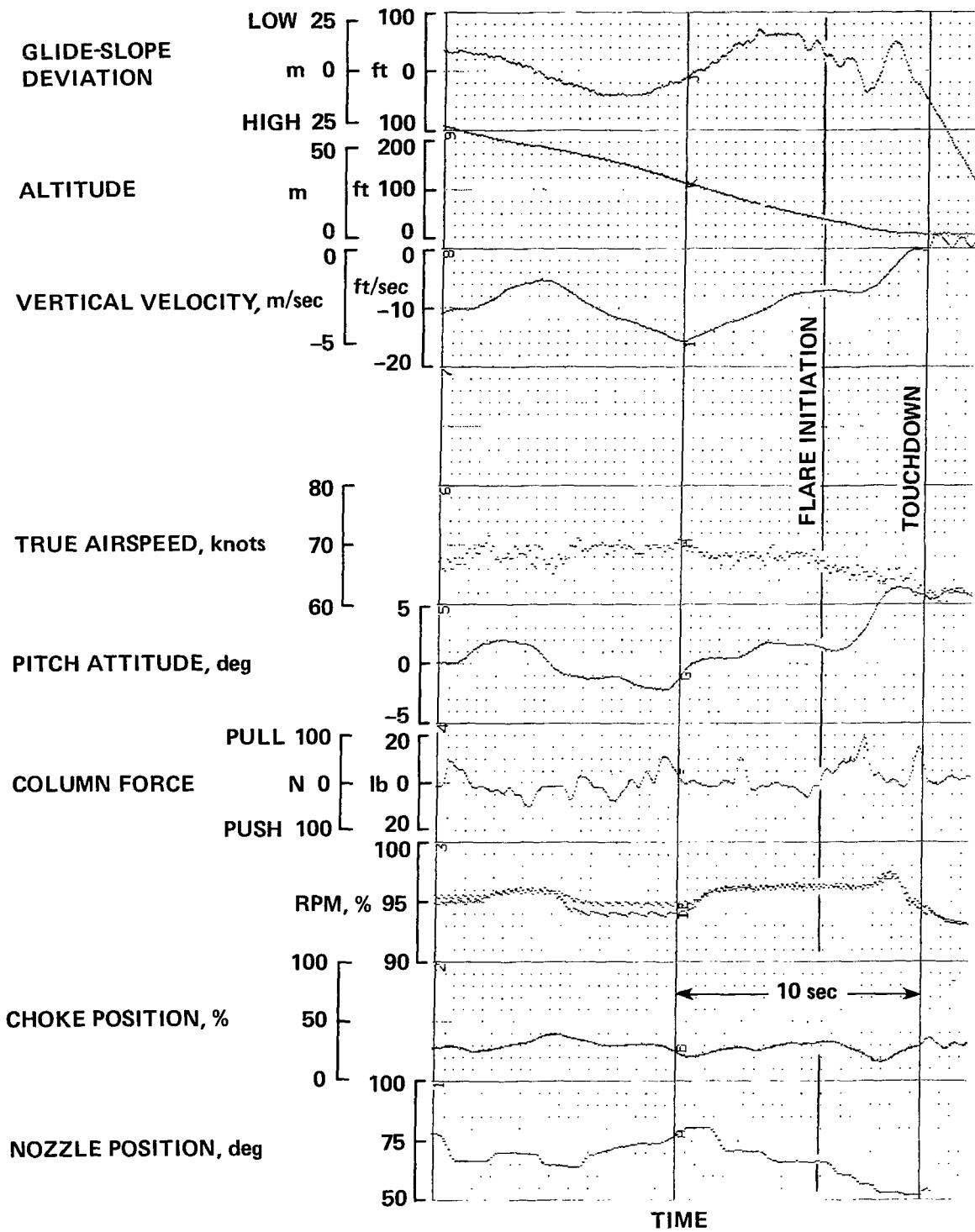
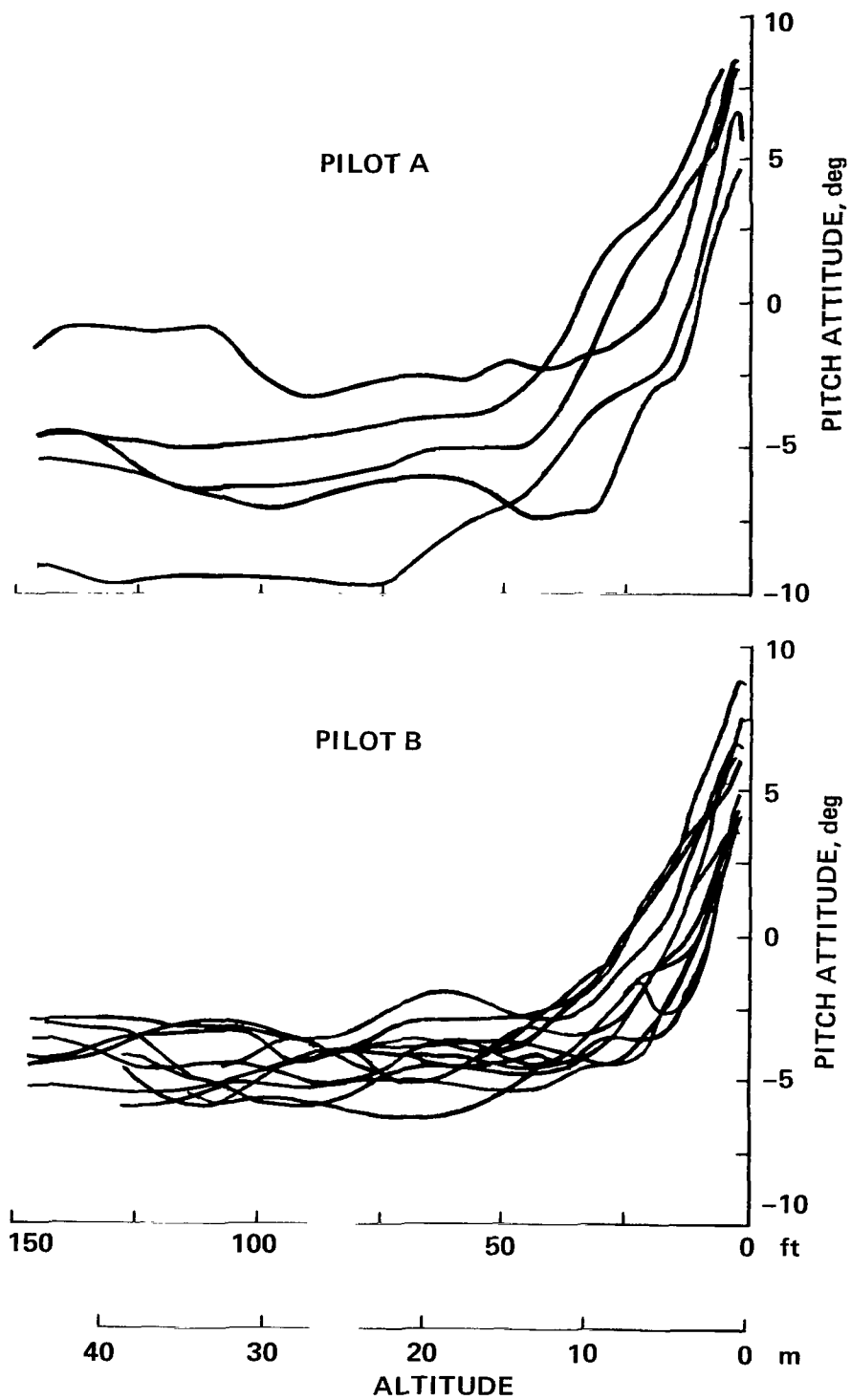
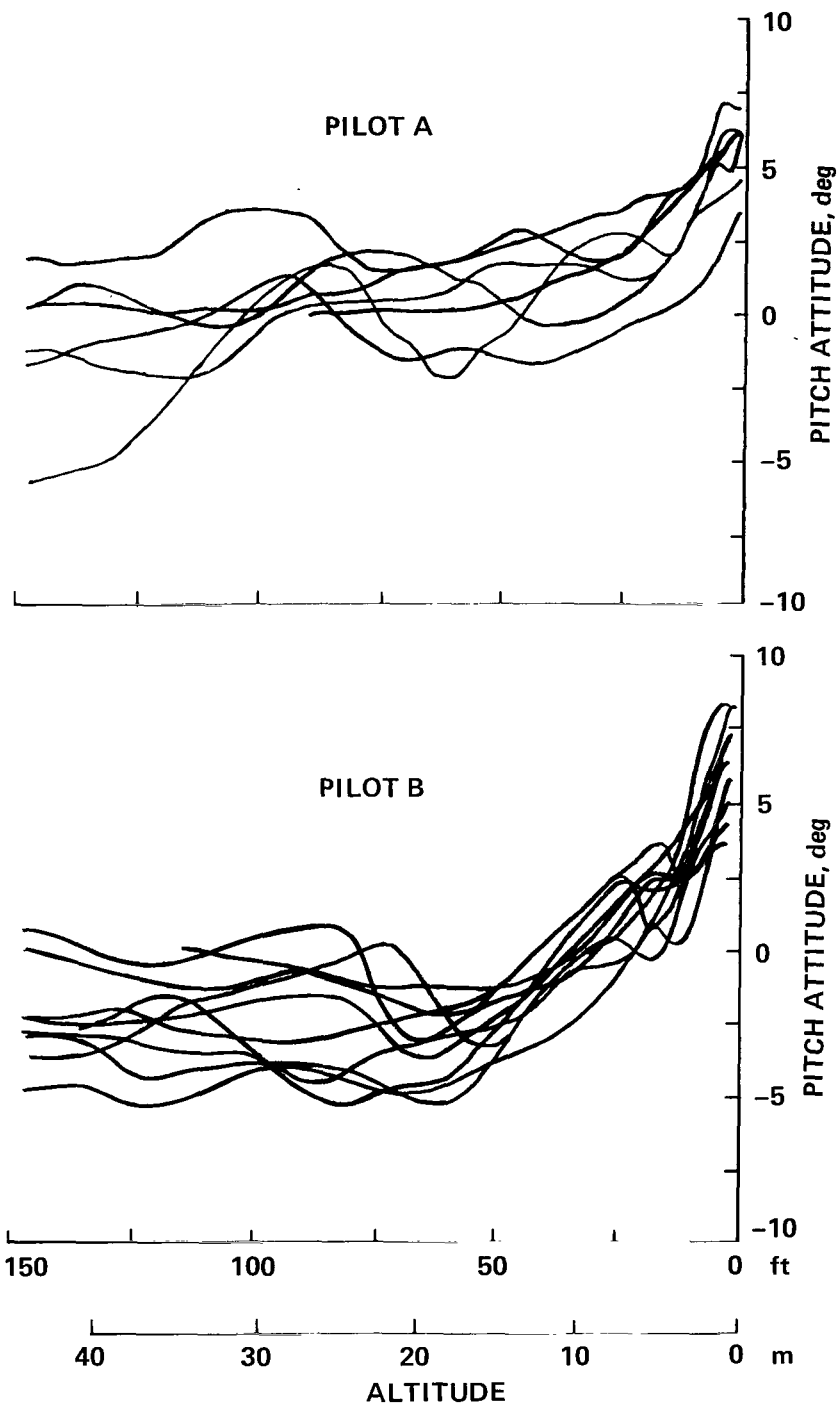


Figure 38.— Flare and landing time history — flightpath-airspeed SCAS.



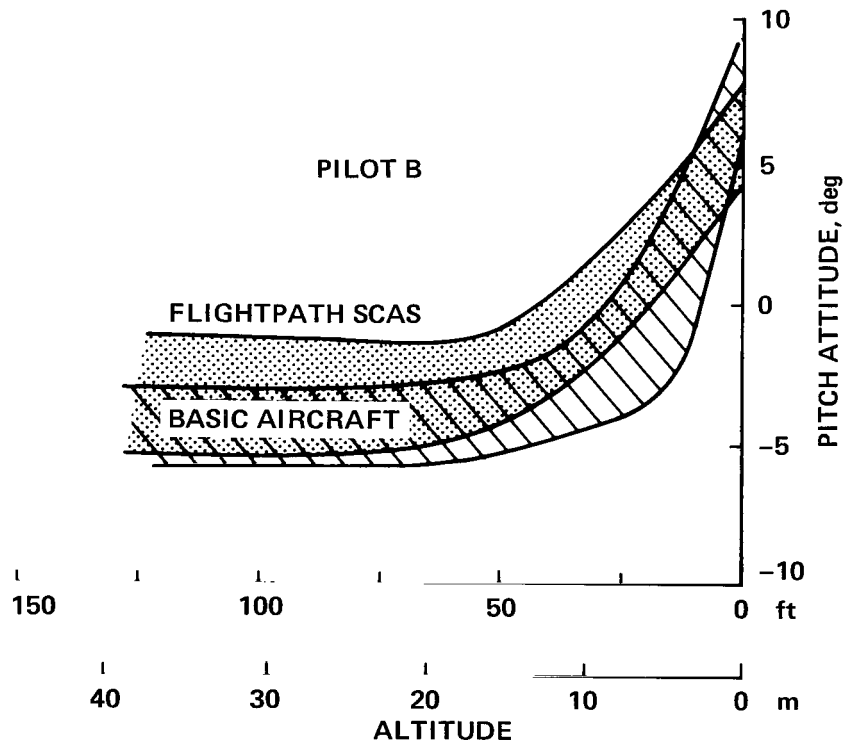
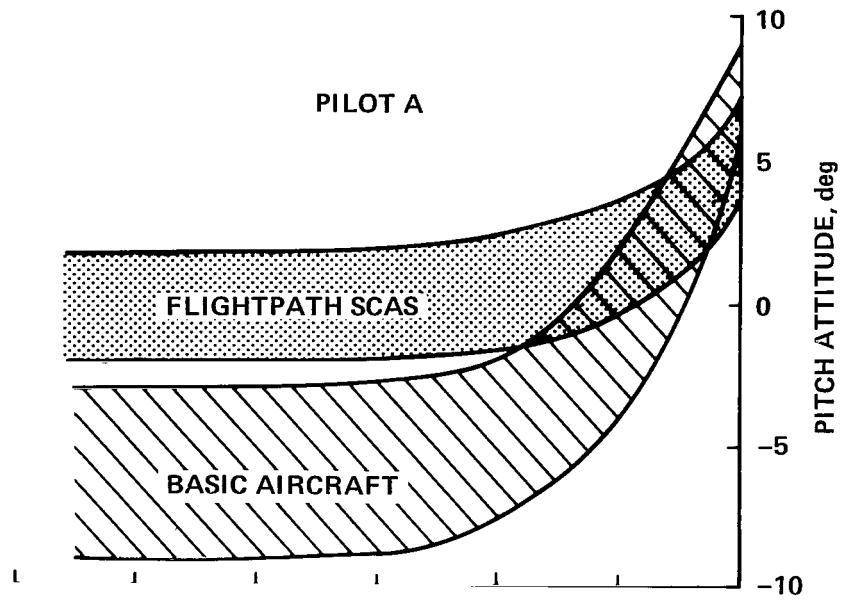
(a) Basic aircraft with pitch, roll, and yaw SCAS.

Figure 39 – Landing flare profiles.



(b) Flightpath SCAS.

Figure 39.— Continued.



(c) General comparison of landing flare profiles.

Figure 39.— Concluded.

	□	▨
CONFIGURATION	BASIC AIRCRAFT + PITCH, ROLL, YAW SCAS	FLIGHTPATH SCAS
NUMBER OF LANDINGS	18	16
MEAN TOUCHDOWN DIST	156 m (514 ft)	151 m (495 ft)
MEAN SINK RATE	1.2 m/sec (3.8 ft/sec)	1.0 m/sec (3.4 ft/sec)

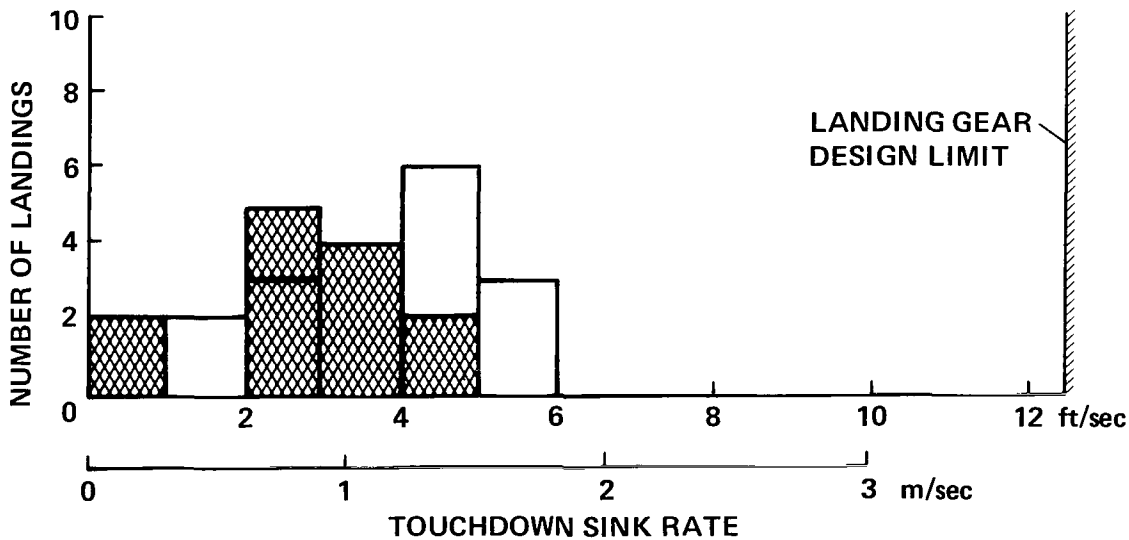
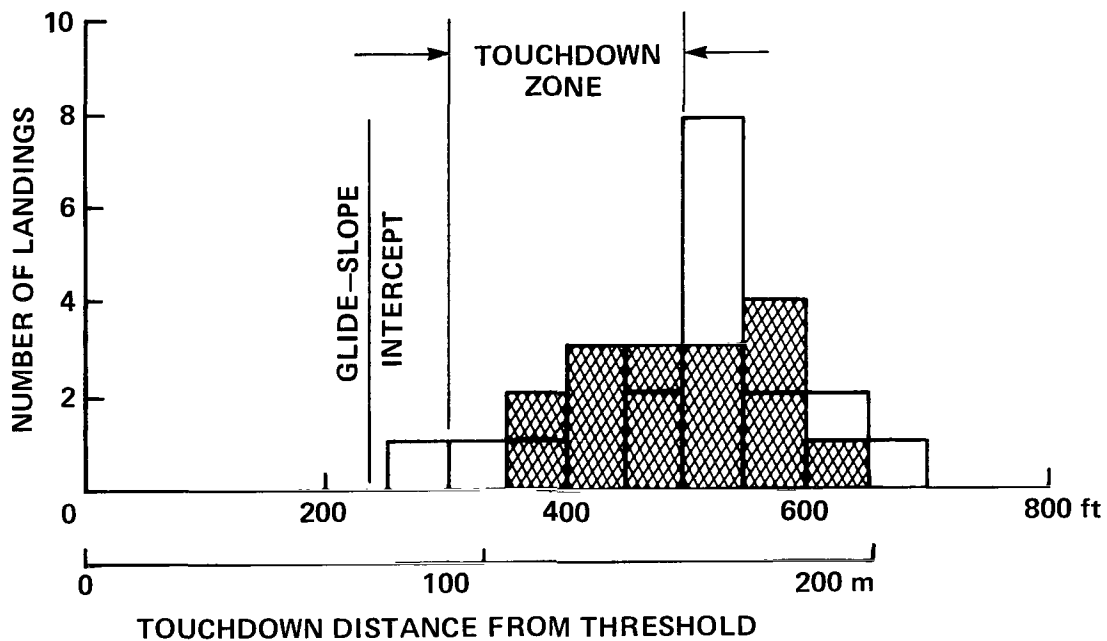


Figure 40.— Comparison of landing performance.

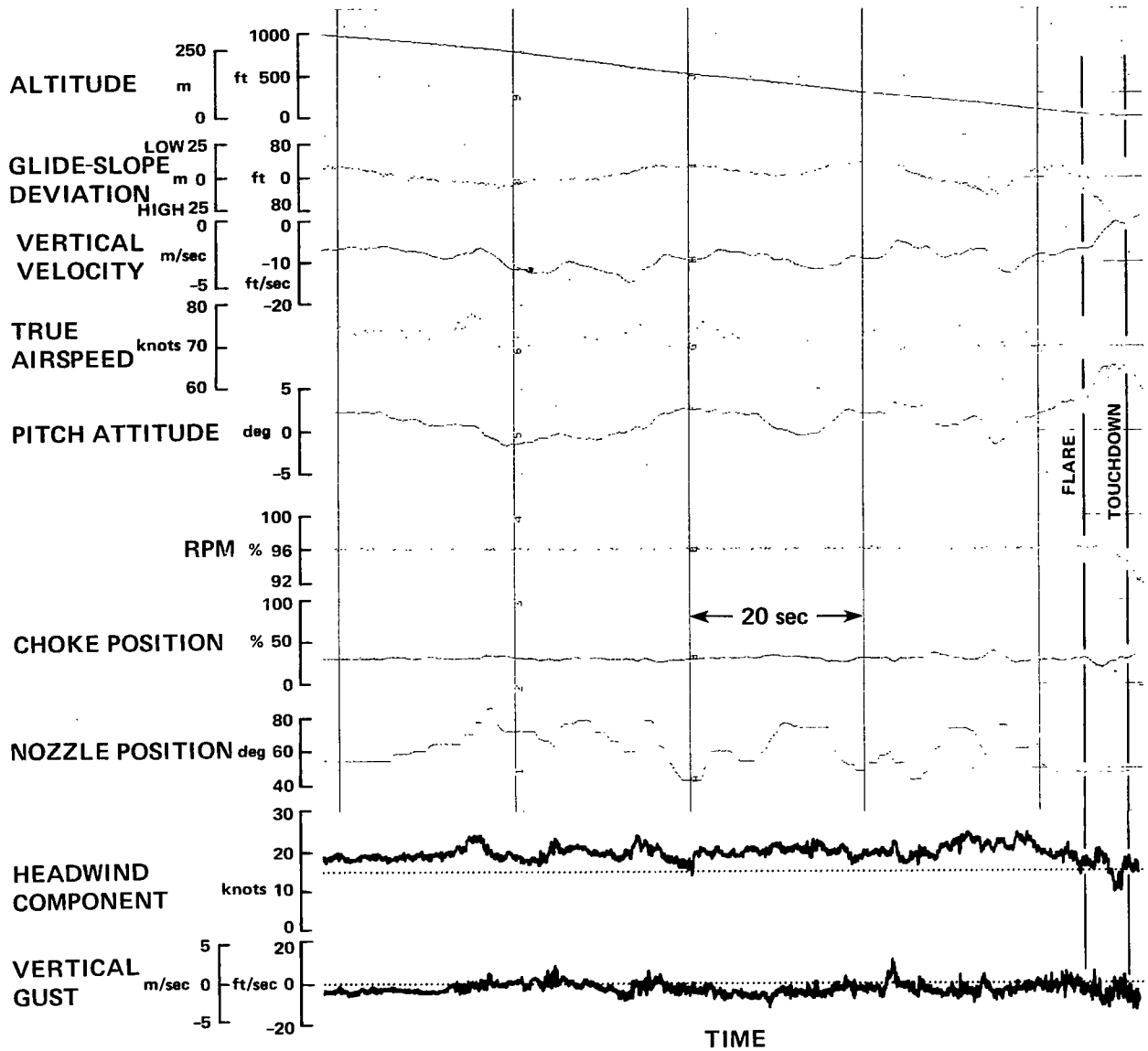


Figure 41.— Landing approach time history — alternate flightpath-airspeed SCAS.

These improvements were felt to warrant a one-half to one unit improvement in pilot rating for the poorer flightpath control configurations. Although the presentation of raw glide-slope and localizer deviation on the MLS box provided a more integrated display, the absence of heading information on the EADI forced the pilots to still scan both the EADI and HSI for localizer tracking. Consequently, little overall improvement in scanning workload was offered by having the MLS box on the EADI.

Flight director— Two flight director concepts were evaluated in conjunction with the flightpath control configurations: one for the throttle-nozzle interconnect system and one for the final flightpath SCAS. Flight director logic for the throttle-nozzle interconnect was tailored to the

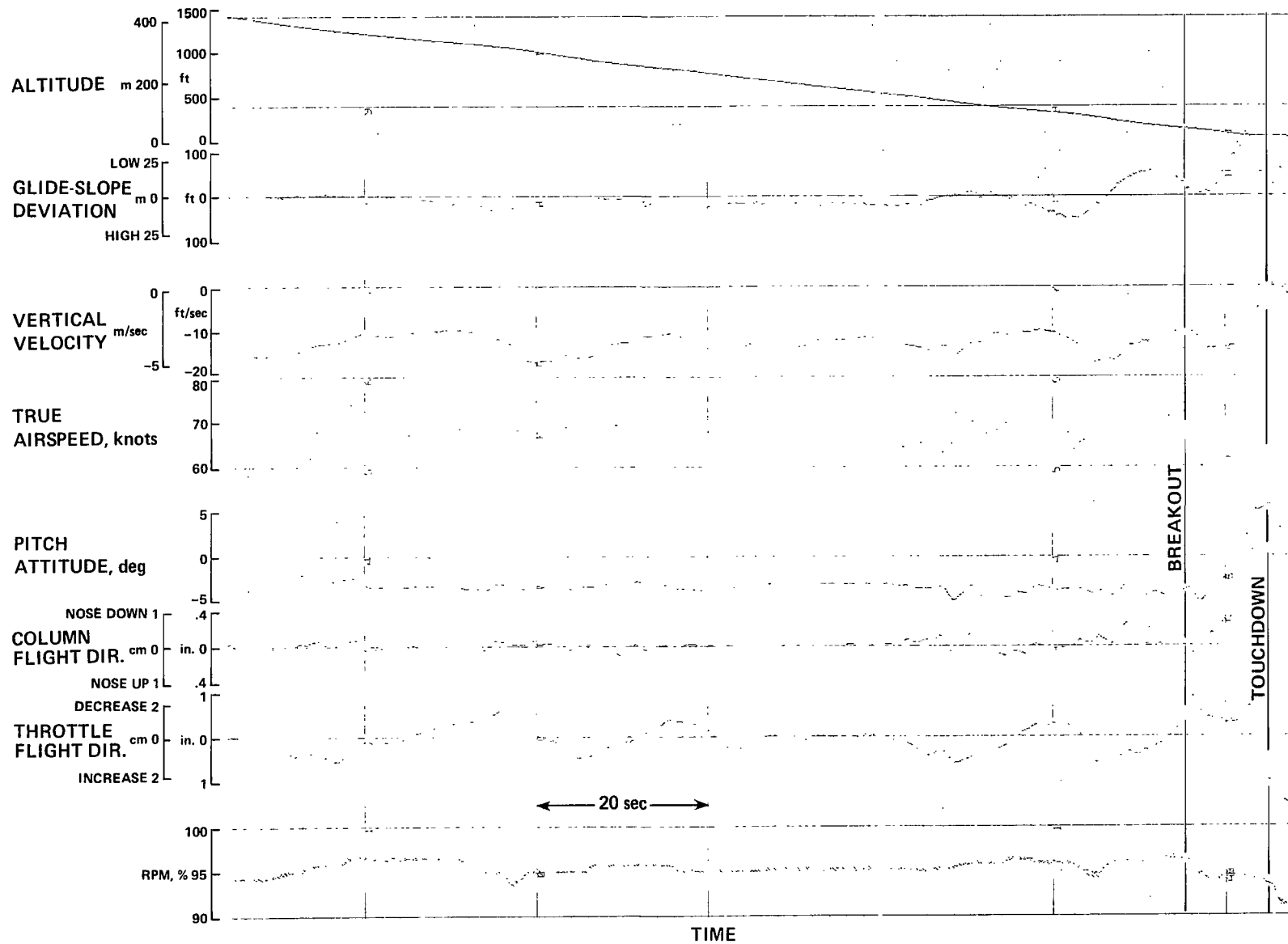
“backside” (*B*) control technique, that is, the use of thrust for glide-slope tracking. The logic for the flightpath SCAS was based on the “frontside” (*F*) control technique, which used pitch attitude for glide-slope control. In either case, the flight director provided a significant reduction in scanning workload and a reduction in vertical and lateral path excursions during the approach; as a result, the aircraft generally arrived at decision height better established for a precise flare and landing.

A time history of an approach for the throttle-nozzle interconnect system combined with the flight director is shown in figure 42. Smooth glide-slope corrections are evident, little throttle control activity exists, and speed excursions are minimal. Localizer capture results in an initial overshoot, and some lateral control activity continues throughout the approach. In general, the pilots felt glide-slope tracking could be performed quite easily with the throttle, and that the flight director activity was appropriate to the task. Localizer tracking was also felt to be quite precise; however, the lateral flight director was considered to be busier than desired. Although no further gain adjustments were made in the lateral flight director for the flight program, a slight reduction in either the roll-rate feedback gain or in the director display gain would reduce the objectionable activity.

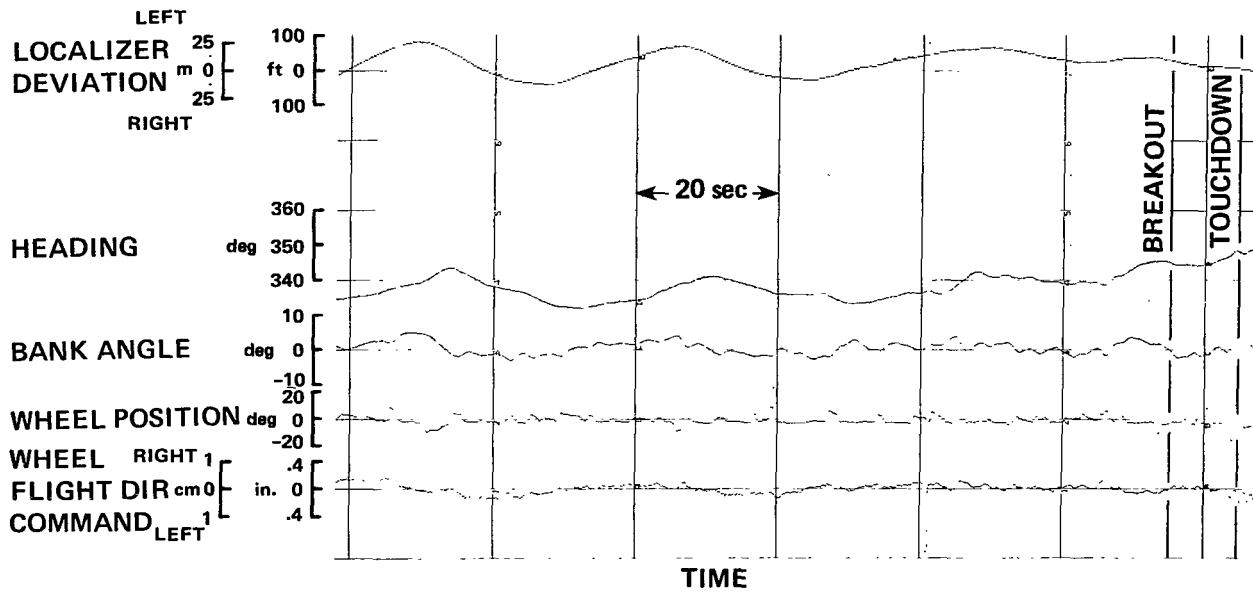
It should be noted that the pilots' perceptions of path tracking performance were based in part on their observations of path deviations as shown by the MLS box. The dimensions of the box were ± 13.5 m (44 ft) vertically by ± 30 m (100 ft) laterally. It is now felt that these dimensions were larger than would be appropriate for operation to instrument minimums that are comparable to those of current commercial jet transports. If the dimensions of the MLS box had been smaller, the pilots' judgments of path tracking performance could have been altered. However, the ultimate judgment of the accuracy of approach path tracking is based on the situation that the pilot observes at breakout and with which he must contend to successfully accomplish the landing. In this sense, it is felt that the pilots' impressions of tracking performance were reflected accurately.

Overall pilot ratings for the instrument approach to a decision height of 30 m (100 ft) ranged from 2 to 3. The ratings apply to the flying qualities of the aircraft associated with the precision approach tracking task to breakout and reflect the fact that the pilots felt comfortable with their ability to track the glide slope and localizer with sufficient accuracy to be able to successfully execute the flare and landing. It should be stated that this experiment was not intended to be an extensive investigation of all the factors that lead to the determination of a decision height for instrument operations, but rather was an exploration of the appropriate flying qualities issues associated with the task.

An example approach is shown in figure 43 for the flightpath SCAS and flight director. Again, good glide-slope tracking is observed, and pitch-attitude corrections are smooth and of generally small magnitude. Wind shears up to 1 knot/sec and persisting for up to 9 sec occurred toward the end of the approach; however, glide-slope tracking was not disturbed appreciably. Overall pilot ratings for this configuration were excellent; they ranged from 1.5 to 2.5 for approach to a 30-m (100-ft) decision height. With the exception of the annoyance with the lateral director's activity, it was felt that few additional improvements could be made in the system.



(a) Throttle-nozzle interconnect-flight director.
 Figure 42.— Landing approach time history.



(b) Lateral flight director.

Figure 42.— Concluded.

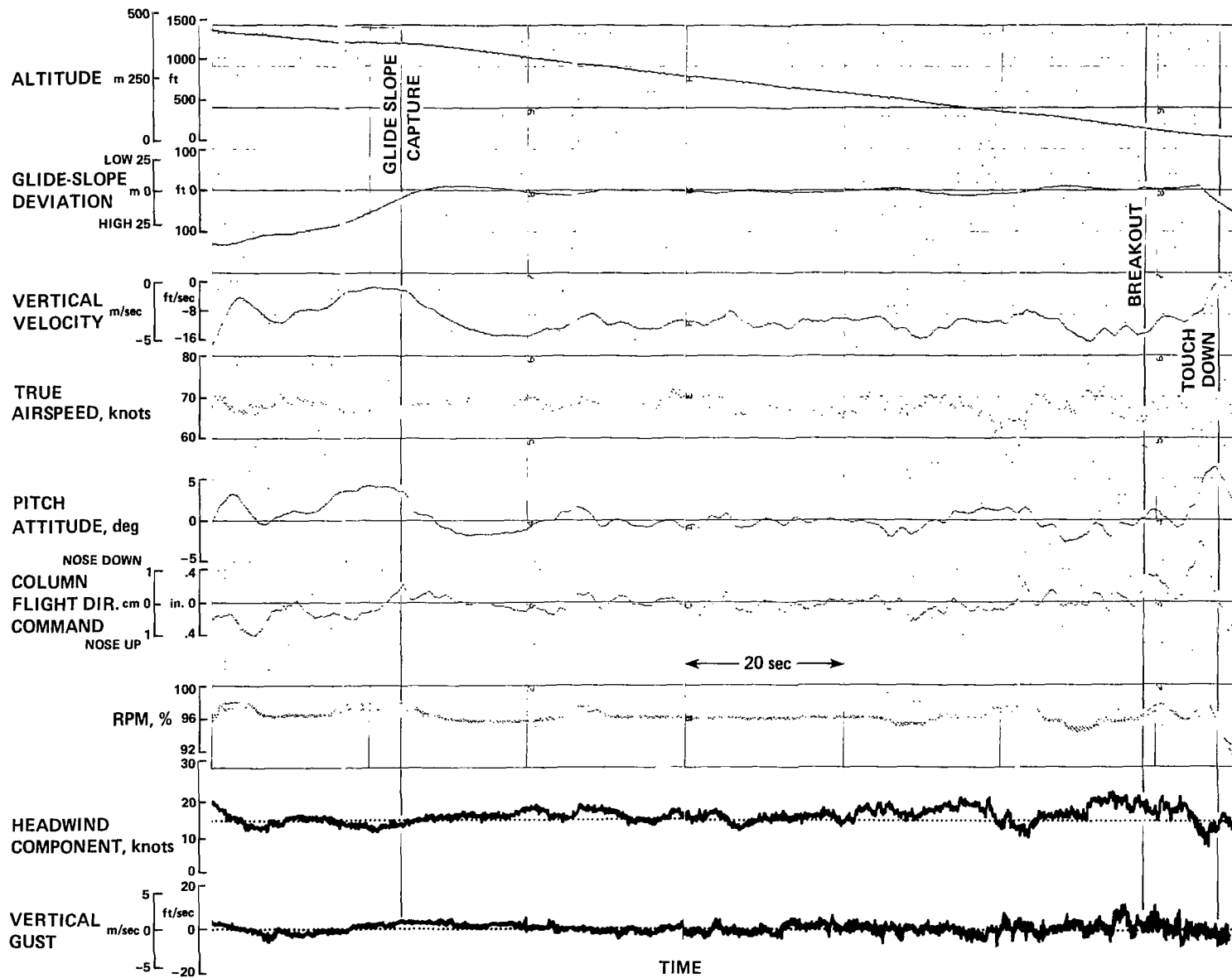


Figure 43.— Landing approach time history – flightpath-airspeed SCAS; flight director.

Summary of Control-Display Results

A graphic summary of the trade-off in flying qualities for the approach and landing with the various control system and display concepts investigated in this program is presented in figure 44. Individual pilot ratings are shown for IFR approaches to instrument minimums, using either raw data information or an appropriate flight director, and for the flare to touchdown. Starting with the basic aircraft configuration — which is only marginally acceptable for the IFR task and for precision, low-sink rate landing — it is possible to achieve essentially satisfactory flying qualities for the approach with the most sophisticated control system evaluated in this program — the flightpath SCAS. It is also possible to obtain completely satisfactory results with a very simple control system (the throttle-nozzle interconnect, which essentially decouples flightpath and airspeed response to the primary flightpath control) in combination with a three-cue flight director. Furthermore, excellent flying qualities can be obtained with the flightpath SCAS and an appropriately configured flight director using only pitch and roll commands. It must be emphasized that these control system and flight director concepts are predicated on good attitude control, and require pitch, roll, and yaw SCAS to insure good flying qualities.

For the flare and landing, satisfactory flying qualities and landing precision at low sink rates can be obtained with the flightpath SCAS. Results of ground-based flight simulator evaluations of STOL landings at low sink rates that were performed using thrust as the primary sink rate control, have indicated the possibility of similarly satisfactory results if the engine thrust response time is sufficiently low (ref. 19). Flight results from the Princeton Variable Stability Navion (ref. 20) and as yet unpublished data obtained during flight experiments at NASA with the Augmentor Wing Research Aircraft verify this capability. One configuration evaluated during the latter experiments incorporated the throttle-nozzle interconnect system combined with a washed-out throttle input to the augmentor chokes to quicken the heave response to throttle inputs. Effective first-order thrust response time constants of about 0.25 sec were produced for wash-out time constants of 3 sec. The resulting pilot ratings for the flare and landing were fully satisfactory (PR < 3.5). Landing precision was equivalent to that obtained with the flightpath SCAS and the pilots were fully confident of their ability to use the thrust control for the flare.

These results indicate a number of options available to the designer to achieve satisfactory flying qualities for STOL operations to minimum decision heights of 30 m (100 ft), and to achieve good landing precision. For the pitch-attitude control, either rate-command-attitude-hold or attitude-command systems are acceptable. For aircraft that require significant pitch maneuvering to maintain the approach flight reference (airspeed, angle of attack, or some more general combination thereof) and to perform the landing flare, the rate-command-attitude-hold concept is preferred. The attitude-command system is likely a better choice for aircraft that do not require appreciable pitch maneuvering during the approach and landing. With either system concept, bandwidths of 2 rad/sec are entirely satisfactory. Control sensitivities of $0.9^\circ/\text{sec}/N$ ($0.4^\circ/\text{sec}/lb$) for the rate-command system and $0.13^\circ/N$ ($0.6^\circ/lb$) for the attitude-command system were found to be satisfactory.

Only a rate-command-bank-angle hold system was evaluated for roll control. When used in conjunction with yaw SCAS, this system was found to be satisfactory when designed for bandwidths of 2 rad/sec and for control sensitivities of $0.9^\circ/\text{sec}/N$ ($4.2^\circ/\text{sec}/lb$).

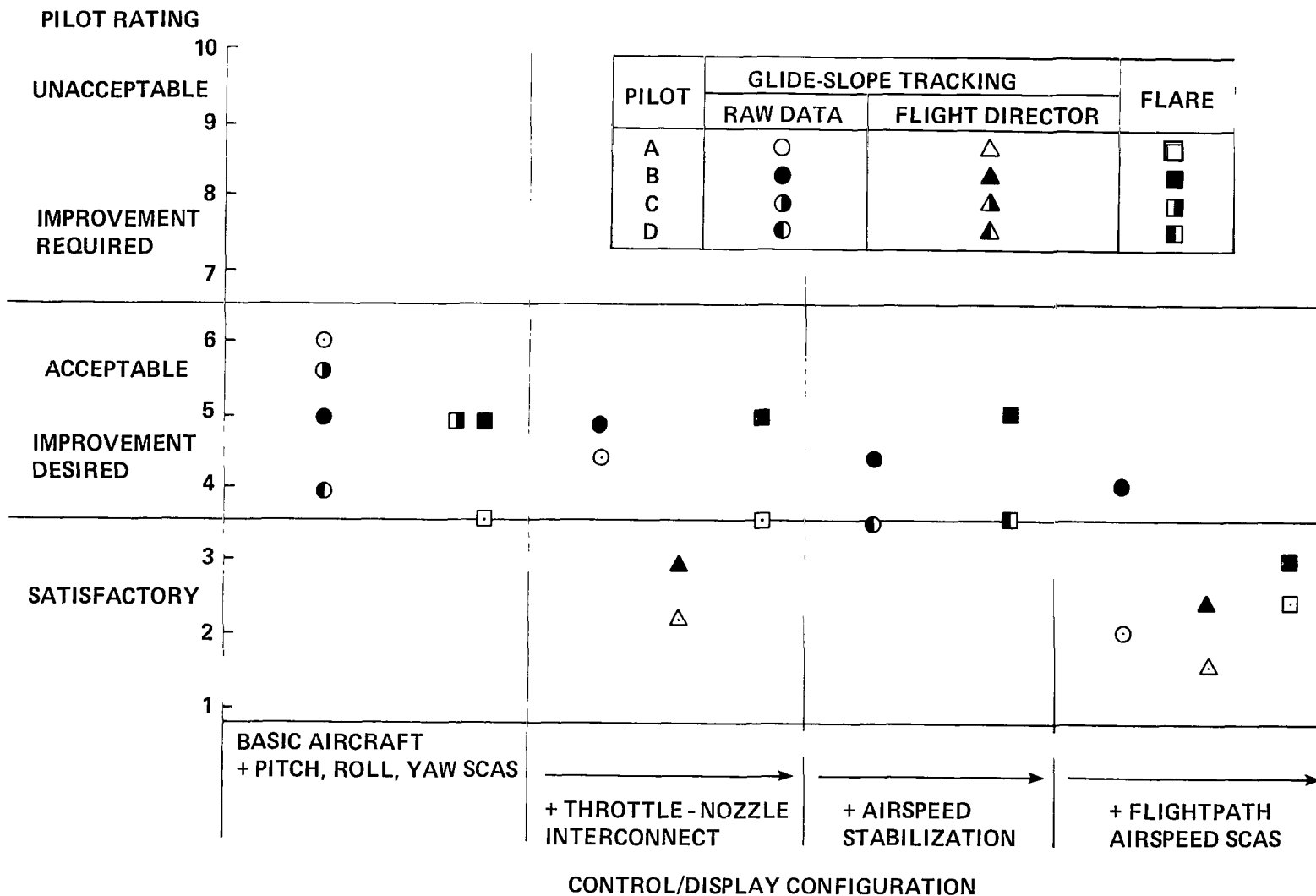


Figure 44.— Summary of pilots' evaluations of IFR glide-slope tracking and landing flare.

For flightpath control during the landing approach, where the backside control technique is to be used, it is necessary to minimize airspeed response to the flightpath controller to obtain satisfactory flying qualities for glide-slope tracking. Levels of vertical velocity damping of the order of -0.45 sec^{-1} and thrust time constants of the order of 0.8 sec are acceptable. When the front-side control technique is to be employed, the ratio of flightpath response to pitch attitude should be greater than 1 in the steady state ($\Delta\gamma_{ss}/\Delta\theta_{ss} > 1.0$) and preferably should be of the order of 1.2. Vertical velocity damping should be about -0.8 sec^{-1} . Speed-stabilization system design should, if possible, incorporate integral error feedback or suitable feed-forward commands to the speed control device to eliminate speed standoff errors during sustained flightpath corrections and to maintain the desired approach reference.

When a requirement exists to execute a landing flare to achieve low touchdown sink rates, and when the maneuver is to be primarily accomplished through pitch rotation, the short-term ratio of flightpath response to attitude should approach 1:1 ($\Delta\gamma_{max}/\Delta\theta_{ss} \doteq 1.0$). If a speed stabilization system is used during the approach, it would be preferable to disengage the system during the flare to allow speed to decay normally in order to reduce the subsequent ground distance. If the flare maneuver is to be accomplished through control of thrust, the generation of propulsion-induced force should follow the pilot's thrust control input with an effective time constant of the order of 0.25 sec to insure satisfactory flare control.

Although only limited data have been published on the two prototype Advanced Medium STOL Transport (AMST) aircraft, the attitude, airspeed, and flightpath control characteristics of the YC-15 closely correspond to those of the throttle-nozzle interconnect configuration. The same control characteristics of the YC-14 closely correspond to those of the flightpath SCAS configuration. The results of the flight experiment reported here indicate that fully satisfactory flying qualities can be obtained readily for either of the AMST prototypes.

CONCLUSIONS

A flight research program was conducted using the Ames Research Center's Augmentor Wing Research Aircraft to assess the effectiveness of manual control concepts and cockpit displays in improving attitude (pitch, roll, and yaw) and longitudinal path control during STOL approaches and landings.

Substantial improvements in manually flown IFR approaches were obtained with stabilization and command augmentation systems ranging in complexity from a simple interconnect between the controls for thrust magnitude (throttles) and thrust deflection (nozzles), to sophisticated path-speed stabilization and command configurations. The basic aircraft is given pilot ratings in the 5-6 range for raw data IFR approaches to a 60-m (200-ft) decision height; those ratings can be improved to the 2.5 to 4 range with the most complex SCAS. The addition of a flight director, to overcome deficiencies of the raw data instrument scan, permit the rating to be improved to the 1.5 to 2.5 category for operation to a 30-m (100-ft) decision height. Thus, it appears feasible to obtain satisfactory flying qualities for powered-lift aircraft for precision approaches to decision heights of the order of current instrument flight minimums.

The capability to accomplish a gentle flare maneuver to a low touchdown sink rate can also be provided by systems that augment the basic aircraft's heave response. Improvements in pilot ratings for the flare to the 2-3 category can be obtained.

Ames Research Center

National Aeronautics and Space Administration

Moffett Field, California 94035, February 14, 1980

APPENDIX A

LONGITUDINAL AND LATERAL-DIRECTIONAL DYNAMICS FOR BASIC AIRCRAFT AND SCAS CONFIGURATIONS

Table 3 describes the various control system configurations that were evaluated in the subject flight experiments; it includes control system gains; time constants, damping ratios, and natural frequencies of the longitudinal and lateral-directional characteristic roots; and the key response parameters for each configuration. Table 4 presents the longitudinal and lateral-directional stability derivatives from which the characteristic roots were derived. These derivatives are appropriate for the aircraft in its landing approach configuration, with flight and loading conditions as indicated in table 4.

TABLE 3.— LONGITUDINAL AND LATERAL-DIRECTIONAL DYNAMIC RESPONSE CHARACTERISTICS

Configuration	Control system gains	Characteristic roots (based on flight-identified derivatives)				Response characteristics
Basic aircraft GW = 18,160 kg (40,000 lb) V = 65 knots $\delta_f = 65^\circ$ $\nu = 80^\circ$	All SCAS off	$\zeta_p = 0.2$	$\omega_p = 0.2 \text{ rad/sec}$	$\frac{n_z}{\alpha} = 1.74 \text{ g/rad}$		
		$\frac{1}{T_{sp1}} = 0.67 \text{ sec}^{-1}$	$\frac{1}{T_{sp2}} = 1.39 \text{ sec}^{-1}$	$\frac{d\gamma}{du} = 0.15^\circ/\text{knot}$		
		$\zeta_d = 0.14$	$\omega_d = 0.9 \text{ rad/sec}$	$\frac{\Delta u_{ss}}{\Delta \theta_{ss}} = -2.5 \text{ knot/deg}$		
		$\frac{1}{T_R} = 1.26 \text{ sec}^{-1}$	$\frac{1}{T_s} = -0.03 \text{ sec}^{-1}$	$\frac{\Delta \gamma_{max}}{\Delta \gamma_{ss}} = 2.1$	$\frac{\Delta u_{ss}}{\Delta \gamma_{ss}} = -2.9 \text{ knots/deg}$	
				$\frac{\Delta \beta}{\Delta \phi} = 0.65$		
Pitch SCAS	$K_\theta = 3^\circ/\text{deg}$ $K_q = 1.2^\circ/\text{deg/sec}$ $K_c = 0.75^\circ/\text{lb}$ $K_{F\theta} = 1.1^\circ/\text{deg}$	$\zeta_p = 0.99$	$\omega_p = 0.27 \text{ rad/sec}$	$\frac{\dot{\theta}}{F_c} = 0.4^\circ/\text{sec/lb}$		
		$\zeta_{sp} = 0.76$	$\omega_{sp} = 2.19 \text{ rad/sec}$	$\frac{\theta_{max}}{\theta_{ss}} = 1.0$		
Roll/yaw SCAS	$K_\phi = 3.3^\circ/\text{deg}$ $K_p = 4^\circ/\text{deg/sec}$ $K_w = 1.5^\circ/\text{deg}$ $K_{F\phi} = -3.8^\circ/\text{deg}$	$\zeta_d = 0.8$	$\omega_d = 1.54 \text{ rad/sec}$	$\frac{\dot{\phi}}{\delta_w} = 0.33^\circ/\text{sec/deg}$		
		$\frac{1}{T_R} = 2.28 \text{ sec}^{-1}$	$\frac{1}{T_s} = 0.55 \text{ sec}^{-1}$	$\frac{\phi_{max}}{\phi_{ss}} = 1.0$		
				$\frac{\Delta \beta}{\Delta \phi} \leq 0.1$		
Airspeed stabilization	$K_v = 8.4^\circ/\text{knot}$	$\zeta_p = 0.91$	$\omega_p = 0.53 \text{ rad/sec}$	$\frac{\Delta \gamma_{ss}}{\Delta \theta_{ss}} = 0.55$		
		$\zeta_{sp} = 0.76$	$\omega_{sp} = 2.19 \text{ rad/sec}$	$\frac{d\gamma}{du} = -0.5^\circ/\text{knot}$		

TABLE 5.— Concluded.

Configuration	Control system gains	Characteristic roots (based on flight-identified derivatives)	Response characteristics
Flightpath-airspeed SCAS	$K_V = 8.4^\circ/\text{knot}$ $K_G = -0.6^\circ/\text{deg}$ $K_T = 1.0^\circ/\text{deg}$ $K_{cc} = 5.7\%/\text{deg}$ $K_{TT} = 1.05\% N_H/\text{deg}$ $\omega_w = 0.5 \text{ rad/sec}$	$\zeta_p = 0.97$ $\omega_p = 0.65 \text{ rad/sec}$ $\zeta_{sp} = 0.77$ $\omega_{sp} = 2.16 \text{ rad/sec}$	$\frac{\Delta\gamma_{ss}}{\Delta\theta_{ss}} = 1.2$ $\frac{d\gamma}{du} = -1.1^\circ/\text{knot}$ $\frac{n_z}{\alpha} = 2.42 \text{ g/rad}$
Throttle-nozzle interconnect	$K_{NT} = -5^\circ/\% N_H$	Same as for pitch SCAS	$\frac{\Delta\gamma_{max}}{\Delta\gamma_{ss}} = 1.0$ $\frac{\Delta u_{ss}}{\Delta\gamma_{ss}} \doteq 0$

TABLE 4.— LONGITUDINAL AND LATERAL-DIRECTIONAL STABILITY DERIVATIVES ^a

Longitudinal		Lateral-Directional	
$X_u = -0.051 \text{ sec}^{-1}$	$Z_u = -0.33 \text{ sec}^{-1}$	$Y_v = -0.11 \text{ sec}^{-1}$	$N_\beta = 0.51 \text{ sec}^{-2}$
$X_w = 0.13 \text{ sec}^{-1}$	$Z_w = -0.51 \text{ sec}^{-1}$	$\frac{Y_{\delta_r}}{V_o} = 0.033 \text{ sec}^{-1}$	$N_p = -0.15 \text{ sec}^{-1}$
$\frac{X_q}{V_o} = 0.0058$	$\frac{Z_q}{V_o} = -0.045$	$L_\beta = -0.93 \text{ sec}^{-2}$	$N_r = -0.34 \text{ sec}^{-1}$
$\frac{X_{\delta_e}}{V_o} = 0.014 \text{ sec}^{-1}$	$\frac{Z_{\delta_e}}{V_o} = -0.049 \text{ sec}^{-1}$	$L_p = -1.06 \text{ sec}^{-1}$	$N_{\delta_w} = 0$
$\frac{X_{\delta_v}}{V_o} = -0.046 \text{ sec}^{-1}$	$Z_{\delta_v} = 0$	$L_r = 0.81 \text{ sec}^{-1}$	$N_{\delta_r} = -0.59 \text{ sec}^{-2}$
$X_{\delta_c} = 0$	$\frac{Z_{\delta_c}}{V_o} = 0.0014 \text{ sec}^{-1} / \%$	$L_{\delta_w} = 0.67 \text{ sec}^{-2}$	
$X_{\Delta T} = 0$	$\frac{Z_{\Delta T}}{V_o} = -0.0075 \text{ sec}^{-1} / \% N_H$	$L_{\delta_r} = 0.33 \text{ sec}^{-2}$	
$M_u = 0$	$M_{\dot{\alpha}} = -0.39 \text{ sec}^{-1}$		
$M_\alpha = -0.37 \text{ sec}^{-2}$	$M_{\delta_e} = -1.4 \text{ sec}^{-2}$		
$M_q = -1.2 \text{ sec}^{-1}$			

^aGross weight = 18,160 kg (40,000 lb) $N_H = 95\%$ $I_{xx} = 357,000 \text{ kg}\cdot\text{m}^2$
 (263,000 slug-ft²)
 $V_o = 65 \text{ knots}$ $\delta_F = 65^\circ$ $I_{yy} = 281,000 \text{ kg}\cdot\text{m}^2$
 (207,000 slug-ft²)
 $\alpha = 3^\circ$ $\nu = 90^\circ$ $I_{zz} = 700,000 \text{ kg}\cdot\text{m}^2$
 (516,000 slug-ft²)

APPENDIX B

SUMMARY OF PILOT COMMENTS

Table 5 presents the pilots evaluations of each of the experimental control system and cockpit display configurations investigated in flight. The table includes pilot opinion ratings for VFR and IFR approaches and for the flare and landing. Detailed pilot commentary accompany the opinion ratings. A summary of the wind conditions encountered for each configuration is provided; it includes the tower-reported wind conditions for an individual approach and landing, or for a series of landings. The most significant encounters of wind and turbulence, as derived from airborne data and from ground-based radar tracking, are also presented; they include sustained headwind gradients, their duration and time of encounter during the approach, and extremes of headwind and vertical gusts, all measured along the aircraft's flightpath.

TABLE 5.— SUMMARY OF PILOTS' EVALUATIONS AND WIND CONDITIONS FOR SELECTED LANDING APPROACHES

Configuration	Tower-reported winds		Measured turbulence				Cooper-Harper ratings of pilots A-D, VFR rating (IFR rating)				Pilot comments
			\dot{U}_w , knots/sec	Δt , sec	T_{TD} , sec	$U_{w\ min\ max}$ $\pm w_{w\ max}$	A	B	C	D	
	knots	deg									
Basic aircraft; Boeing roll-yaw SAS	25	310					4				Pitch attitude control Pitch attitude control acceptable when tightly controlling attitude during VFR glide-slope tracking in light to moderate turbulence. Considerable attention to attitude control required for landing flare and during flap and nozzle deployment. Roll and yaw attitude control Difficulty in tracking localizer. Poor bank-angle and heading control.
	15	320						3 (3)			
	20-30	280								5	
Pitch SCAS; Attitude command, Boeing roll-yaw SAS	10	150									Pitch attitude control Ability to make small corrections satisfactory. No tendency to drift. Trim rate OK. Control sensitivity and forces OK for large corrections. Bothersome to hold forces for sustained corrections. Difficult to hold precisely. Unattended attitude hold good. Ease of adjustment of sink rate poor. Forces seem high. Another control (trim button) adds to workload. Attitude-command system less desirable than RCAH for this aircraft when continuous attitude control is required during approach and flare.
	7	360					3 (3)				
	10	150								3.5-4 (4.5-5)	
Pitch SCAS; Rate-command attitude-hold, Boeing roll-yaw SAS	10	160					2 (2)				Pitch attitude control Good precision of attitude control. Sensitivity good. No tendency to overshoot or drift for small or large corrections. Attitude held satisfactorily during unattended operation. Precise control of flare and landing. Control forces low. Easy to adjust attitude to modulate sink rate. Low control workload.
	20-30	250						2 (2)			
	20	300								2.5-3 (3.5-4)	
	15	270									

TABLE 5.— Continued.

Configuration	Tower-reported winds		Measured turbulence				Cooper-Harper ratings of pilots A-D, VFR rating (IFR rating)				Pilot comments	
			\dot{U}_w , knots/sec	Δt , sec	T_{TD} , sec	$U_{w \min \max}$ $\pm w_{w \max}$	A	B	C	D		
	knots	deg										
Roll-yaw SCAS								3	3		3	Bank angle control Roll stability and damping satisfactory. Good control sensitivity. No tendency to overshoot. Good control harmony between pitch and roll. Some difficulty in establishing small bank angles around zero.
Basic aircraft; pitch, roll yaw SCAS	5	360						4.5	(6)			Localizer tracking Difficulty with heading and localizer control due to instrument scan workload.
	30-38	320										Glide-slope tracking Control technique -- thrust for flightpath control, attitude for airspeed control, nozzles fixed except for large sustained path corrections. Difficulty with coupled flightpath-airspeed-angle-of-attack responses to thrust control. Airspeed variations influence flightpath response and landing distance. Angle-of-attack variations influence safety margins. Sluggish flightpath response when correcting to glide slope from low offset. Easy to get low-slow due to path-speed coupling. Pilot must either control attitude to hold airspeed to obtain acceptable flightpath response during glide-slope corrections or accept degraded flightpath response if allowing pitch SCAS to hold attitude. Large attitude changes required to hold speed. Pitch attitude control required to hold airspeed while making flightpath corrections with thrust is unconventional in that a nose-down change in attitude must be coordinated with an increase in thrust for a correction up to the glide slope and vice versa. Workload evenly
	5	360										
	8	360								5		
	25-30	270								(5)		
	30-40	310										
	35-42	320	-1.0	10	70	16 to 30 ± 7.5		(5.5-6) in turb			(5.5)	
	20	350										
	12	360									2.5-3 (3.5-4)	

TABLE 5.— Continued.

Configuration	Tower-reported winds		Measured turbulence				Cooper-Harper ratings of pilots A–D, VFR rating (IFR rating)				Pilot comments	
			\dot{U}_w	Δt	T_{TD}	$U_{w_{min}}$	A	B	C	D		
	knots/sec	sec	sec	$\pm w_{max}$								
	knots	deg										
												divided between glide-slope and localizer task. Workload increased for wind conditions demanding coordinated throttle-nozzle control for glide-slope tracking (PR 6). Effects of turbulence and shears encountered degrade ratings by 0.5 to 1 unit. Reduced sink rate in strong headwinds.
Basic aircraft; pitch, roll yaw SCAS	5	360						3.5				Flare and landing Control technique – initiate and modulate flare with pitch rotation. Use discrete thrust inputs to compensate for high sink rates. Maintain positive sink rate to touchdown. Gradually reduce thrust when touchdown is assured. Landing precision reasonably good. Large pitch rotation required. Use of both pitch and thrust control not objectionable.
	25-30	300										
	8	360							5			
	30-40	310										
	20	350								5		
Throttle-nozzle interconnect pitch, roll, yaw SCAS	5	320						3.5				Glide-slope tracking Control technique – thrust for flightpath control, attitude for airspeed control. Decoupling of flightpath and airspeed response allows approach to be made at more constant pitch attitude which simplifies tracking task. Glide-slope tracking reasonably good. No 0.5 to 1 unit change in rating for shears and turbulence encountered. Minimum decision height for IFR approach for this configuration is 61 m (200 ft) when tracking raw glide slope and localizer. Most deficiencies attributed to raw data instrument scan.
	10	360										
	25-30	310										
	37	320	0.8	8	20	9 to 24	3.5					
			-1.4	8	37	± 18	in					
			0.8	7	45		turb					
	30-38	320	1.4	8	22	10 to 30						
			1.0	7	75	± 12						
	5	320	1.0	7	18	0 to 7	(4.5)					
			-1.0	7	28	± 6						
15	300							4				
20-30	270							(4.5)				
35-40	320							(5-5.5)				
								in turb				
	5	360	-1.1	9	20	-6 to 7						
			1.5	8	30	± 9						
			-1.5	7	60							

TABLE 5.— Continued.

Configuration	Tower-reported winds		Measured turbulence				Cooper-Harper ratings of pilots A-D, VFR rating (IFR rating)				Pilot comments
			\dot{U}_w , knots/sec	Δt , sec	T_{TD} , sec	U_w U_w^{min} U_w^{max}	A	B	C	D	
	knots	deg									
Airspeed-stabilization; pitch, roll, yaw SCAS	12	110									(3.5) Glide-slope tracking Control technique – pitch attitude for flightpath control augmented by thrust if necessary for large, sustained corrections. Large attitude changes required for glide-slope tracking. Not objectionable early in approach when pitch rates can be kept low, but is objectionable to make large rotations during last 30-61 m (100-200 ft). Heave response not adequate for rapid glide-slope corrections during latter stages of approach. Must augment control with thrust to get adequate response. Some variation in speed noted. Crisp nozzle response when maneuvering.
	20	300					(4.5)				
	20	330									
	20-30	300									
	10	100									
	20	300						5			3.5 Flare and landing Flare with pitch, coordinated with reduction in thrust to counteract floating tendency. No speed bleed-off in flare.
	20-30	300									
	10	100									
Flightpath airspeed SCAS; pitch roll, yaw SCAS	5	360					(2)				(4) Glide-slope tracking Control technique – pitch attitude for flightpath control. Good glide-slope tracking. Airspeed held within acceptable limits during large corrections. Can make rapid corrections without overshooting. Good fly-up capability. Magnitude of pitch changes for precise glide-slope tracking down to decision height is acceptable.
	20-25	310	-0.7	15	20	14 to 25 ±6					
	5	150	-1.0	9	30	-9 to 4		(4)			
	5	150	1.0	8	55	±4.5					
	5	150	-0.7	10	20	-6 to 3 ±3.0					
	12	320	1.0	7	15	5 to 14					
	15	180	1.5	7	40	± 6					

TABLE 5.— Continued.

Configuration	Tower-reported winds		Measured turbulence				Cooper-Harper ratings of pilots A-D, VFR rating (IFR rating)				Pilot comments		
			\dot{U}_w ,	Δt ,	T_{TD} ,	U_w	A	B	C	D			
	knots/sec	sec	sec	$_{min}^{max}$	$\pm w_{w_{max}}$								
	5	360						2.5				Flare and landing	
	12	320								3.0		Flare with pitch, coordinated with reduction in thrust. Flare and touchdown quite comfortable. Little pitch rotation required. Good consistency of touchdown point.	
Flightpath airspeed SCAS; reduced gain ($K_T = 0.6$)	10-20	340						(3.5)				Glide-slope tracking	
	20-25	270								(5)		Corrections from low were slow and speed tended to bleed-off. Required fairly large pitch corrections. Tight glide-slope tracking when approaching decision height was uncomfortable. Not much throttle activity.	
Alternate flightpath- airspeed SCAS; pitch, roll yaw SCAS	10	320						(2-2.5)				Glide-slope tracking	
	25	320	-1.0	8	15	15 to 24						Control technique — pitch attitude for flightpath control. Glide-slope tracking pretty good. Response seemed sluggish when correcting from below. Heave response improved in comparison to airspeed-stabilization configuration.	
			1.0	7	28	± 6							
			-1.0	7	60								
	20	330	-2.5	4	7	17 to 25			(4)			Some what large pitch corrections still required. Occasionally required thrust increase to augment large, long-term path corrections.	
			-0.8	7	35	± 9							
	5	150											
20	190												
	18	340	1.8	5	33	18 to 28				(3)			
			-1.0	8	42	± 4.5							
	20	340	-0.7	10	29	12 to 24							
						± 9							
	20	330								4.5		Flare and landing	
	20	350										3.5	Flare capability OK. Improved heave response in comparison to basic aircraft. Flare entry condition not as critical as basic aircraft. Good touchdown precision. Need to reduce thrust to counteract floating tendency.

TABLE 5.— Concluded.

Configuration	Tower-reported winds		Measured turbulence				Cooper-Harper ratings of pilots A-D, VFR rating (IFR rating)				Pilot comments
			\dot{U}_w , knots/sec	Δt , sec	T_{TD} , sec	U_w min max $\pm w_{wmax}$	A	B	C	D	
	knots	deg									
Throttle-nozzle interconnect;	20	320	-1.5	6	6						Glide-slope tracking Control technique – flightpath control with thrust, airspeed control with attitude. Flight director does a good job. Makes task significantly easier. Good glide-slope and localizer tracking performance. Pitch commands smooth and easy to follow. Throttle and lateral directors seem a little busy and perhaps too sensitive. Minimum decision height of 30 m (100 ft) looks practical.
	20-25	320	-1.2	7	10	9 to 19 ± 3					
flight director, pitch, roll yaw SCAS	10	340					(3)				
	25	320									
Flightpath airspeed SCAS;	20-25	320	-1.2	10	15	8 to 22 ± 4.5	(1.5)				Glide-slope tracking Control technique – Flightpath control with pitch attitude. Simplifies pilot's task significantly. Overall instrument scan workload reduced. Good glide-slope and localizer performance. Lateral director is a little sensitive. Minimum decision height of 30 m (100 ft) is acceptable.
flight director, pitch, roll yaw SCAS			-1.0	5	30						
			-1.4	6	45						
			-1.0	7	30	12 to 20 ± 4.5		(2.5)			

APPENDIX C

NOTATION

<i>AGL</i>	above ground level
a_x	longitudinal body axis acceleration
a_y	lateral body axis acceleration
a_z, n_z	vertical body axis acceleration
<i>B</i>	backside control technique
<i>BLC</i>	boundary layer control
<i>c.g.</i>	center of gravity
<i>DLC</i>	direct lift control
<i>d</i>	deviation from the glide-slope beam
$d\gamma/du$	change of flightpath angle with airspeed for constant thrust
<i>F</i>	front-side control technique
F_{BO}	electrical breakout force for column
F_c	column force
F_w	wheel force
F_p	pedal force
<i>g</i>	gravitational acceleration
<i>h</i>	altitude
\dot{h}	vertical velocity
<i>IFR</i>	instrument flight rules
I_{xx}	roll moment of inertia
I_{yy}	pitch moment of inertia

I_{zz}	yaw moment of inertia
K_c	column force sensitivity gain
K_{cc}	master gain for inboard choke controls
$K_{F\theta}$	pitch control feed-forward gain
$K_{F\phi}$	roll control feed-forward gain
K_G	aerodynamic flightpath angle gain to throttles and chokes
K_I	pitch command integral feed-forward gain
K_{NT}	engine rpm gain to nozzles
$K_{N\theta}$	pitch-attitude gain to nozzles
K_p	roll rate gain to lateral controls
K_q	pitch-rate gain to elevator
K_T	pitch-attitude gain to throttles and chokes
K_{TT}	master gain for throttle controls
K_v	airspeed gam to nozzles
K_w	wheel position sensitivity gain
K_θ	pitch-attitude gain to elevator
K_ϕ	bank-angle gain to lateral controls
L_a	rolling moment, derivative with respect to variable a , $\frac{1}{I_{xx}} \frac{\partial L}{\partial a}$
MSL	mean sea level
M_a	pitching moment derivative with respect to variable a , $\frac{1}{I_{yy}} \frac{\partial M}{\partial a}$
m	aircraft mass
N_a	yawing moment derivative with respect to variable a , $\frac{1}{I_{zz}} \frac{\partial N}{\partial a}$
N_H	high-pressure engine rotor rpm
N_{H_0}	initial value of N_H at flight director engage

p, p_B	body axis roll rate
q, q_B	body axis pitch rate
R	turn radius for reference flightpath
r, r_B	body axis yaw rate
s	Laplace operator
$T_{L\theta}$	pitch SCAS lead time constant, $T_{L\theta} = K_q/K_\theta$
$T_{L\phi}$	roll SCAS lead time constant, $T_{L\phi} = K_p/K_\phi$
T_R	roll mode time constant
T_S	spiral mode time constant
T_{sp_1}, T_{sp_2}	time constants of the longitudinal characteristic equation normally associated with the short period mode
T_{TD}	time to go to touchdown
U_w	longitudinal wind component – positive for headwind
\dot{U}_w	rate of change of longitudinal wind (headwind shear with respect to time)
u	perturbation airspeed
V	airspeed
VFR	visual flight rules
V_c	calibrated airspeed
V_E	equivalent airspeed
V_F	complementary filtered airspeed
V_G	ground speed
V_o	initial airspeed
V_{REF}	pilot selected reference airspeed for airspeed SCAS and flight director
V_T	true airspeed
v	lateral velocity

WP	waypoint
w	vertical velocity
w_w	vertical wind velocity
X_a	longitudinal force derivative due to variable a , $\frac{1}{M} \frac{\partial X}{\partial a}$
Y_a	lateral force derivative with respect to variable a , $\frac{1}{M} \frac{\partial Y}{\partial a}$
Z_a	vertical force derivative with respect to variable a , $\frac{1}{M} \frac{\partial Z}{\partial a}$
α	angle of attack
$\dot{\alpha}$	rate-of-change of angle of attack
α_O	threshold angle of attack for throttle flight director
β	angle of sideslip
γ	flightpath angle
ΔT	incremental change in thrust
Δt	time duration of longitudinal wind gradient
$\Delta u_{SS}/\Delta \gamma_{SS}$	ratio of change of steady-state airspeed to flightpath due to a change in thrust (constant pitch attitude)
$\Delta u_{SS}/\Delta \theta_{SS}$	ratio of change of steady-state airspeed to pitch attitude for constant thrust
Δy	lateral deviation from localizer beam
$\Delta \beta/\Delta \phi$	ratio of peak sideslip to peak bank angle occurring during a turn entry maneuver
$\Delta \gamma_{max}/\Delta \gamma_{SS}$	ratio of peak to steady-state change of flightpath angle due to a change in thrust (constant pitch attitude)
$\Delta \gamma_{max}/\Delta \theta_{SS}$	peak change in flightpath angle in response to a step change in pitch attitude
$\Delta \gamma_{SS}/\Delta \theta_{SS}$	ratio of change of steady-state flightpath angle to pitch attitude
δA_{TOTAL}	sum of right and left aileron deflection
δ_c	column position
δ_{cFD}	column flight director bar deflection

δ_{CH}	inboard or outboard augmentor choke position
$\dot{\delta}_{CH}$	inboard augmentor choke deployment rate
δ_e	elevator position
δ_{eSAS}	pitch SAS series servo position
δ_f	flap position
δ_r	rudder position
δ_p	pedal position
δ_T	throttle position
δ_{TRIM}	pitch-trim command from column switch
δ_{TFD}	throttle flight director bar deflection
δ_w	wheel position
δ_{wBO}	electrical breakout position for wheel
δ_{wFD}	wheel flight director bar deflection
δ_v	cockpit nozzle control handle position
ϵ	glide-slope tracking or altitude-hold error signal for flight director
ζ_d, ω_d	damping ratio and natural frequency of the Dutch-roll mode
ζ_p, ω_p	damping ratio and natural frequency of the phugoid mode
ζ_{sp}, ω_{sp}	damping ratio and natural frequency of the short period mode
θ	pitch attitude
$\dot{\theta}$	pitch rate
θ_{BIAS}	pitch attitude bias for flight director
θ_{max}/θ_{ss}	ratio of peak to steady-state pitch attitude
ν	nozzle position

ϕ	bank angle
$\dot{\phi}$	roll rate
ϕ_c	bank angle command to lateral flight director for reference flightpath turn
ϕ_{max}/ϕ_{ss}	ratio of peak to steady-state bank angle
ω_{SAS}	SCAS actuator natural frequency
ω_w	washout frequency for choke control



REFERENCES

1. Quigley, Hervey C.; and Innis, Robert C.: Handling Qualities and Operational Problems of a Large Four-Propeller STOL Transport Airplane. NASA TN D-1647, 1963.
2. Quigley, Hervey C.; Innis, Robert C.; Vomaske, Richard F.; and Ratcliff, Jack W.: A Flight and Simulator Study of Directional Augmentation Criteria for a Four-Propellered STOL Airplane. NASA TN D-3909, 1967.
3. Quigley, Hervey C.; Innis, Robert C.; and Holzhauser, Curt A.: A Flight Investigation of the Performance, Handling Qualities, and Operational Characteristics of a Deflected Slipstream STOL Transport Airplane Having Four Interconnected Propellers. NASA TN D-2231, 1964.
4. Innis, Robert C.; Holzhauser, Curt A.; and Gallant, Richard P.: Flight Tests Under IFR with an STOL Transport Aircraft. NASA TN D-4939, 1968.
5. Grantham, William D.; Nguyen, Luat T.; Patton, James M., Jr.; Deal, Perry L.; Champine, Robert A.; and Carter, C. Robert: Fixed-Base Simulator Study of an Externally Blown Flap STOL Transport Airplane During Approach and Landing. NASA TN D-6898, 1972.
6. Powers, Bruce G.; and Kier, David A.: Simulator Evaluation of the Low-Speed Flying Qualities of an Experimental STOL Configuration with an Externally Blown Flap Wing or an Augmentor Wing. NASA TN D-7454, 1973.
7. Allison, R. L.; Mack, M.; and Rumsey, P. C.: Design Evaluation Criteria for Commercial STOL Transports. NASA CR-114454, 1972.
8. Berg, R. A.; and Shirley, W. A.: A Flight Simulator Study of STOL Transport Longitudinal Control Characteristics. FAA-RD-72-56, July 1972.
9. Vincent, James H.: STOL Tactical Aircraft Investigation – Flight Control Technology: Piloted Simulation of a Medium STOL Transport with Vectored Thrust/Mechanical Flaps. AFFDL-TR-73-19, Vol. V, Part 2, May 1973.
10. Campbell, J. E.; Elsanker, W. K.; and Okumoto, V. H.: STOL Tactical Aircraft Investigation – Externally Blown Flap. Flight Control Technology: Simulation Studies/Flight Control System Validation. AFFDL-TR-73-20, Vol. V, Part 2, Apr. 1973.
11. Feinreich, Benjamin; Seckel, Edward; and Ellis, David R.: In-Flight Simulation Study of Decoupled Longitudinal Controls for the Approach and Landing of a STOL Aircraft. NASA CR-2710, 1977.
12. Lane, John P.: YC-15 Development and Test Highlights – Phase III. Society of Experimental Test Pilots Technical Review, Vol. 13, No. 4, Oct. 1977, pp. 85-111.
13. McPherson, Raymond L.: YC-14 Flight Test Program. Society of Experimental Test Pilots Technical Review, Vol. 13, No. 4, Oct. 1977, pp. 112-127.
14. Quigley, Hervey C.; Innis, Robert C.; and Grossmith, Seth W.: A Flight Investigation of the STOL Characteristics of an Augmented Jet Flap STOL Research Aircraft. NASA TM X-62,334, 1974.

15. Vomaske, Richard F.; Innis, Robert C.; Swan, Brian E.; and Grossmith, Seth W.: A Flight Investigation of the Stability, Control, and Handling Qualities of an Augmented Jet Flap STOL Airplane. NASA TP-1254, 1978.
16. Neuman, Frank; Watson, Delmar M.; and Bradbury, Peter: Operational Description of an Experimental Digital Avionics System for STOL Airplanes. NASA TM X-62,448, 1975.
17. Hoh, Roger H.; Klein, Richard H.; and Johnson, Walter A.: Development of an Integrated Configuration Management/Flight Director System for Piloted STOL Approaches. NASA CR-2883, 1977.
18. Cooper, George E.; and Harper, Robert P.: The Use of Pilot Rating in the Evaluation of Aircraft Handling Qualities. NASA TN D-5153, 1969.
19. Hefley, Robert K.; Stapleford, Robert L.; and Rumold, Robert C.: Airworthiness Criteria Development for Powered-Lift Aircraft – A Program Summary. NASA CR-2791, 1977.
20. Ellis, David R.: An In-Flight Simulation of Approach and Landing of a STOL Transport with Adverse Ground Effect. NASA CR-154875, 1976.

1. Report No. NASA TP-1551	2. Government Accession No.	3. Recipient's Catalog No.
4. Title and Subtitle FLIGHT EVALUATION OF STABILIZATION AND COMMAND AUGMENTATION SYSTEM CONCEPTS AND COCKPIT DISPLAYS DURING APPROACH AND LANDING OF A POWERED-LIFT STOL AIRCRAFT		5. Report Date November 1980
7. Author(s) James A. Franklin, Robert C. Innis, and Gordon H. Hardy		6. Performing Organization Code
9. Performing Organization Name and Address Ames Research Center, NASA Moffett Field, Calif. 94035		8. Performing Organization Report No. A-7968
12. Sponsoring Agency Name and Address National Aeronautics and Space Administration Washington, D.C. 20546		10. Work Unit No. 532-02-11
15. Supplementary Notes		11. Contract or Grant No.
16. Abstract A flight research program was conducted to assess the effectiveness of manual control concepts and various cockpit displays in improving attitude (pitch, roll, and yaw) and longitudinal path control during STOL approaches and landings. The NASA-Ames Powered-Lift Augmentor Wing Jet STOL Research Aircraft was used in the research program. Satisfactory flying qualities were demonstrated to minimum-decision heights of 30 m (100 ft) for selected stabilization and command augmentation systems and flight director combinations. Precise landings at low touchdown sink rates were achieved with a gentle flare maneuver.		13. Type of Report and Period Covered Technical Paper
17. Key Words (Suggested by Author(s)) STOL aircraft Handling qualities Stability augmentation Flight director Approach and landing Flight research	18. Distribution Statement Unclassified - Unlimited	14. Sponsoring Agency Code
19. Security Classif. (of this report) Unclassified	20. Security Classif. (of this page) Unclassified	21. No. of Pages 94
		22. Price* \$6.00

*For sale by the National Technical Information Service, Springfield, Virginia 22161

National Aeronautics and
Space Administration

THIRD-CLASS BULK RATE

Postage and Fees Paid
National Aeronautics and
Space Administration
NASA-451



Washington, D.C.
20546

Official Business

Penalty for Private Use, \$300

6 1 1U, A, 103180 S00903DS
DEPT OF THE AIR FORCE
AF WEAPONS LABORATORY
ATTN: TECHNICAL LIBRARY (SUL)
KIRTLAND AFB NM 87117

NASA

POSTMASTER: If Undeliverable (Section 158
Postal Manual) Do Not Return
